In cooperation with the Upper Elkhorn, Lower Elkhorn, Upper Loup, Lower Loup, Middle Niobrara, Lower Niobrara, Lewis and Clark, and Lower Platte North Natural Resources Districts

Apparent Resistivity and Estimated Interaction Potential of Surface Water and Groundwater along Selected Canals and Streams in the Elkhorn-Loup Model Study Area, North-Central Nebraska, 2006–07

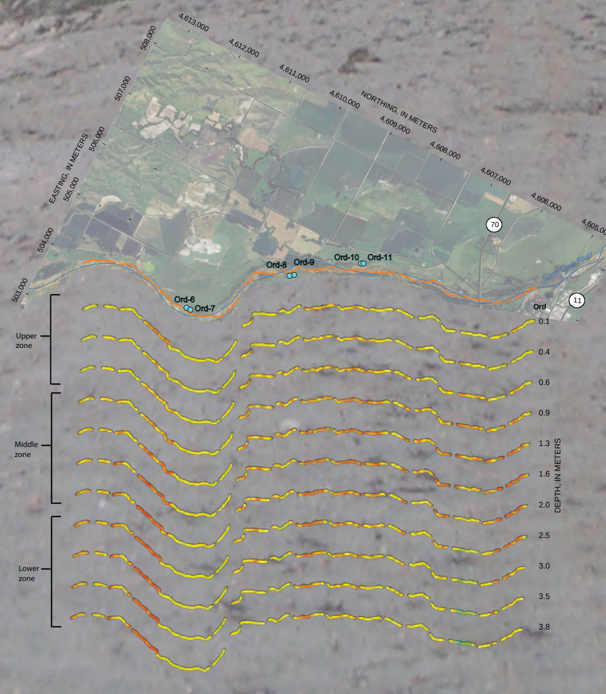

Scientific Investigations Report 2009–5171

U.S. Department of the Interior
U.S. Geological Survey

Front cover:

Left, GEM-2 frequency domain electromagnetic continuous-resistivity profiling equipment;

Right top, Geoprobe machine mounted on a utility vehicle (top);

Right bottom, Inverse modeling results for waterborne direct-current resistivity profile near Ord, Nebraska.

Apparent Resistivity and Estimated Interaction Potential of Surface Water and Groundwater along Selected Canals and Streams in the Elkhorn-Loup Model Study Area, North-Central Nebraska, 2006–07

By Andrew P. Teeple, Joseph Vrabel, Wade H. Kress, and James C. Cannia

In cooperation with the Upper Elkhorn, Lower Elkhorn, Upper Loup, Lower Loup, Middle Niobrara, Lower Niobrara, Lewis and Clark, and Lower Platte North Natural Resources Districts

Scientific Investigations Report 2009–5171

U.S. Department of the Interior
U.S. Geological Survey

U.S. Department of the Interior
KEN SALAZAR, Secretary

U.S. Geological Survey
Suzette M. Kimball, Acting Director

U.S. Geological Survey, Reston, Virginia: 2009

This and other USGS information products are available at http://store.usgs.gov/
U.S. Geological Survey
Box 25286, Denver Federal Center
Denver, CO 80225

To learn about the USGS and its information products visit http://www.usgs.gov/
1-888-ASK-USGS

Suggested citation:
Teeple, A.P., Vrabel, Joseph, Kress, W.H., and Cannia, J.C., 2009, Apparent resistivity and estimated interaction potential of surface water and groundwater along selected canals and streams in the Elkhorn-Loup Model study area, north-central Nebraska, 2006–07: U.S. Geological Survey Scientific Investigations Report 2009–5171, 66 p.

Contents

Figures

Table

Conversion Factors and Datums

SI to Inch/Pound

Multiply	By	To obtain
	Length	
meter (m)	3.281	foot (ft)
kilometer (km)	0.6214	mile (mi)
kilometer (km)	0.5400	mile, nautical (nmi)
meter (m)	1.094	yard (yd)
millimeter (mm)	0.003281	foot (ft)
	Area	
square meter (m^2)	0.0002471	acre
square kilometer (km^2)	247.1	acre
square meter (m^2)	10.76	square foot (ft^2)
square kilometer (km^2)	0.3861	square mile (mi^2)
	Resistivity	
ohm-meter (ohm-m)	3.281	ohm-foot (ohm-ft)

Datums

Vertical coordinate information is referenced to the North American Vertical Datum of 1988 (NAVD 88).

Horizontal coordinate information is referenced to the North American Datum of 1983 (NAD 83).

Altitude, as used in this report, refers to distance above the vertical datum.

Blank Page

Apparent Resistivity and Estimated Interaction Potential of Surface Water and Groundwater along Selected Canals and Streams in the Elkhorn-Loup Model Study Area, North-Central Nebraska, 2006–07

By Andrew P. Teeple, Joseph Vrabel, Wade H. Kress, and James C. Cannia

Abstract

In 2005, the State of Nebraska adopted new legislation that in part requires local Natural Resources Districts to include the effect of groundwater use on surface-water systems in their groundwater management plan. In response the U.S. Geological Survey, in cooperation with the Upper Elkhorn, Lower Elkhorn, Upper Loup, Lower Loup, Middle Niobrara, Lower Niobrara, Lewis and Clark, and Lower Platte North Natural Resources Districts, did a study during 2006–07 to investigate the surface-water and groundwater interaction within a 79,800-square-kilometer area in north-central Nebraska. To determine how streambed materials affect surface-water and groundwater interaction, surface geophysical and lithologic data were integrated at four sites to characterize the hydrogeologic conditions within the study area. Frequency-domain electromagnetic and waterborne direct-current resistivity profiles were collected to map the near-surface hydrogeologic conditions along sections of Ainsworth Canal near Ainsworth, Nebraska; Mirdan and Geranium Canals near Ord, Nebraska; North Loup River near Ord, Nebraska; and Middle Loup River near Thedford, Nebraska. Lithologic data were collected from test holes at each site to aid interpretation of the geophysical data. Geostatistical analysis incorporating the spatial variability of resistivity was used to account for the effect of lithologic heterogeneity on effective hydraulic permeability. The geostatistical analysis and lithologic data descriptions were used to make an interpretation of the hydrogeologic system and derive estimates of surface-water/groundwater interaction potential within the canals and streambeds.

The estimated interaction potential at the Ainsworth Canal site and the Mirdan and Geranium Canal site is generally low to moderately low. The sediment textures at nearby test holes typically were silt and clay and fine-to-medium sand. The apparent resistivity values for these sites ranged from 2 to 120 ohm-meters. The vertical and horizontal variability of the apparent resistivity data were consistently low. Low resistive variability indicates little lithologic heterogeneity for either canal site. The surface-water/groundwater interaction-potential estimates are in agreement with the narrow frequency distribution of resistivity, low apparent resistivities, low spatial heterogeneity, and test-hole grain-size ranges.

The estimated surface-water/groundwater interaction potential at the North Loup and Middle Loup River sites is moderate to moderately high. The sediment textures at nearby test holes were predominantly fine, medium, and coarse sand with some silt and silty to sandy clay. The apparent resistivity values for these sites ranged from 34 to 1,338 ohm-meters. The vertical variability of the resistivity data was moderately high. The horizontal variability at these sites is low to moderately low. The higher resistive variability at these sites indicates generally greater lithologic heterogeneity than at either the Ainsworth Canal site or the Mirdan and Geranium Canal site. The surface-water/groundwater interaction-potential estimates are in agreement with the generally moderate to high apparent resistivity, the greater spatial heterogeneity, and the variable lithologic texture. A higher interaction potential as compared to the canal sites is expected because of the higher subsurface resistivity and greater lithologic heterogeneity.

Introduction

In 2005, the State of Nebraska adopted new legislation requiring an annual evaluation to determine the water appropriation status of all river basins in the state (North Platte Natural Resources District, 2004). A basin is considered fully appropriated when the current use of surface-water resources is equal to the available surface-water supply. The water supply of the Loup and Elkhorn River Basins in central Nebraska was identified by the Nebraska Department of Natural Resources as having a high potential for being designated as fully appropriated (Bleed, 2006, 2007). The 2005 law also requires Natural Resources Districts (NRDs) to include the effect of groundwater use on surface-water systems as part of their groundwater management plan. In response to these new demands for water planning, the Upper Elkhorn, Lower Elkhorn, Upper Loup, Lower Loup, Middle Niobrara, Lower Niobrara, Lewis and Clark, and Lower Platte North NRDs (hereinafter referred to collectively as the Elkhorn-Loup Model (ELM) sponsors) cooperated with the U.S. Geological Survey (USGS) to study the surface-water and groundwater system within a 79,800-square kilometer (km^2) area of north-central Nebraska (Peterson, 2007).

Determining how streambed materials affect surface-water/groundwater interaction was identified as a concern by the ELM sponsors. One tool for understanding surface-water and groundwater systems is groundwater flow models, which can be used to apply theoretical relations between physical properties and model variables. Flow models can also be used to simulate how stresses affect an aquifer system (Appel and Bredehoeft, 1976). Specific hydrogeologic values, such as hydraulic conductivity, must be known for the groundwater flow model to accurately simulate current or future conditions (Merry and others, 2003). Borehole data and surficial geologic mapping are commonly used to determine geologic and hydrogeologic conditions. For example, the grain size and character of the streambed regulates the flow of water between the stream and the groundwater system. Often, however, needed information is either unavailable or too spatially sparse to adequately define the subsurface. This could require streambed characteristics to be estimated from test-hole information that was collected several kilometers away. An alternative approach is inverse modeling, wherein model input is adjusted until it reproduces measured stream behavior to an “acceptable” level. In either case, the lack of information can increase uncertainties in estimated geologic and hydrogeologic properties, which in turn can lead to problems with conceptualization, calibration, and simulation of the flow system.

Acquiring lithologic data by drilling test holes can be time-consuming, expensive, and difficult in an active stream (Ball and others, 2006). In addition, lithologic data collected from test holes represent individual locations and do not accurately define the lateral variability of grain-size distribution along a stream. By integrating surface geophysical and lithologic (test-hole) data, a laterally extensive framework can be developed to characterize the hydrogeologic conditions of a streambed within a defined area.

Surface geophysical resistivity methods can be used to detect spatial changes in the electrical properties of the subsurface (Zohdy and others, 1974). The electrical properties of soil and rock are determined by water content, porosity, clay content, and conductivity (reciprocal of electrical resistivity) of the pore water (Lucius and others, 2007). Typically, the resistivity of the water has a large effect on the bulk resistivity of the subsurface. Ball and others (2006) demonstrated that surface geophysical resistivity methods can be used to map spatial changes in relative grain-size distributions of alluvial sediment in irrigation-supply canals. Within their study area, fine-grained sediment generally had lower resistivity values than did coarse-grained sediment such as sand and gravel. Electrical resistivity values of geologic material are typically less than 10 ohm-meters (ohm-m) for clay and shale, less than 50 ohm-m for saturated sands and gravels, and more than 200 ohm-m for dry sands and gravels (Lucius and others, 2007). This physical property of the lithology makes surface geophysical resistivity methods an effective tool, when integrated with test-hole lithologic data, for mapping changes in relative grain-size distribution within a streambed. These spatially continuous data depicting relative grain-size distribution can be analyzed to estimate the potential for surface-water and groundwater interaction.

Purpose and Scope

This report documents the results of a surface geophysical investigation conducted during 2006–07 to map the near-surface lithologies to estimate the surface-water/groundwater interaction potential and determine how streambed materials affect the interaction of surface-water and groundwater systems in north-central Nebraska. Using surface geophysical continuous-resistivity profiling (CRP) techniques, changes in the relative grain-size distribution in the upper 3.8 meters (m) of bed materials were mapped along Ainsworth Canal near Ainsworth, Nebraska; Mirdan and Geranium Canals near Ord, Nebraska; North Loup River near Ord, Nebraska; and Middle Loup River near Thedford, Nebraska. Sites were selected to include contrasting streambed character, stream morphology, stream size, local geology, and local topography. Continuous cores were collected from lithologic test holes near the CRP-mapped areas to aid interpretation of subsurface materials and to verify the resistivity results. Methods used to collect, process, and analyze the surface geophysical and test-hole data are presented. Estimated surface-water/groundwater interaction potential is quantified using geostatistical analysis of the CRP data.

Description of Study Sites

The study sites selected for CRP data collection are within the boundaries of the ELM groundwater model study area (fig. 1), which includes the majority of the Loup River Basin. The ELM groundwater model study area is contained between the Niobrara River to the north and the Platte River to the south, with Columbus, Nebraska, located at the eastern extent of the study area and the western end of Lake McConaughy at the western extent (Peterson and others, 2008). Four sites were chosen within the ELM groundwater model study area to map the local near-surface lithology. Previous investigations by Darton (1903a, 1903b) and Swinehart and others (1994) describe the geology and occurrence of groundwater in the study area.

The study site located near Ainsworth, Nebraska (hereinafter referred to as the Ainsworth Canal site), extends from midtown Ainsworth in the west to a point approximately 11 kilometers (km) east from Ainsworth (fig. 2). This study site includes approximately 14 km of the Ainsworth Canal. The

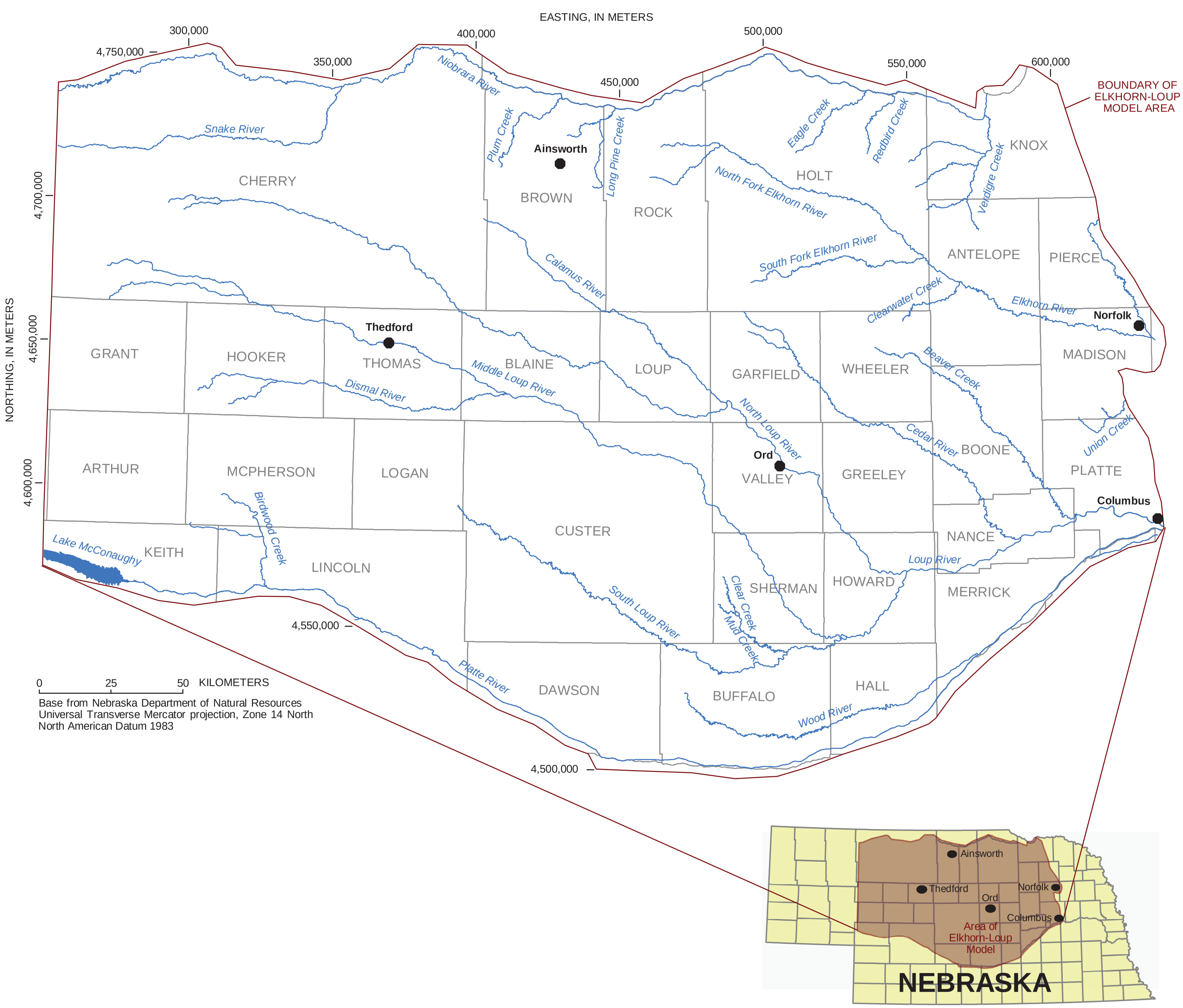

Figure 1. Elkhorn-Loup Model study area, north-central Nebraska.

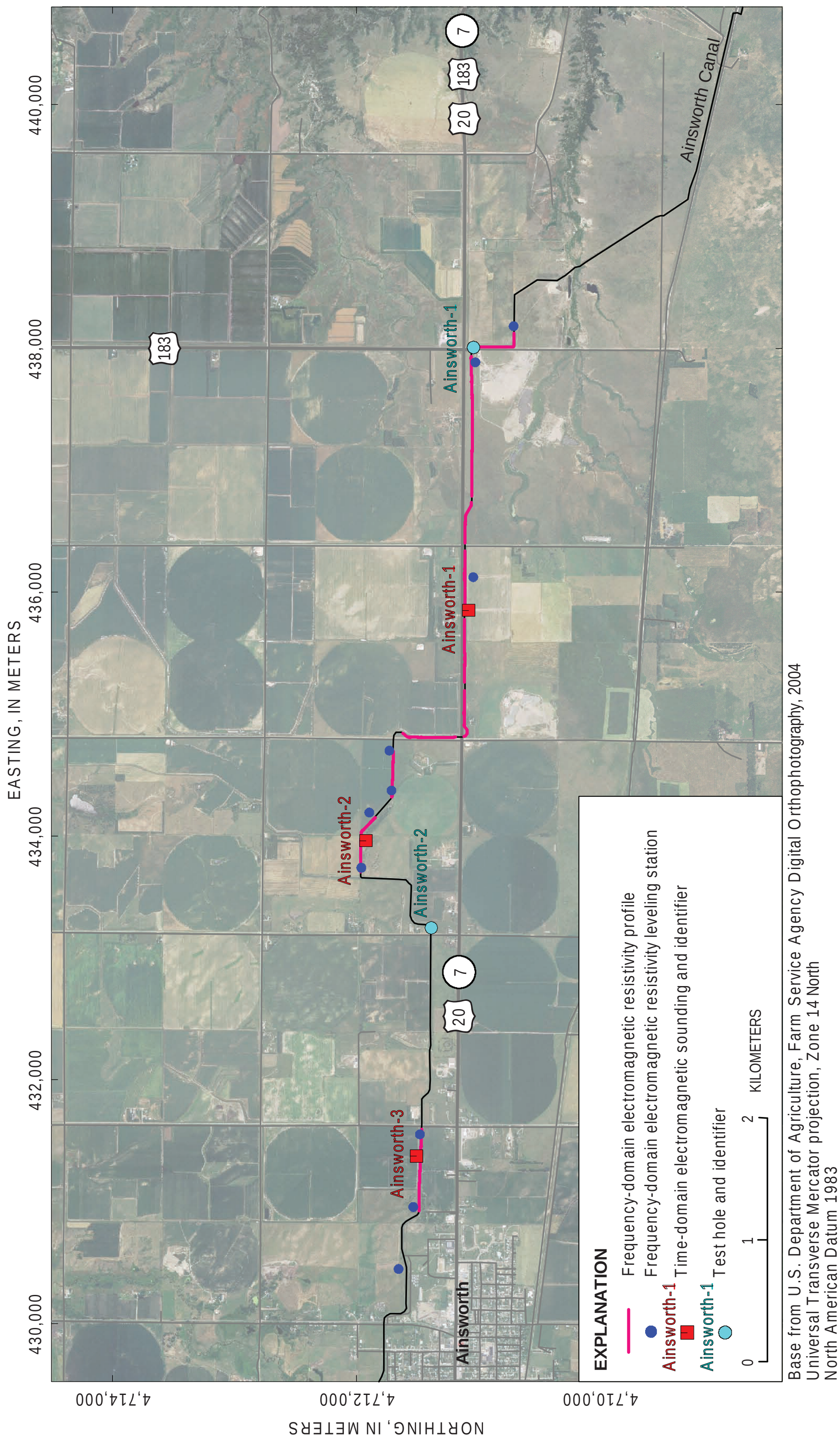

Figure 2. Location of frequency-domain electromagnetic continuous-resistivity profiles Ainsworth Canal near Ainsworth, Nebraska.

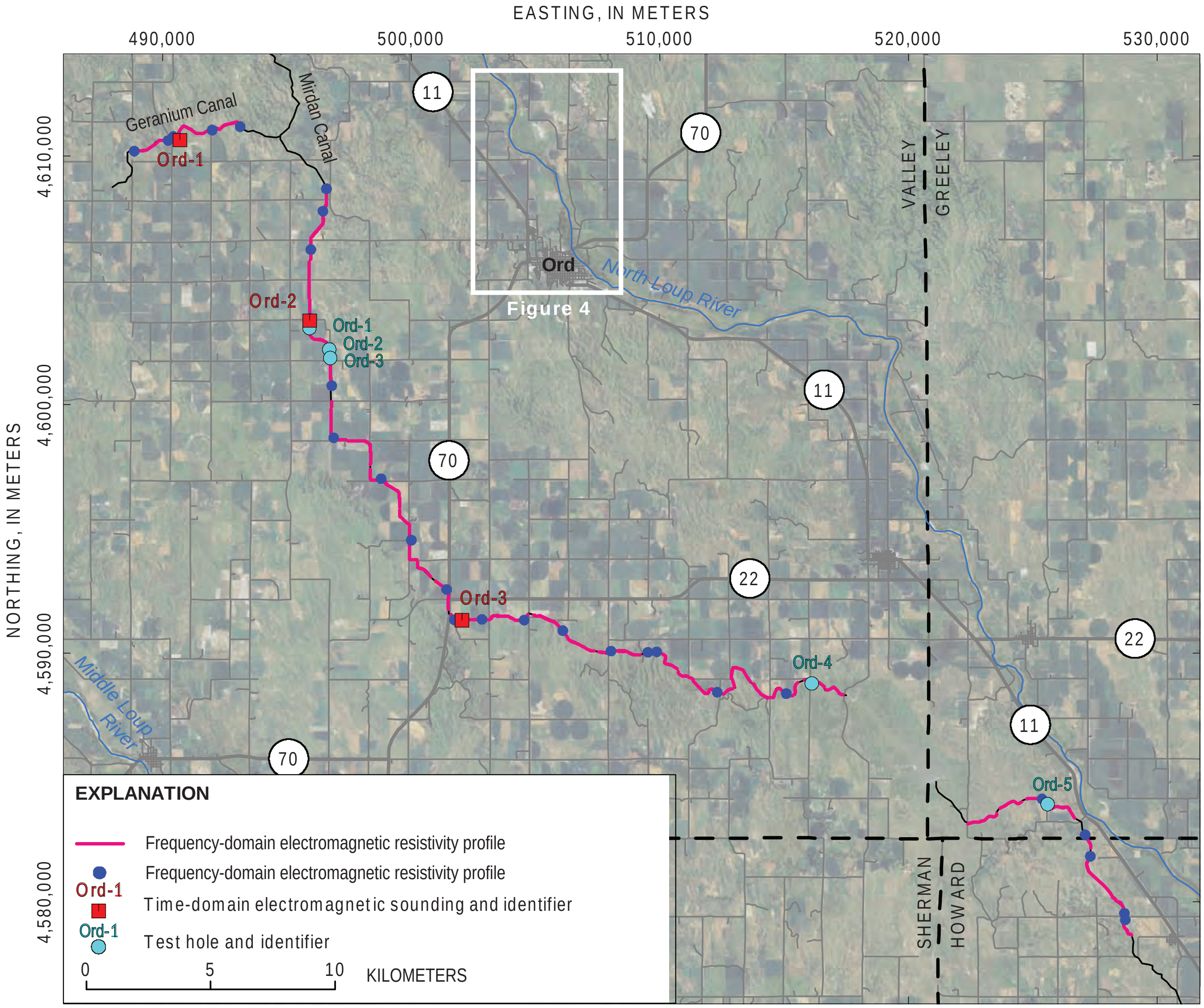

Base from U.S. Department of Agriculture, Farm Service Agency Digital Orthophotography, 2004
Universal Transverse Mercator projection, Zone 14 North
North American Datum 1983

Figure 3. Location of frequency-domain electromagnetic continuous-resistivity profiles along Mirdan and Geranium Canals near Ord, Nebraska.

Ainsworth Canal overlies Quaternary alluvial and eolian deposits. The adjacent prairie is underlain by eolian deposits of well-sorted fine sand with minor silt. The alluvium consists of coarse gravel to fine sand (Swinehart and others, 1994).

The study site located near Ord, Nebraska, extends from about 8.5 km north of Ord to a downstream, southern terminus approximately 6.7 km into Howard County (fig. 3). The study site includes approximately 65 km of the Mirdan Canal and approximately 9 km of the Geranium Canal. The profiled sections of Mirdan Canal and Geranium Canal (hereinafter referred to as the Mirdan and Geranium Canal site) within this area are primarily constructed upon eroded loess hills. The loess is generally well-sorted silt with minor amounts of clay and fine sand. The canals also cross areas of valley fill consisting of locally derived sediment which includes silt, sand, and minor gravel (Souders, 2000).

The surveyed section of the North Loup River (hereinafter referred to as the North Loup River site) (fig. 4) trends northwest to southeast in a broad alluvial valley flanked by deeply incised loess hills. This study site includes approximately 12 km of the North Loup River. The sediment of the riverbed is predominately sand with some components of silt and minor gravel. The source of this sediment is primarily the Sand Hills to the west and nearby loess of Holocene- to Pleistocene-age (Souders, 2000). The loess is composed predominately of well-sorted silt that may occasionally be slightly

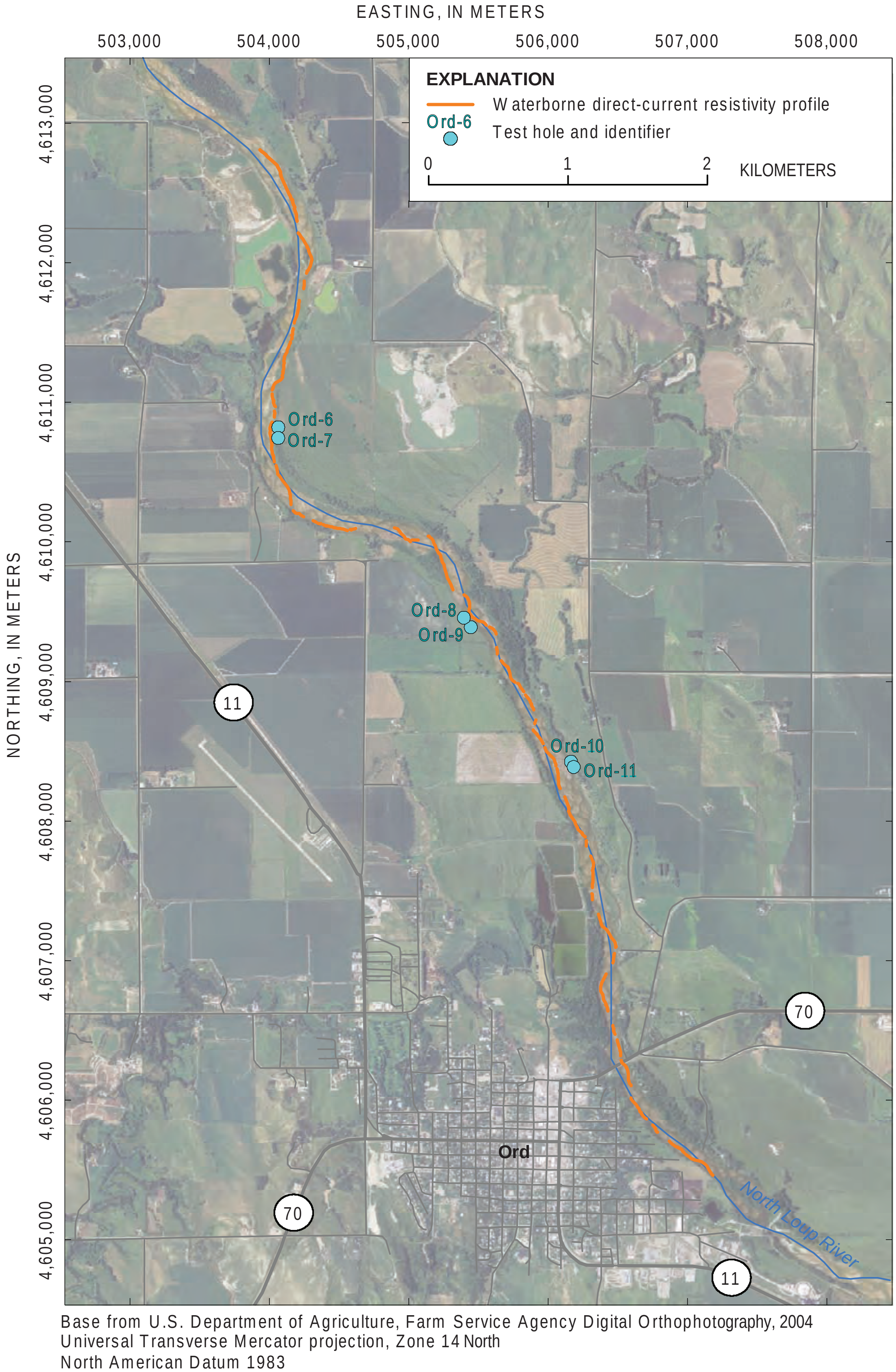

Figure 4. Location of waterborne direct-current continuous-resistivity profiles along North Loup River near Ord, Nebraska.

Figure 5. Location of waterborne direct-current continuous-resistivity profiles along Middle Loup River near Thedford, Nebraska.

clayey to sandy. Soil development has occurred on most of the terraces and flood plains.

The surveyed section of the Middle Loup River (hereinafter referred to as the Middle Loup River site) near Thedford, Nebraska, extends from about 10 km west of Thedford to its eastern, downstream terminus approximately 5 km west of Thedford (fig. 5). The surveyed section of the Middle Loup River, which is approximately 5 km in length, trends west to east in an alluvial valley flanked by sand hills. The sediment of the riverbed is predominately sand with small fractions of silt and minor gravel. The source of this sediment is primarily the surrounding Sand Hills along with other nearby deposits, which are mostly sand hills of Holocene- to Pleistocene-age (Souders, 2000). The river has incised the hills, exposing the stratification at the water edge in some locations along the surveyed section. Soil development has occurred on most of the terraces and flood plains.

Test-Hole Coring and Lithologic Descriptions

Test-hole samples were collected with a Geoprobe (Geoprobe Systems, Salina, Kansas) (fig. 6A), a hydraulically driven direct-push probe machine. The Geoprobe collected core samples in 1.2-m increments. Each 1.2-m core sample was extracted and stored in a 50.8-millimeter diameter polyethylene tube (fig. 6B). Each core was capped and labeled with sampling date, location, sampled interval, latitude, and longitude. Each test hole comprises multiple cores collected at one location.

Following core collection, a detailed lithologic description of the core samples was compiled. A 10X hand lens, Munsell soil-color chart, tape measure, and geotechnical gage were used to examine the core samples. Lithologic intervals were categorized into major grain-size divisions such as clay, silt, sand, and gravel. These were subdivided into concise descriptions including color, grain size, roundness, sorting, sedimentary characteristics, some mineralogy, and other distinctive traits. After the sample was described, a duplicate subsample was archived. The lithologic descriptions of the core samples collected are in table 1 (at end of report). Because of recovery problems, there are several instances of missing depth intervals in the core descriptions.

To aid in verifying the resistivity results, the detailed lithologic descriptions (table 1) were aggregated into eight lithologic texture categories: silty clay, clayey silt, sandy clay, sandy silt, clayey sand, silty sand, fine to medium sand, and medium to coarse sand. These categories were chosen as representative of a wide range of permeability and electrical resistivity characteristics. The depths included with each lithologic description were used to compute total thickness for each category, resulting in a measure (in meters) of the total amount of each lithology type. The relative percentage of each texture category was computed by dividing the sum of each individual category by the total sum of all categories. The percentage of each texture category determined by this procedure was plotted in a histogram chart. The texture categories were ordered from less to progressively more permeable from left to right. In previous investigations, textures with lower permeability generally had lower resistivity values (Ball and others, 2006).

Methods for Continuous Resistivity Profiling

Two CRP methods were used to measure vertical and lateral variations in the resistivity of the subsurface. Resistivities were then compared with test-hole lithology to define the correlation between electrical resistivity and relative grain size. CRP methods detect spatial changes in the electrical properties of the subsurface (Zohdy and others, 1974). The electrical properties of the subsurface lithology are determined by water content, porosity, clay content, and conductivity (reciprocal of electrical resistivity) of the pore water (Lucius and others, 2007). Typically, the resistivity of water has a large effect on the bulk resistivity of the subsurface. Two of the most commonly used CRP methods for estimating subsurface variations in resistivity are frequency-domain electromagnetic (FDEM) and direct-current (DC) resistivity.

Interpretations from CRP measurements can be used to image the distribution of physical properties of the subsurface. Comprehensive descriptions of FDEM and DC resistivity methods, as well as tables of the electrical properties of earth materials, are available in Zohdy and others (1974) and Lucius and others (2007). FDEM and DC resistivity instruments are used to measure the voltage response of the earth from a current field that is applied to the earth through electromagnetic induction or DC injection. The raw data collected by these instruments are filtered statistically to remove poor quality (noisy) data and are then used to calculate apparent resistivity of the subsurface. Apparent resistivity represents the resistivity of completely uniform (homogenous and isotropic) earth material (Keller and Frischknecht, 1966). Because the subsurface tends to contain layers of varying lithology and the apparent resistivity assumes a static one-layer scenario, a process is needed to convert the apparent resistivity values to resistivity values that are associated with multiple lithologic layers. To estimate the resistivity of nonuniform earth material, inverse modeling software is used. Inverse modeling theory is described for DC resistivity data in Loke (2000) and in Advanced Geosciences, Inc. (2008). The methods used for FDEM and DC resistivity data acquisition and processing, as well as the application of inverse modeling methods used in this investigation, are described in detail in Abraham and others (2006) and Ball and others (2006), respectively.

Frequency-Domain Electromagnetic Profiling

The FDEM method uses multiple frequencies to measure conductivities of the earth at different depths. This is achieved

Figure 6. Test-hole coring equipment used in Nebraska: (A) Geoprobe machine mounted on a utility vehicle; and (B) core sample collected at the site, stored in a polyethylene tube.

by injecting an alternating current into a transmitter (Tx) coil at a known frequency (Lucius and others, 2007). The current induces a primary magnetic field (fig. 7). The primary field creates a current in the subsurface that, in turn, induces a secondary magnetic field. The magnitude of both the primary magnetic field and the secondary magnetic field are measured using a receiver (Rx) coil. In-phase and quadrature responses are calculated from the measured magnitudes of the primary and secondary magnetic fields, respectively. These responses are then used to calculate the apparent resistivity of the subsurface. Further explanation of how apparent resistivity values are calculated from the in-phase and quadrature responses is provided by Huang and Won (2000).

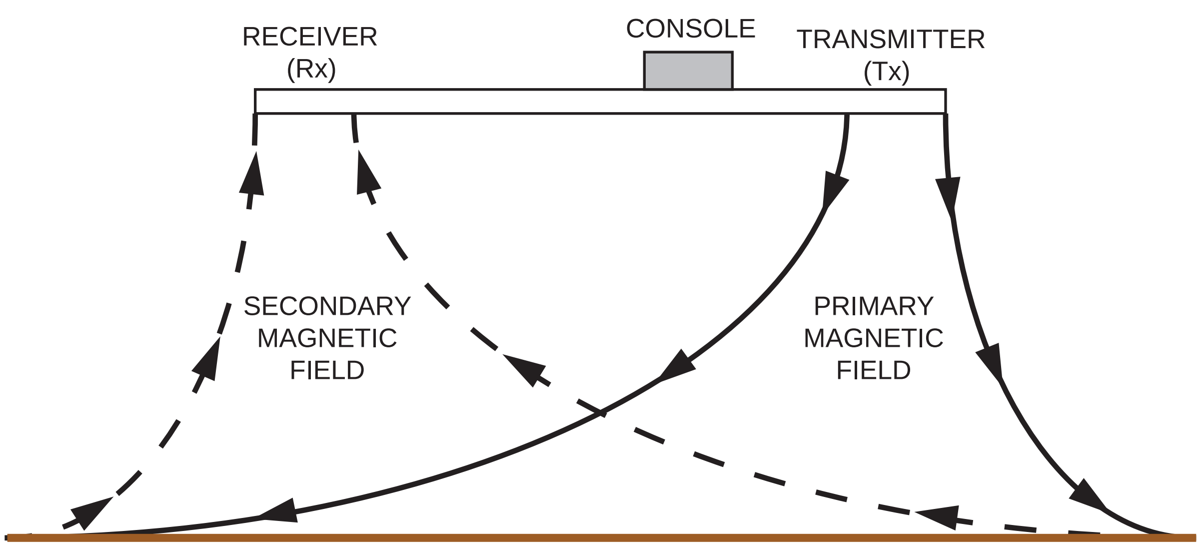

Figure 7. Schematic representation of the frequency-domain electromagnetic method.

Figure 8. GEM-2 frequency-domain electromagnetic continuous-resistivity profiling equipment used in north-central Nebraska.

The GEM-2 electromagnetic sensor (fig. 8) (Geophex Ltd., Raleigh, North Carolina) was selected for FDEM CRP on the basis of considerations of the local geology, portability, and speed of data collection. The GEM-2 is a broadband sensor that can collect multiple frequencies simultaneously. The unit has a fixed spacing (1.67 m) between the Tx and Rx coils with a bucking coil between them to remove the primary magnetic field from the Rx signal. A Trimble DSM 232 Global Positioning System (GPS) was used to georeference each frequency sounding with a spatial coordinate. The GPS device was separated from the unit by 5 m and tethered to the GEM-2 through a bluetooth wireless link. Bluetooth communication across 5 m was determined to be reliable through on-site testing. A more detailed discussion on the GEM-2 and its operations is available in Won and others (1996).

An environmental noise test, completed by recording Rx data while the transmitter was turned off, was performed to aid in the selection of Tx frequencies that did not coincide with natural or anthropogenic noise, such as frequencies associated with power lines at 60 Hertz (Hz). Following the environmental noise test, frequencies of 60; 5,490; 16,290; 27,210; 35,310; and 42,690 Hz were selected as the Tx frequencies because there was little or no noise near those frequencies. The 60-Hz frequency was collected as a quality-control band only to aid in identifying areas that may be affected by nearby power lines. Soundings were collected at the default interval of 100 milliseconds while the instrument was held approximately 1 m above land surface. The GEM-2 sensor is sensitive to all types of metal. To reduce the interference from metal, the operator wore clothing without metallic fasteners and did not carry or wear any electronic devices.

Over the course of collecting measurements with the GEM-2 unit, the instrument has the potential for drift because of (for example) battery voltage depletion or temperature variations. To allow drift correction, leveling stations (figs. 2–3) were established to compare static measurements (no operator movement) over time to a single reference measurement. Because of the extensive survey area, multiple leveling stations were required. Each successive leveling station was referenced to the first leveling station for final data correction. At the beginning of a survey line, the first leveling station was established and data were collected for 3 to 5 minutes. The operators then collected data within the canals until the battery voltage decreased by approximately 5 percent or the survey was otherwise interrupted (for example, by canal obstructions). At such a point, a second leveling station was established and occupied for 3 to 5 minutes to collect static reference data. To close the loop, the operators returned to the first leveling station and performed a final static measurement. By doing this, the second leveling station could be drift corrected using the measured drift at the first leveling station. The second leveling station was reoccupied and data collection was resumed. The process was continued with the establishment of additional leveling stations as needed. In this manner, the entire study site was referenced to the first leveling station for final drift correction. If a problem occurred with the unit, such as accidental shutdown or Tx failure, the survey was repeated only from the last-established leveling station. This

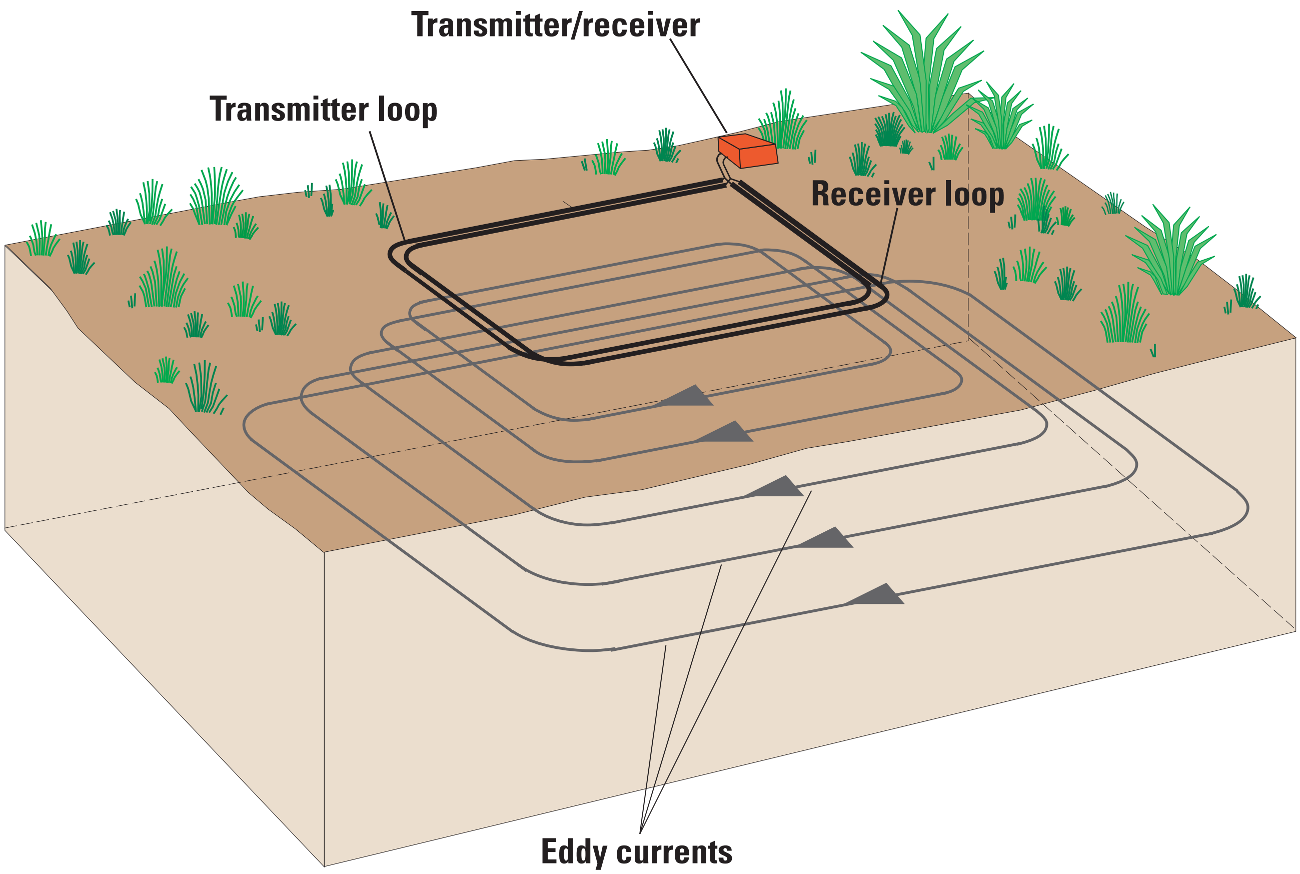

Figure 9. Coincident loop configuration for time-domain electromagnetic sounding (modified from North Carolina Division of Water Resources, 2004).

loop-closure technique was adapted from the methods discussed in Abraham and others (2006).

After collection, the in-phase and quadrature responses were drift corrected by applying linear corrections and then smoothed by using a 35-point low-pass filter. The data were smoothed because the GEM-2 collected data at 1 Hz and can be erratic in nature. The smoothing of the data removes any anomalous spikes but the overall trend of the data remains the same. The 35-point low-pass filter was used after comparison with narrower and wider filters to determine which was most effective at removing erroneous data with minimal changes to other data points. Because the GEM-2 only records relative changes in apparent resistivity, the data required calibration to reference the “true” electrical response of the earth. The “true” in-phase and quadrature response was calculated from the layered-earth resistivity model obtained from the time-domain electromagnetic (TDEM) data described in the “Time-Domain Electromagnetic Soundings” section of this report. The in-phase and quadrature values of the GEM-2 were shifted to match the in-phase and quadrature responses at the locations of TDEM soundings. Apparent resistivity values along the profile were calculated for each frequency using these calibrated in-phase and quadrature responses as described in the “Calibration of Frequency-Domain Electromagnetic Data” section of this report. The test-hole data indicated that the lithology at these sites was relatively homogeneous; therefore, inverse modeling of the FDEM data was deemed unnecessary.

Time-Domain Electromagnetic Soundings

Electromagnetic measurements are made by transmitting an alternating current into a square-loop antenna of insulated wire, or a transmitter loop, deployed on the land surface. The current consists of equal periods of time-on and time-off base frequencies (North Carolina Division of Water Resources, 2004) that produce a primary electromagnetic field in the immediate vicinity of the wire antenna. Termination of the current flow is not instantaneous but occurs over a period of a few microseconds, known as the ramp time, during which the magnetic field is time-variant. The time-variant nature of the primary electromagnetic field creates a secondary electromagnetic field in the ground beneath the antenna. This secondary field immediately begins to decay, and in the process generates additional eddy currents (fig. 9) that propagate downward

Figure 10. Time-domain electromagnetic sounding equipment used in north-central Nebraska: (A) complete unit including transmitter/receiver, current controller, and battery pack; (B) close up of terraTEM transmitter/receiver unit; and (C) close up of current controller.

and outward into the subsurface like a series of smoke rings. The secondary currents are measured by a second square-loop antenna, or a receiver loop, during the time-off period. The depth of investigation depends on the time interval after current shutoff; as the time interval lengthens, the receiver measures eddy currents at progressively greater depths. The intensity of the eddy currents at specific times and depths is determined by the combined conductivity of the subsurface lithology and pore fluid (Stewart and Gay, 1986). An apparent resistivity value can be calculated using the magnitude of the eddy current strength at specific times. Multiple TDEM measurements, or “stacks,” are averaged to obtain a final TDEM sounding.

A terraTEM (Alpha GeoScience, 2007) (fig. 10) was used to collect TDEM soundings at six TDEM sites near the FDEM data-collection sites: three along the Ainsworth Canal site (fig. 2) and three along the Mirdan and Geranium Canals site (fig. 3). A single-turn coincident antenna (equivalent Tx and Rx antenna sizes with parallel antennas separated approximately 1 m apart) was used. Because the TDEM data were used to calibrate the in-phase and quadrature response of the GEM-2 sensor, a maximum depth of investigation of 20 m was desired. A coincident square antenna with 20-m side length was used to reach a maximum depth of about 60 m. At each TDEM data-collection site, 10 replicate soundings (five with a high current setting and five with a low

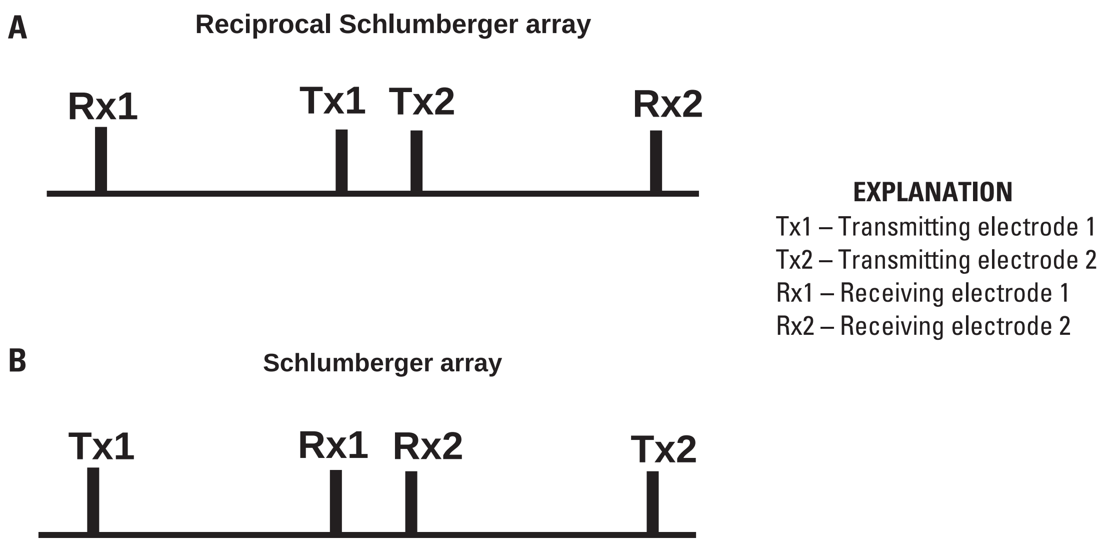

Figure 11. Direct-current transmitter and receiver electrode configurations of (A) reciprocal Schlumberger array and (B) Schlumberger array.

current setting) were collected, as well as a background-noise sounding. One thousand stacks per sounding were measured using the high-resolution sampling rate. The high-resolution sampling rate uses high temporal resolution for measuring the signal amplitude. Times and widths of the high-resolution sampling rate are listed in appendix 1.

The raw TDEM data collected for each location was filtered using the following procedure. To eliminate voltage samples with the greatest uncertainty, replicate voltage samples with a relative standard deviation exceeding 35 percent were removed from the data set. Relative standard deviation is the standard deviation of a sample divided by the sample mean, expressed as a percentage. The mean of the remaining replicate voltage samples was then calculated. Finally, any negative voltages were removed to obtain the voltages used for inverse modeling.

Calibration of Frequency-Domain Electromagnetic Data

The filtered TDEM data were imported into the inverse modeling software package IX1D, version 3.39 (Interpex Ltd., 2007). This software was used to estimate the resistivity of nonuniform earth material as layered models of (inverted) resistivity and depth. Apparent resistivity values (resistivity values that assume a homogenous and isotropic earth) were first computed from the filtered voltages and plotted as a function of time using logarithmic resistivity and time scales. Then, a smooth inverse model (a multi-layered model that holds the depth values fixed and allows the resistivities to vary during inversion) was fit to the data using Occam's inversion principle (Constable and others, 1987). Data points that substantially deviated from the smooth-model curve were removed, per the analyst's judgment, on a case-per-case basis. Finally, a layered-earth model, generally limited to 1 to 5 layers, was estimated based on the smooth inverse model. The depth and resistivity values from the final layered-earth model were used to back-calculate the in-phase and quadrature responses for the frequencies used by the GEM-2 instrument during FDEM data collection. In this manner, the relative changes in apparent resistivity measured by the GEM-2 were calibrated to the modeled (best-fit) electrical response of the earth, as indicated by the TDEM soundings. All TDEM inversion results are shown in appendix 2.

Direct-Current Resistivity Profiling

DC resistivity methods use an array of four electrodes (two Tx and two Rx) to measure electrical resistivity beneath the earth's surface. A known current is injected into the subsurface through the Tx electrodes and the resulting electrical potential is measured as a voltage change between the two Rx electrodes. Using the known current and the measured voltage values, a resistance, or the ability of the earth to transmit a current, can be calculated using Ohm's law. The apparent resistivity of the subsurface can be obtained by multiplying the resistance by a geometric factor dependent on the array geometry (Zohdy and others, 1974). By increasing the distance between electrodes, data can be collected at greater depth. A description of the DC resistivity method and tables of the electrical properties of earth materials can be found in Zohdy and others (1974), Sumner (1976), and Sharma (1997).

DC resistivity data were collected using the reciprocal Schlumberger array (fig. 11A), a modified version of the Schlumberger array (fig. 11B). The reciprocal Schlumberger array was selected because it is superior in distinguishing

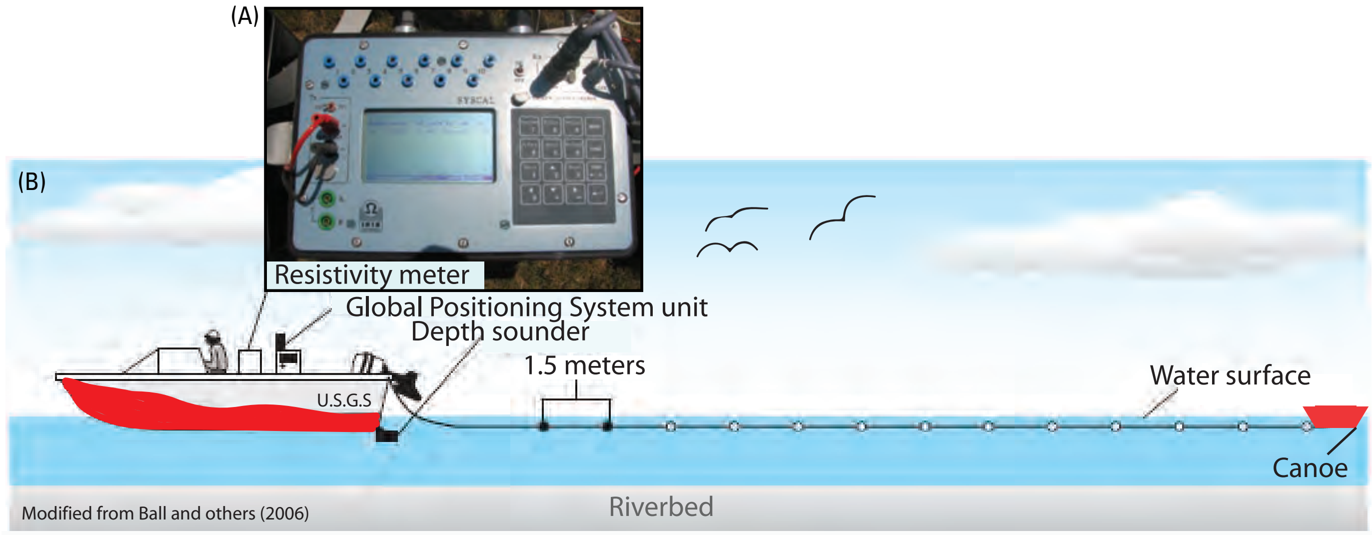

Figure 12. Waterborne direct-current continuous-resistivity-profiling method setup used in north-central Nebraska: (A) photograph of the IRIS Syscal Pro 10-channel multi-electrode direct-current resistivity meter used to collect two-dimensional direct-current resistivity data; and (B) diagram of the waterborne profiling system.

lateral from vertical variations in resistivity (U.S. Army Corps of Engineers, 1995). The reciprocal Schlumberger array was optimized to allow for the maximum number of potential pairs (channels) to be measured with a single current injection. Waterborne direct-current (WDC) resistivity data were collected along the North Loup River site (fig. 4) and Middle Loup River site (fig. 5). The following section describes the data-collection methods of the WDC surveys in further detail.

Data Collection

The IRIS Syscal Pro (IRIS Instruments, Orleans, France) 10-channel multi-electrode DC resistivity meter (fig. 12A) was used to collect resistivity data using the reciprocal Schlumberger array in a CRP configuration along the North and Middle Loup Rivers (figs. 4–5). A floating cable was deployed with 13 stainless-steel electrodes spaced at 1.5-m intervals (fig. 12B). With this method, the water serves as an electrical contact with the ground (Ball and others, 2006).

The floating cable was towed upstream by a boat at a constant speed to collect continuous data. A canoe was attached to the downstream end of the cable to help keep it as straight as possible. Because river depth during the time of collection was generally less than 0.5 m, an echo sounder would not have been an effective depth sounder and therefore not used. A Garmin (Garmin International, Inc., Olathe, Kansas) GPSmap 188 sounder was used to provide a geospatial reference for the resistivity data. The transducer was positioned at the stern of the boat and the GPS receiver was located in the center of the boat. A laptop computer running the Sysmar software package (IRIS Instruments, 2007a) was attached directly to the IRIS Syscal Pro resistivity meter to acquire the CRP data.

The raw data were imported into IRIS Instruments (IRIS Instruments, 2007b) ProsysII software. GPS offsets were applied and data were imported into Oasis montaj software (Geosoft, Inc., 2008), where georeferenced data were plotted onto National Agricultural Imagery Project (NAIP) digital photography (U.S. Department of Agriculture, 2007) to verify GPS accuracy as well as the data coverage of the study area. Unsuitable data (such as areas where the electrode cable was beached, curved, or suspended in debris) were removed, and the data were plotted for quality-assurance inspections.

Inverse Modeling

The filtered WDC data were inverted using the inverse modeling program AGI EarthImager 2D, version 2.2.6 Build 554 (Advanced Geosciences, Inc., 2008). A model consisting of multiple rectangular blocks, each assigned a centered resistivity value, was used by the program to determine electrical resistivity values for a nonuniform subsurface (Ball and others, 2006). The average value of all the apparent resistivities in the input data was selected as the starting apparent resistivity value for all model blocks. The apparent resistivity values in the model were then compared to the apparent resistivity values computed from the field measurements and a root mean-square (RMS) difference was calculated. The inverse modeling program, through numerical optimization, minimized the RMS difference by altering the resistivity values of each model block. Each optimization trial is known as “an iteration.” When the RMS difference did not decrease by more than 3 percent between iterations, a satisfactory solution condition was reached. The inverse modeling process is described in detail by Loke (2004).

Each WDC data set was inverted using the smooth model inversion setting of EarthImager. The smooth model inversion setting used gradual resistivity changes within the model to arrive at a smooth model fit. In addition, the "CRP-Freshwater" default settings of EarthImager were used to invert all WDC data. The following parameters were adjusted from the default settings: the damping factor was reduced from 100 to 10, the maximum apparent resistivity was increased from 1,000 to 10,000, and the mesh was refined to two divisions (the equivalent of a half-cell). For more information regarding the smooth model inversion and "CRP-Freshwater" settings of EarthImager, the reader is referred to Advanced Geosciences, Inc. (2008). Final inverted data sets were imported into Oasis montaj and were rejoined to their geographic coordinates.

Methods for Estimating Surface-Water/Groundwater Interaction Potential

Resistivity measurements have a direct relation to sediment grain size, a critical factor controlling hydraulic permeability. Specifically, less permeable fine-grained sediments are less electrically resistive than more permeable coarse-grained sediments (Ball and others, 2006). For this reason, the resistivity values can be used to estimate the relative potential for surface-water/groundwater interaction (hereinafter referred to as "interaction") of a stream or canal bed for use in a flow model. A variability adjustment method was used to characterize the CRP data as a one-dimensional (1D), down-line representation (distance traversed along the stream or canal bed) of the overall hydraulic behavior of the shallow subsurface. This method was chosen to be an appropriate method to represent the surface-water/groundwater interaction.

The variability adjustment method adjusts a resistivity profile based on the local heterogeneity (relative variability) of the resistivity values. Unlike inverse modeling, which calculates a resistivity value using surrounding data points and minimizes the difference between modeled and field-derived apparent resistivity values, this method uses the variability of nearby resistivity values and calculates an estimated interaction potential. Local lithologic heterogeneity can have direct bearing on water transport through the subsurface geology (Smith and Wheatcraft, 1993). Locally homogeneous, high resistivity units (fig. 13A), such as contiguous layers of sand, would tend toward greater bulk hydraulic permeabilities. Conversely, locally homogeneous, low resistivity units (fig. 13B), such as contiguous layers of clay, would tend toward lower bulk hydraulic permeabilities. However, a locally heterogeneous unit with areas of high resistivity and low resistivity (fig. 13C) has a potential for a moderate hydraulic permeability because water has the ability to flow through the more permeable areas in the immediate vicinity of less permeable areas. Thus, it was deemed appropriate to incorporate local lithologic heterogeneity into an adjustment method that uses resistivity values as a basis for estimating interaction potential and that is not biased to either a gaining or losing stream.

The coefficient of *L*-variation (*L*-CV), a measure of data dispersion, was applied to the resistivity data to quantify local lithologic heterogeneity. *L*-CV was computed as the ratio of the second *L*-moment to the mean of the data sample. *L*-moments are defined in Hosking (1990), and Asquith (2007) has summarized the mathematics and theory of *L*-moments in further detail. The *L*-CV is analogous to, but not numerically equal to, the coefficient of variation (CV, the standard deviation of a sample divided by its mean). *L*-CV provides a dimensionless measure of the relative variability of a data sample. *L*-moment statistics, among other advantages, have the benefit of greater robustness and less bias than other statistics that measure variability when sample sizes are small. These advantages were instrumental in selecting the *L*-CV over the CV or other measures of relative variability.

Both the vertical variability (changes with depth) and horizontal variability (changes with down-line distance) of the resistivity profiles were analyzed to visually evaluate the heterogeneity of the study sites. Local lithologic heterogeneity (change within a specified range of depths and down-line distances) was used to adjust the resistivity values to represent the expected permeability on the basis of variability of the profile. From these adjusted resistivity values an estimated interaction potential was calculated.

Vertical Heterogeneity

Vertical heterogeneity, an expression of variability with depth, provides information on how the geophysical properties of the subsurface lithology change from shallow to greater depths. To examine vertical heterogeneity, the inverted WDC resistivity data were partitioned into three depth zones (upper, middle, and lower) (fig. 14). The partitioning of the data into zones allowed the analysis of the heterogeneity of each zone individually along the profile, as well as visual (not computational) comparisons of relative heterogeneity among the zones. The WDC data consisted of resistivity values at 12 discrete depths ranging from 0 to 3.8 m below land surface. The 12 depths were equally partitioned into upper, middle, and lower zones. The *L*-CV for each of the zones and each down-line distance was then computed. Because each of the three zones contained four discrete depths, each down-line distance corresponded to a sample size of four data values per depth zone.

The FDEM apparent resistivity data consisted of only five sampling frequencies, corresponding to five distinct depth levels. Because the five depth levels cannot be partitioned into multiple depth zones while still retaining a meaningful sample size per zone, the five depth levels were grouped into a single depth zone. In this case, no visual comparison between different depth zones is possible.

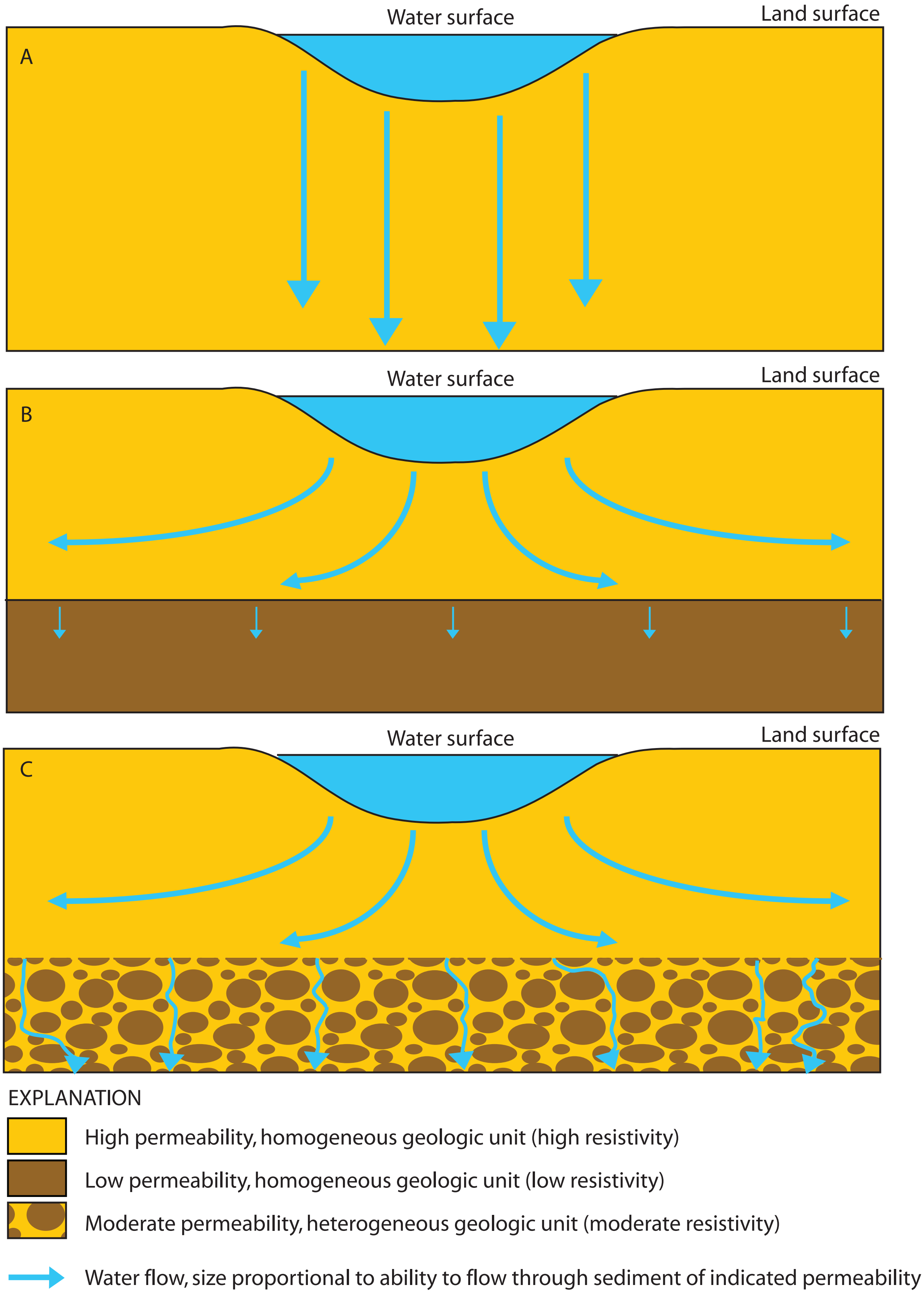

Figure 13. Conceptual model of water transport in (A) homogeneous, high permeability units, (B) homogeneous, low permeability units, and (C) heterogeneous units having low permeability sediment within higher permeability sediment.

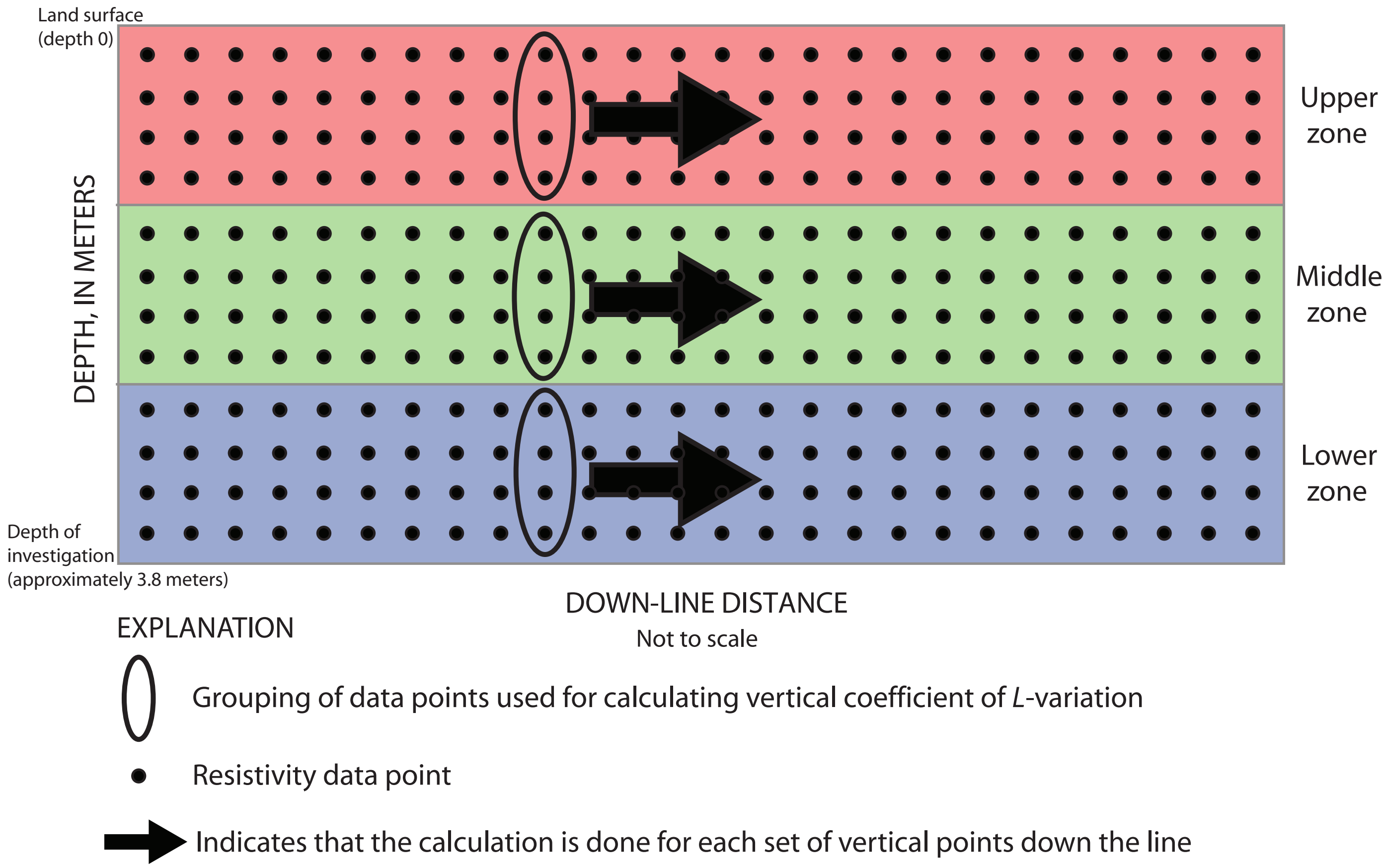

Figure 14. Schematic representation of the vertical heterogeneity analysis method.

Horizontal Heterogeneity

Horizontal heterogeneity, an expression of variability with down-line distance, provides information on how the geophysical properties of the subsurface lithology change laterally along the profile. For the inverse modeling results of the WDC resistivity data, horizontal heterogeneity was examined at depths of 0.64, 2.0, and 3.8 m (shallow, moderate, and deep) (fig. 15). These depths were chosen because they correspond to the bottom depth of each of the three depth zones listed in the "Vertical Heterogeneity" section of the report. For the FDEM apparent resistivity data, horizontal heterogeneity was examined at frequencies of 42,690; 27,210; and 5,490 Hz. For each depth or frequency, the horizontal collection of summarized data values was defined by a 5-m line length, or bin, sequentially positioned at 1-m down-line intervals. The *L*-CV statistic was calculated for each bin, resulting in a measure of the local relative variability of resistivity. This process is similar to a moving-window average, except the *L*-CV statistic was calculated instead of a mean. Although the number of data values in each bin varied because of nonuniform measurement spacing and data gaps, the *L*-CV statistic was applied to sample sizes averaging about 15 resistivity values per bin.

Heterogeneity Adjustment

The WDC and FDEM resistivity values were statistically analyzed to simultaneously assess both the vertical and horizontal local heterogeneity of the subsurface geology. A 5-m by 5-m cell centered at each data point was established to define a collection of neighboring data values above, below, and to the sides of the central value (fig. 16). The *L*-CV was calculated for this subset of points as a relative measure of the local variability of resistivity at the central data point. This procedure was repeated for each data value in the data set so that each data value had an associated dimensionless measure of local relative variability. Because of the nonuniform spacing of the measurements, the number of data points enclosed by the cell varied, but the count did not fall below 30 for any *L*-CV calculation.

After the *L*-CV was determined for each data value within the data set, the resistivity was adjusted to a value that is representative of the effective permeability relative to the local heterogeneity. *L*-CV is proportionally related to the local lithologic heterogeneity. Consequently, minimally heterogeneous areas have smaller *L*-CV values than highly heterogeneous areas. Additionally, it was assumed that greater heterogeneity results in either: (1) proportionally

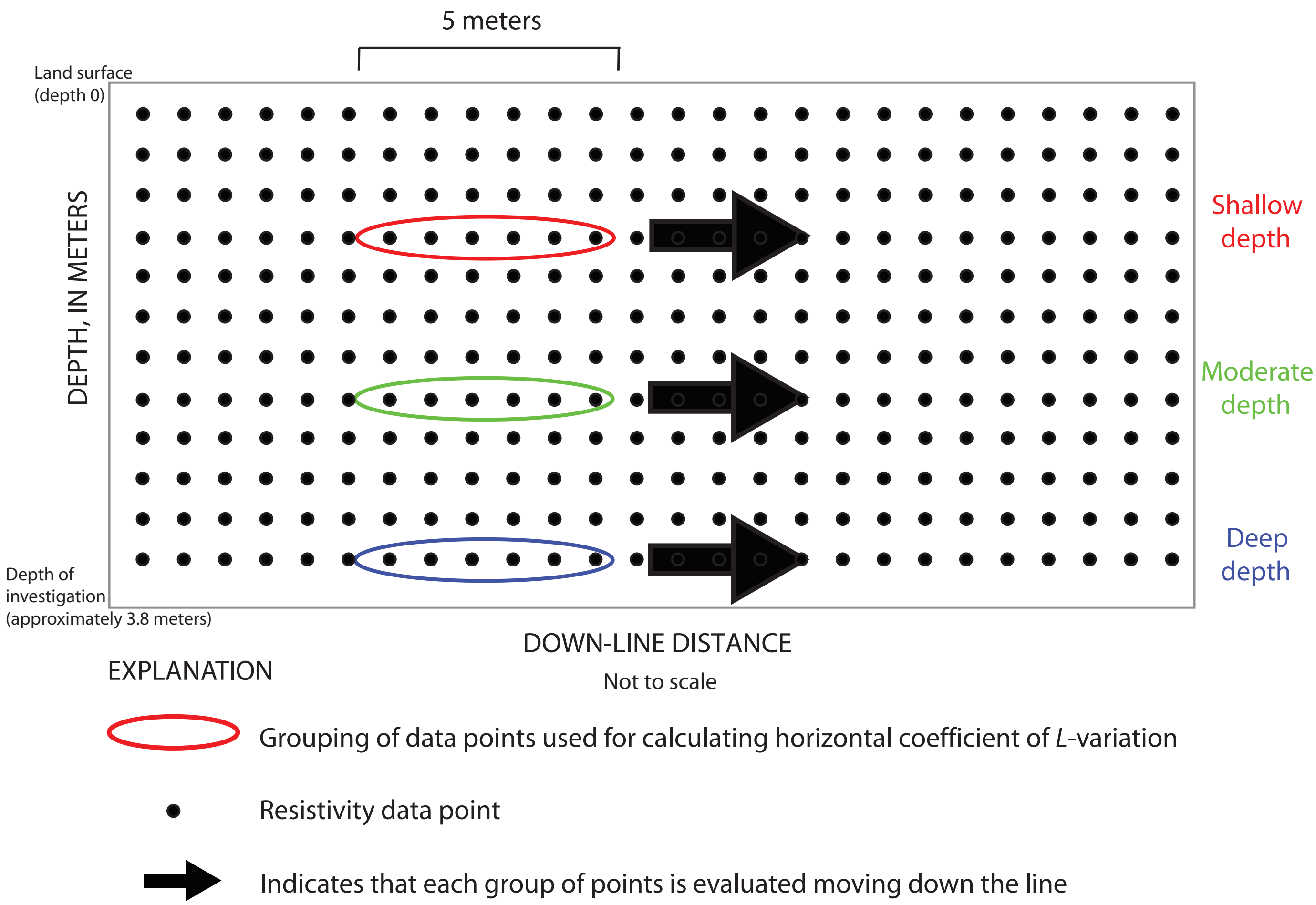

Figure 15. Schematic representation of the horizontal heterogeneity analysis method.

higher effective hydraulic permeability if the surrounding region is, on average, more permeable (greater average electrical resistivity) than the central point, or (2) proportionally lower effective hydraulic permeability if the surrounding region is, on average, less permeable (less average electrical resistivity) than the central point. For example, a low-resistivity data point within a heterogeneous, electrically resistive unit would have a proportionally higher effective permeability, and a high-resistivity data point within a heterogeneous, electrically conductive unit would have a proportionally lower effective permeability. Thus, it is reasonable to use the *L*-CV values as a basis for adjusting the resistivity values to better represent the hydrologic effects of lithologic heterogeneity.

To accommodate both increases and decreases in hydraulic permeability, the *L*-CV values were linearly transformed (rescaled and translated) to a relative-change scale. Linear transformation preserves the relational characteristics of a data set while changing its upper and lower bounds (Friedberg and others, 1997). For the lowest *L*-CV value in a data set (corresponding to the most homogenous area), the potential for increases or decreases of hydraulic permeability related to lithologic heterogeneity is least. Thus, the lower bound of the transformed data was set to 0, resulting in zero change to the resistivity value. An upper bound of 0.5 was chosen to allow a maximum adjustment of 50 percent for the most heterogeneous region. Although further investigation of the chosen maximum value might determine the optimum adjustment value, that was outside the scope of this report. Applying these lower and upper bounds restricted the potential effects of the heterogeneity adjustment to within reasonable limits. A relative increase was applied to values where the surrounding locality was, on average, higher in resistivity than the central resistivity value; a relative decrease was applied to values where the surrounding locality was, on average, lower in resistivity than the central resistivity value.

To obtain a 1D estimate of interaction potential along the streambed, the minimum of the adjusted resistivity values for each vertical column of points at each down-line distance along the profile was computed. The minimum was selected because hydraulic permeability is most affected by the least permeable (hence least electrically resistive) unit in the subsurface (Smith and Wheatcraft, 1993). For example, an area containing a confining unit of clay will result in low

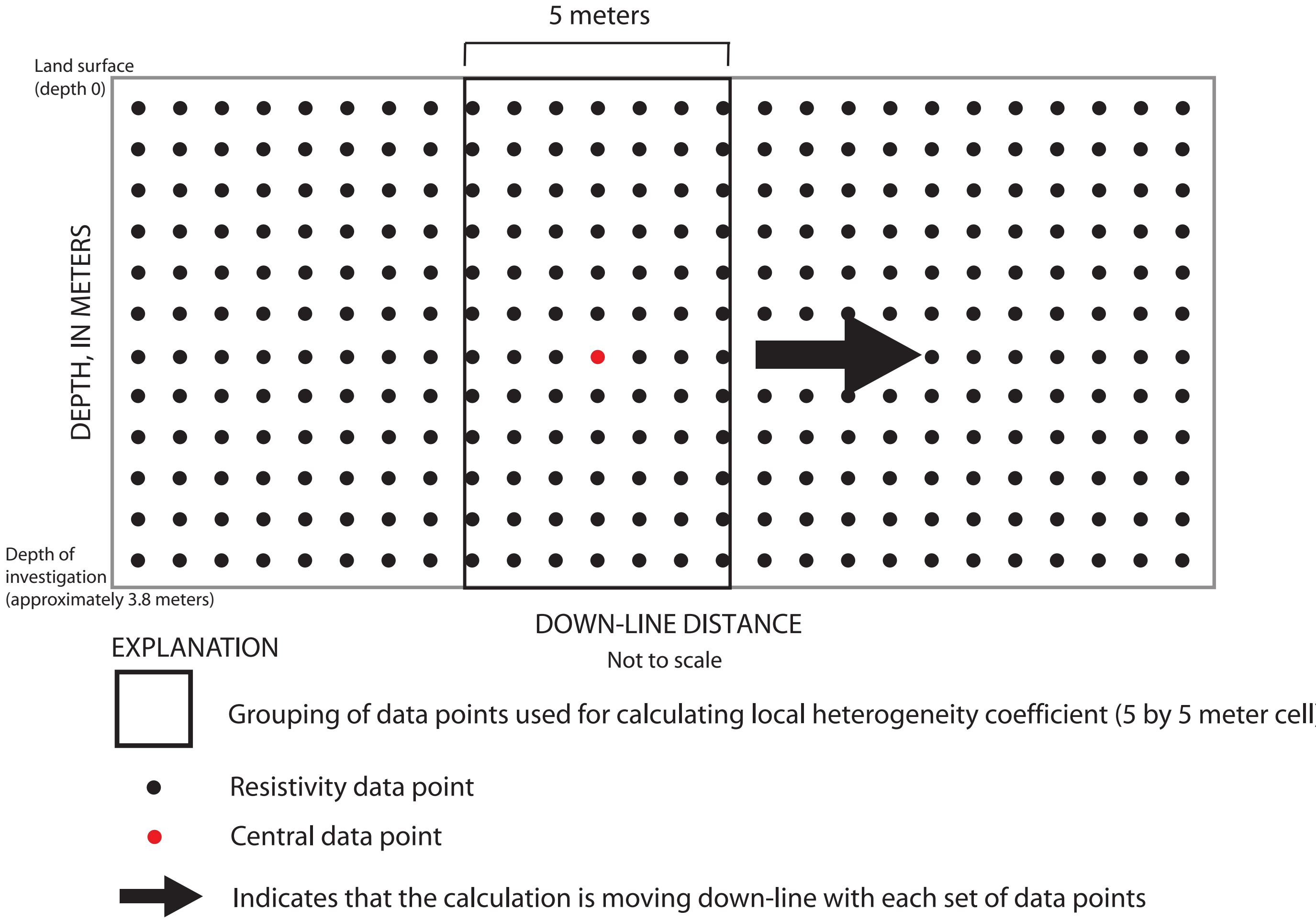

Figure 16. Schematic representation of the local heterogeneity analysis method.

overall interaction potential for that area regardless of the permeability of the overlying and underlying material. In this manner, impermeable subsurface units, when present, tend to govern the 1D representation of the two-dimensional (2D) profile.

The minimum adjusted resistivity values retain units of ohm-meters. As a final step, dimensionless estimates of interaction potential were obtained by dividing each minimum of the adjusted resistivity values by the greatest minimum adjusted resistivity value from all four sites. This normalized the estimates by bounding them between 0 and 1 and scaled relative interaction potential for comparability with other sites in this study.

Data from the FDEM collection method have resistivity values associated with sampling frequency (Hertz). The frequencies correspond to distinct depth levels, with higher frequencies corresponding to shallower depths and lower frequencies corresponding to deeper depths. Because of this, the FDEM data can also be analyzed using the same heterogeneity adjustment procedure as outlined above. Although inverse modeling techniques are available that adjust for frequency-depth relations, this was deemed unnecessary because the apparent resistivity data closely resembled the test-hole data at the sites where FDEM data were collected.

Apparent Resistivity and Estimated Interaction Potential of Surface Water and Groundwater

The apparent resistivities from the FDEM profiles collected at the Ainsworth Canal site and the Mirdan and Geranium Canal site are described in this section as well as the inverse modeling results from the WDC resistivity profiles collected at the North Loup River and Middle Loup River sites. The estimated interaction potential along the respective canals and streambeds also is presented. Discussion of the resistivity data, and the vertical and horizontal heterogeneity of resistivity is provided. Estimated surface-water/groundwater interaction potential is described within the context of the test-hole lithologies at each site. Because the data-collection path spanned large distances, the horizontal heterogeneity, vertical heterogeneity, and interaction potential charts were divided and presented on three consecutive figure pages to enhance clarity. The vertical axes were adjusted to a common range for all sites to facilitate comparison.

Ainsworth Canal

The Ainsworth Canal site is generally electrically conductive throughout, with apparent FDEM resistivities of the shallow subsurface ranging from about 22 to 71 ohm-m. A histogram of the apparent resistivity is presented with summary statistics in figure 17A, depicting a relatively narrow distribution with the majority of the values between 22 to 42 ohm-m. Similarly, the interquartile range (containing 50 percent of the data) extends between 30 and 36 ohm-m, a change of only 6 ohm-m; 75 percent of the resistivities were between 22 and 36 ohm-m, a change of only 14 ohm-m. Lithologic descriptions of the Ainsworth test holes (Ainsworth-1 and Ainsworth-2, fig. 2) are in table 1. The distribution of different lithology textures is shown as the relative percentage for each category (fig. 17B). The lithologic categories are ordered from less to progressively more permeable from left to right in figure 17B. Sediments at the Ainsworth Canal test holes are predominantly fine-to-medium sand, with some clay and silt. Although large percentages (totaling about 60 percent) of fine to medium sand and medium to coarse sand are present, the descriptions for these test holes indicate that the majority of these lithology textures are at depths greater than 3.8 m, which is below the range of the CRP investigation. Therefore, a correlation between these lithology textures and the resistivity data collected for this site was not expected.

Apparent resistivity results for each frequency collected using the GEM-2 FDEM profiler are shown in figure 18. There is an approximately 2-km gap in the FDEM data between TDEM soundings Ainsworth-2 and -3 along the profile because of transmission problems that occurred with the GEM-2 unit. Each sampled frequency ranging from 42,690 to 5,490 Hz is depicted as a parallel trace of the collection path. Because sampling frequency correlates to depth below land surface (higher to lower frequencies correspond to shallower to deeper depths, respectively), each trace depicts resistivity at progressively increasing depth. Resistivity shows little variance with depth. The highest resistivities (50 ohm-m and above) are located at the west end of the profile near the town of Ainsworth. Resistivity decreased towards the east (beyond the gap) starting near TDEM sounding Ainsworth-2, where resistivity values ranged typically between 20 to 40 ohm-m.

Results of the vertical heterogeneity analysis are shown in figure 19A. The data profile spanned about 8.6 km. The vertical heterogeneity of the apparent resistivity data is generally low, bounded above by an *L*-CV (dimensionless) of about 0.05. This indicates small lithologic variability with depth for this site, as is also seen in the resistivity profile (fig. 18). The data for the nearby test-hole indicate that there is little vertical variability, with the near-surface sediment composed of mainly fine-grained silt and clay with lithologic texture becoming slightly coarser with depth.

Results of the horizontal heterogeneity analysis are shown in figure 19B. The horizontal heterogeneity analysis was performed on frequencies of 42,690; 27,210; and 5,490 Hz as representing shallow, moderate, and deep depths, respectively. The horizontal heterogeneity of the apparent resistivity data is generally low, bounded above by an *L*-CV (dimensionless) of about 0.02. This suggests that local horizontal lithologic variability for this site is small. The abrupt change in resistivity between TDEM soundings Ainsworth-1 and Ainsworth-2 is not shown in figure 19B because the large discontinuity (gap) in the data exceeds the 5-m local-binning width of the analysis. The small horizontal variability of the resistivity data is consistent with the resistivity profiles shown in figure 18, which show gradual changes in resistivity along the canal at all depths (except across the large data gap).

Interaction potential (dimensionless) estimated by application of the heterogeneity-adjustment method on the resistivity profile is shown in figure 19C. Estimated interaction potential is consistently low along the entire profile, ranging from about 0.01 to 0.025. Uniformly low interaction potential is consistent with low apparent resistivities and the narrow apparent-resistivity distribution (fig. 17A), as well as with the lithologic distribution (fig 17B). The apparent-resistivity interquartile range of 6 ohm-m further indicates the relatively uniform nature of the lithology. Overall, the interaction potential at the Ainsworth Canal site is estimated to be low relative to the other three sites. A color-scaled map of the estimated interaction potential is presented in figure 20.

Mirdan and Geranium Canal

The Mirdan and Geranium Canal site is generally electrically conductive throughout, with apparent FDEM resistivities of the shallow subsurface ranging from about 2 to 120 ohm-m. A histogram of the apparent resistivity is presented with summary statistics in figure 21A, depicting a relatively narrow distribution with the majority of the values between about 14 to 30 ohm-m. Lithologic descriptions of the test holes for this site are in table 1. The percentages by texture category for the combined Mirdan and Geranium Canal test holes (Ord-1, Ord-2, Ord-3, Ord-4, and Ord-5) are graphed in figure 21B. Lithologic textures are almost entirely silt and clay (about 95 percent), consistent with the low, narrowly distributed electrical resistivities (fig. 21A).

Apparent resistivity results for each frequency collected using the GEM-2 FDEM profiler are shown in figure 22. Large gaps are present in the data approximately between TDEM soundings Ord-1 and Ord-2 (about 5 km in length) and between test holes Ord-4 and Ord-5 (about 7 km in length). The data gap between TDEM soundings Ord-1 and Ord-2 was caused by instrument transmission problems, whereas the data gap between test holes Ord-4 and Ord-5 corresponds to a lake. Each sampled frequency is depicted as a parallel

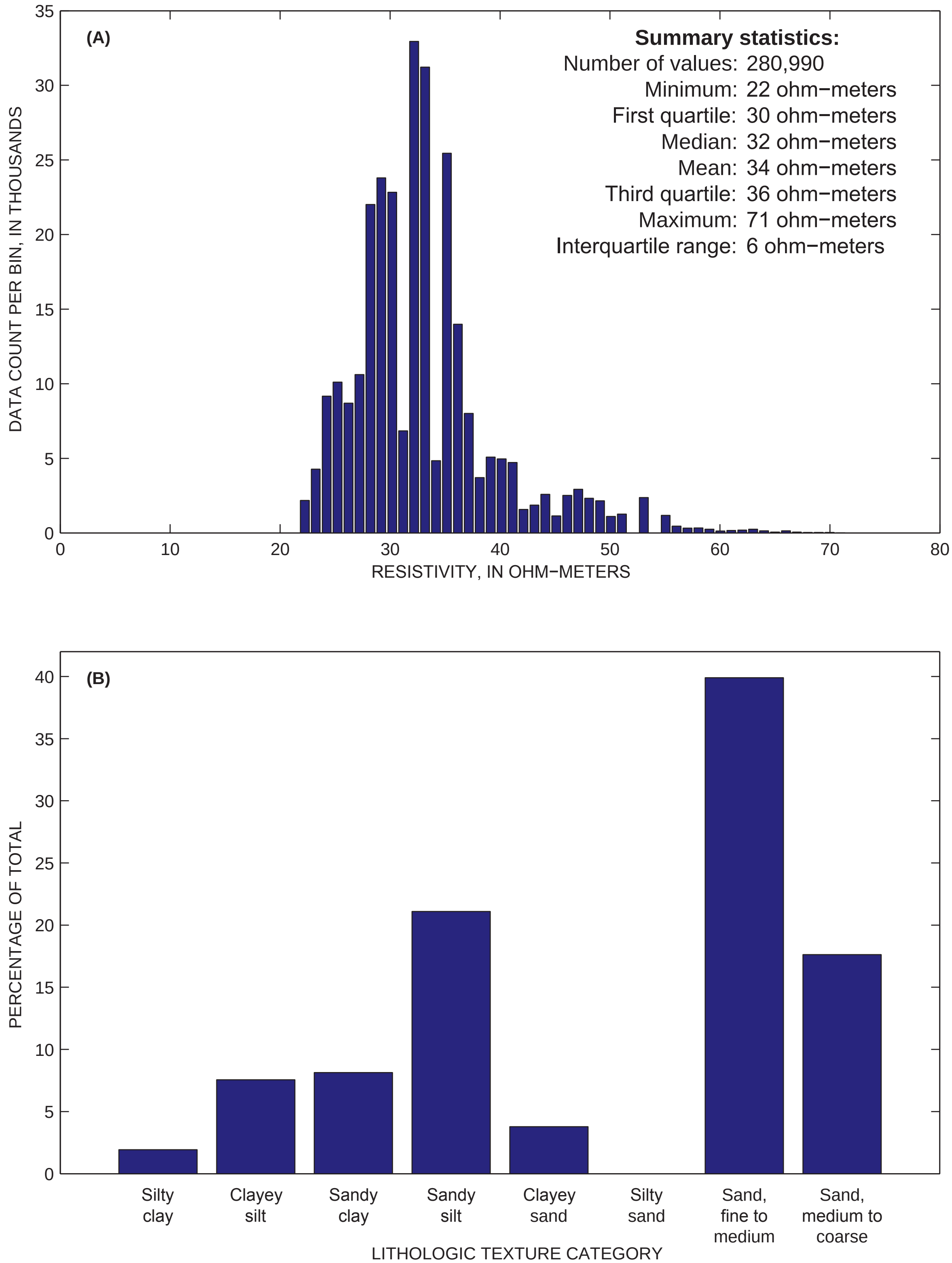

Figure 17. (A) Histogram with summary statistics for resistivity results for frequency-domain electromagnetic profiles; and (B) distribution of lithologic texture categories found at test holes Ainsworth-1 and Ainsworth-2 along Ainsworth Canal near Ainsworth, Nebraska, 2006–07.

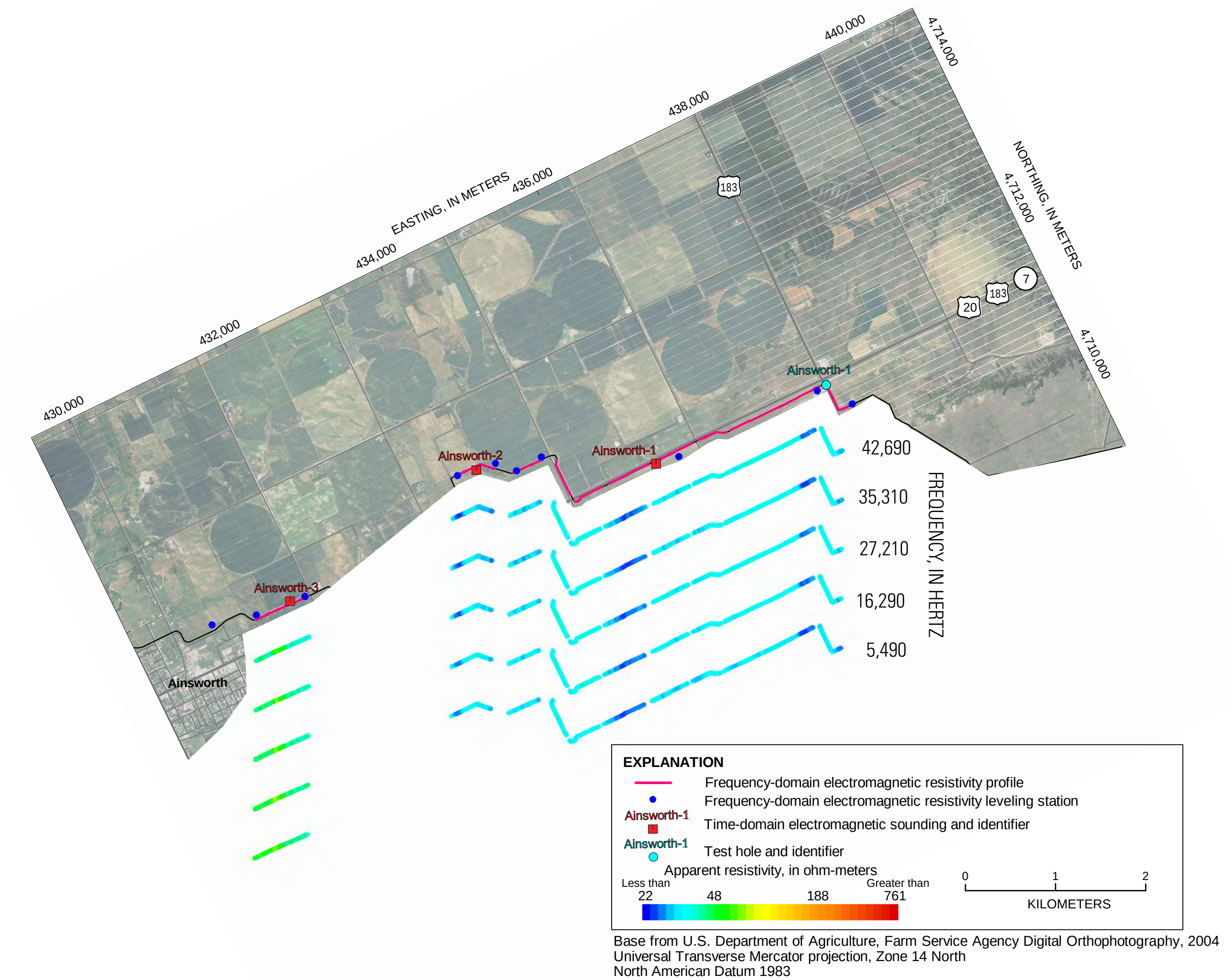

Figure 18. Apparent resistivity results for each frequency collected using the GEM-2 frequency-domain electromagnetic profiler along Ainsworth Canal near Ainsworth, Nebraska, 2006–07.

trace of the profile, with higher to lower frequencies corresponding to shallower to deeper depths, respectively. Slight variance with depth was observed, particularly in the more resistive areas. As shown in figure 22, the highest resistivities (above 50 ohm-m) are located towards the northwest end of the profile, near TDEM sounding Ord-2. Resistivities for the remainder of the profile generally range between 14 and 30 ohm-m.

Results of the vertical heterogeneity analysis are shown in figure 23A. For the first 5 km and last 40 km of the profile, the vertical heterogeneity of the apparent resistivity is low, similar to that for the Ainsworth Canal, with *L*-CV (dimensionless) less than 0.05. This indicates small lithologic variability with depth, consistent with the generally uniform resistivity across frequencies in the resistivity profiles (fig. 22) in these areas. Slightly higher *L*-CV from about 10 to 30 km along the profile indicates greater lithologic vertical variability for this 20-km stretch of the canal. As shown in the resistivity profile (fig. 22), the greatest resistivities occur within this 20-km stretch, with peak values nearer the surface. The higher surface resistivity contributes to the greater vertical variability in this area.

Results of the horizontal heterogeneity analysis are shown in figure 23B. The horizontal heterogeneity analysis was performed on frequencies of 42,690; 27,210; and 5,490 Hz as representing shallow, moderate, and deep depths, respectively. Generally, the horizontal heterogeneity of the apparent resistivity is moderately higher than that for the Ainsworth Canal site, bounded above by an *L*-CV (dimensionless) of about 0.05, with occasional peak *L*-CV exceeding 0.05. This indicates low horizontal lithologic heterogeneity on a local scale (5 m). The high percentages of

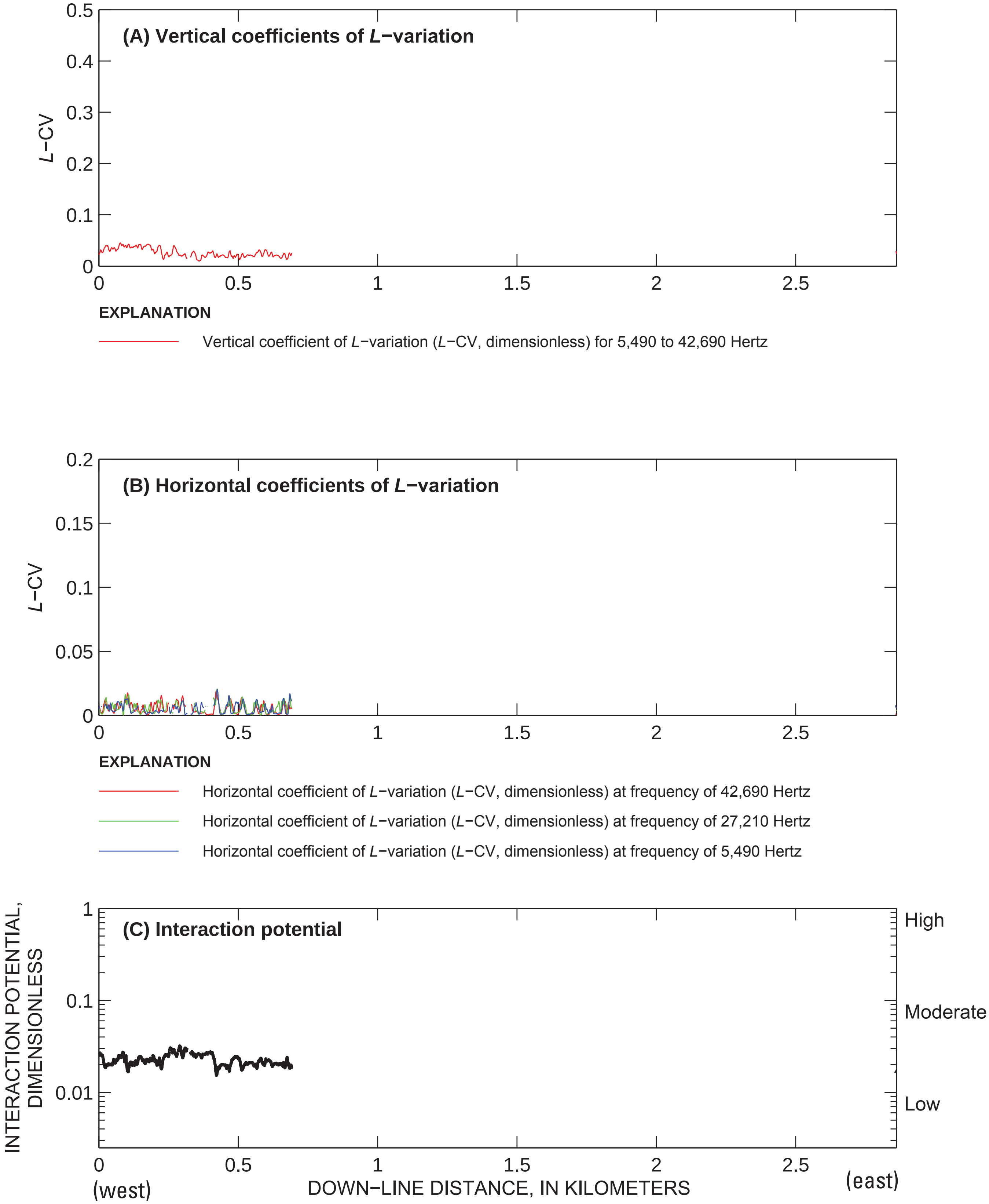

Figure 19. (A) Vertical heterogeneity results, (B) horizontal heterogeneity results, and (C) interaction potential estimated from resistivity data collected along Ainsworth Canal near Ainsworth, Nebraska, 2006–07.

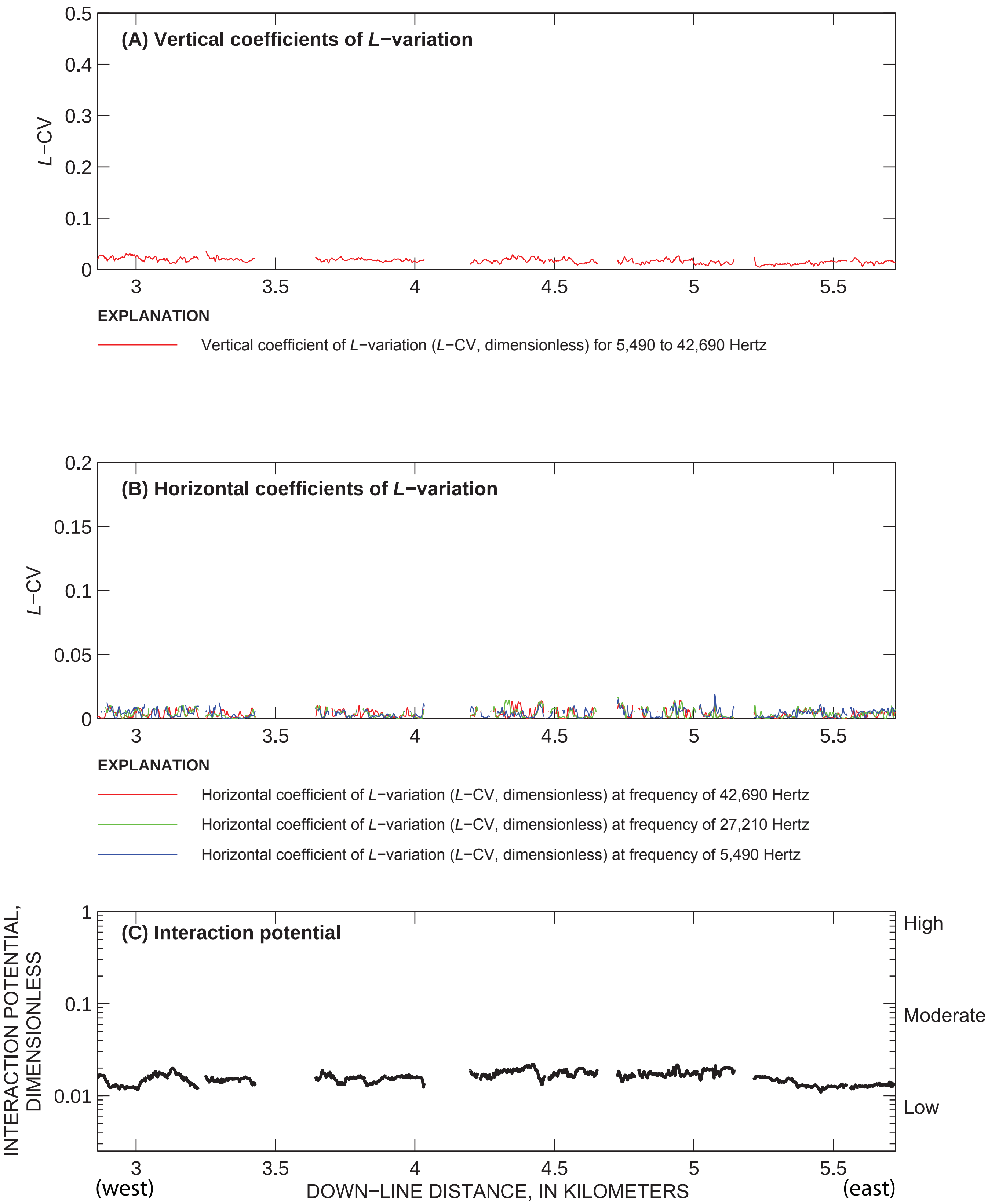

Figure 19.—Continued.

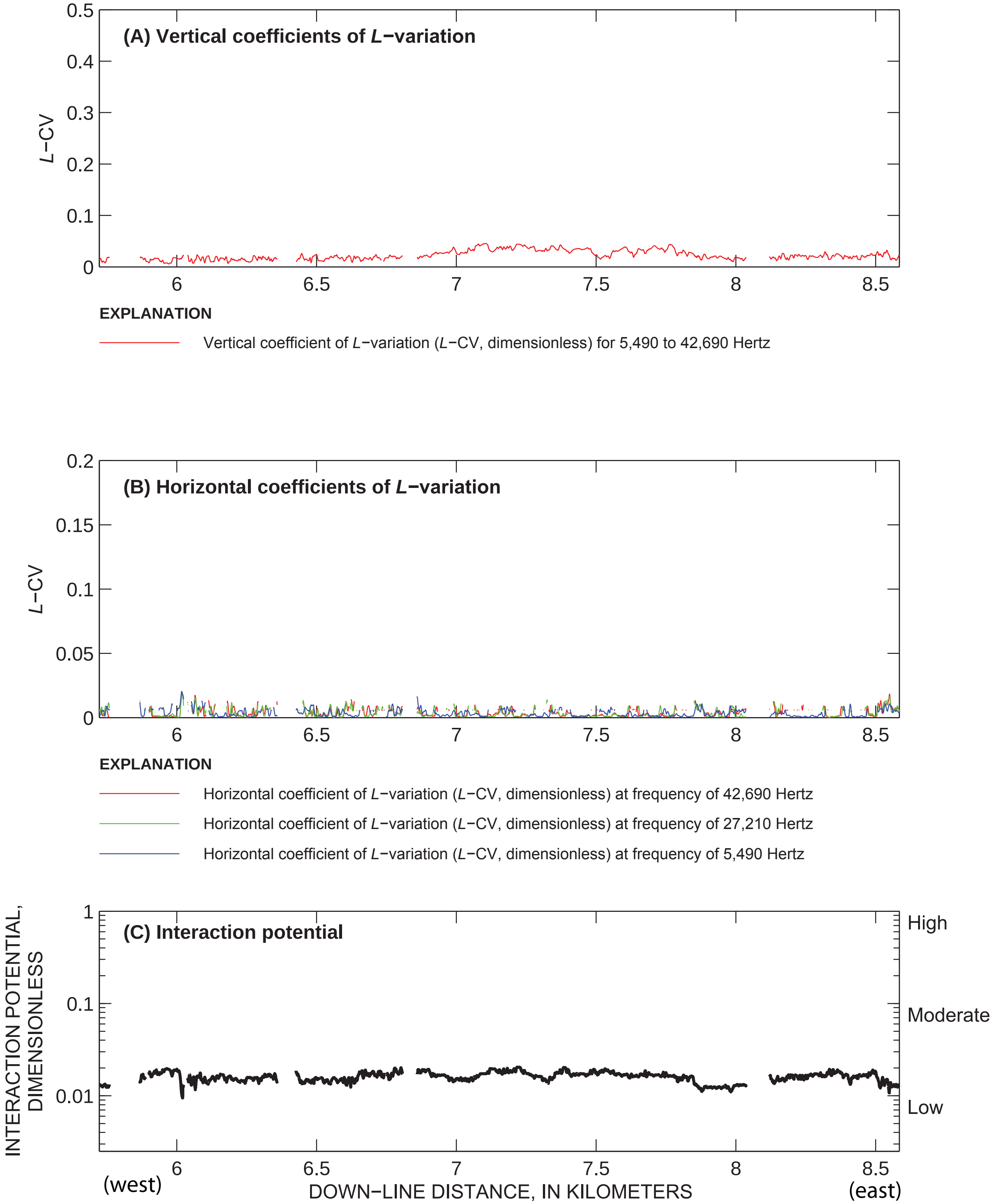

Figure 19.—Continued.

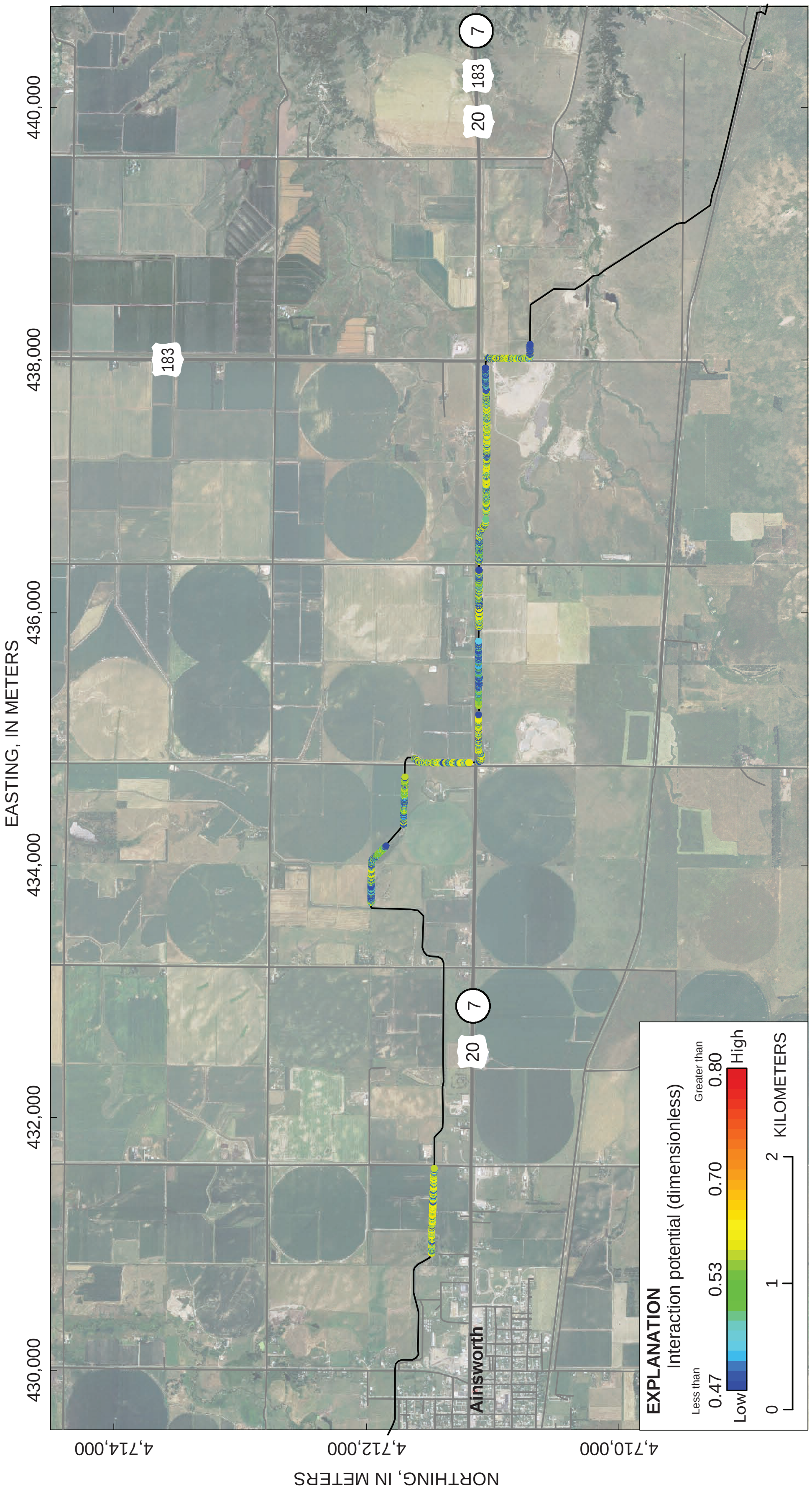

Base from U.S. Department of Agriculture, Farm Service Agency Digital Orthophotography, 2004
Universal Transverse Mercator projection, Zone 14 North
North American Datum 1983

Figure 20. Interaction potential estimates along Ainsworth Canal near Ainsworth, Nebraska.

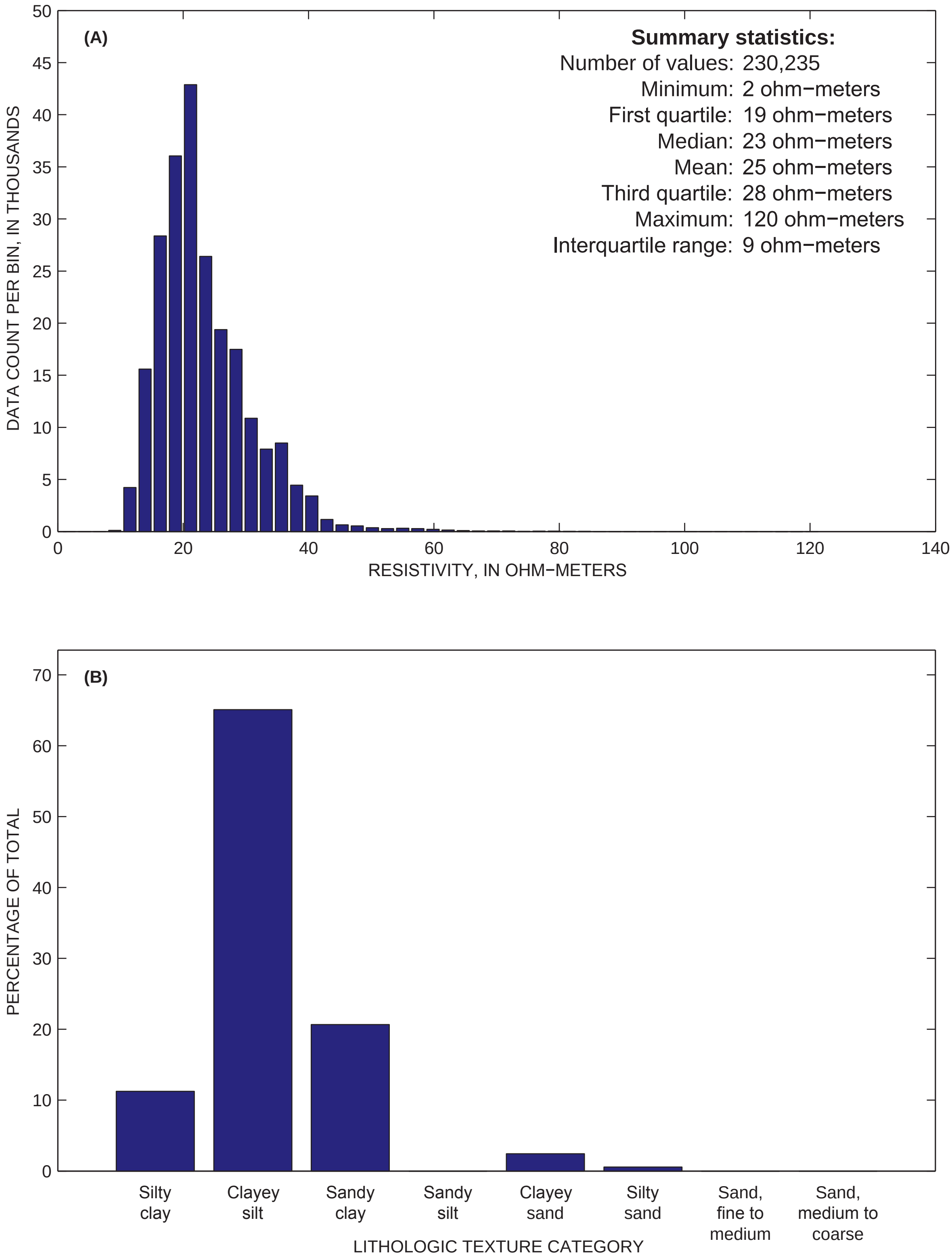

Figure 21. (A) Histogram with summary statistics for resistivity results for frequency-domain electromagnetic profiles; and (B) distribution of lithologic texture categories found at test holes Ord-1, Ord-2, Ord-3, Ord-4, and Ord-5 along Mirdan and Geranium Canals near Ord, Nebraska, 2006–07.

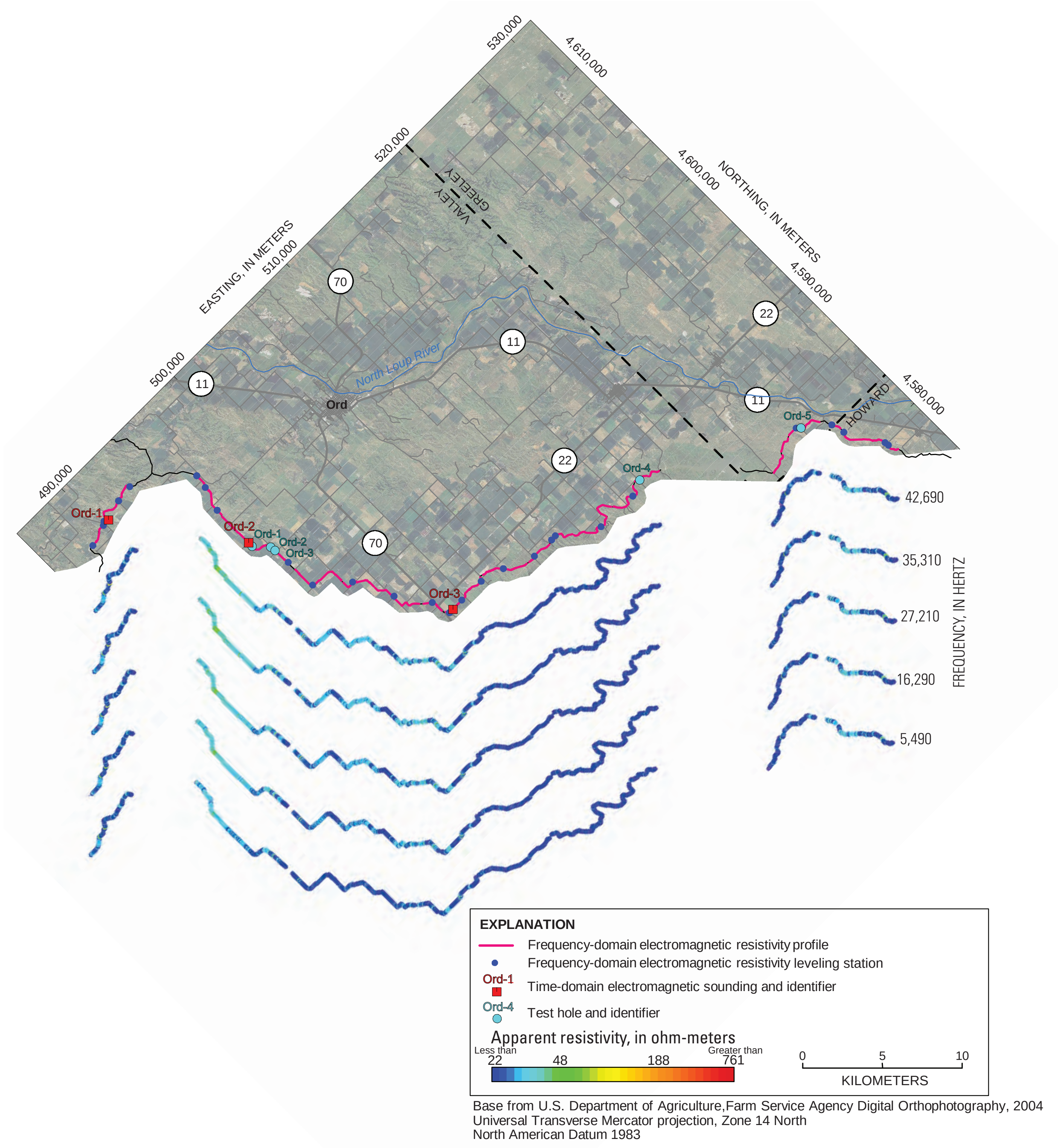

Figure 22. Apparent resistivity results for each frequency collected using the GEM-2 frequency-domain electromagnetic profiler along Mirdan and Geranium Canals near Ord, Nebraska, 2006–07.

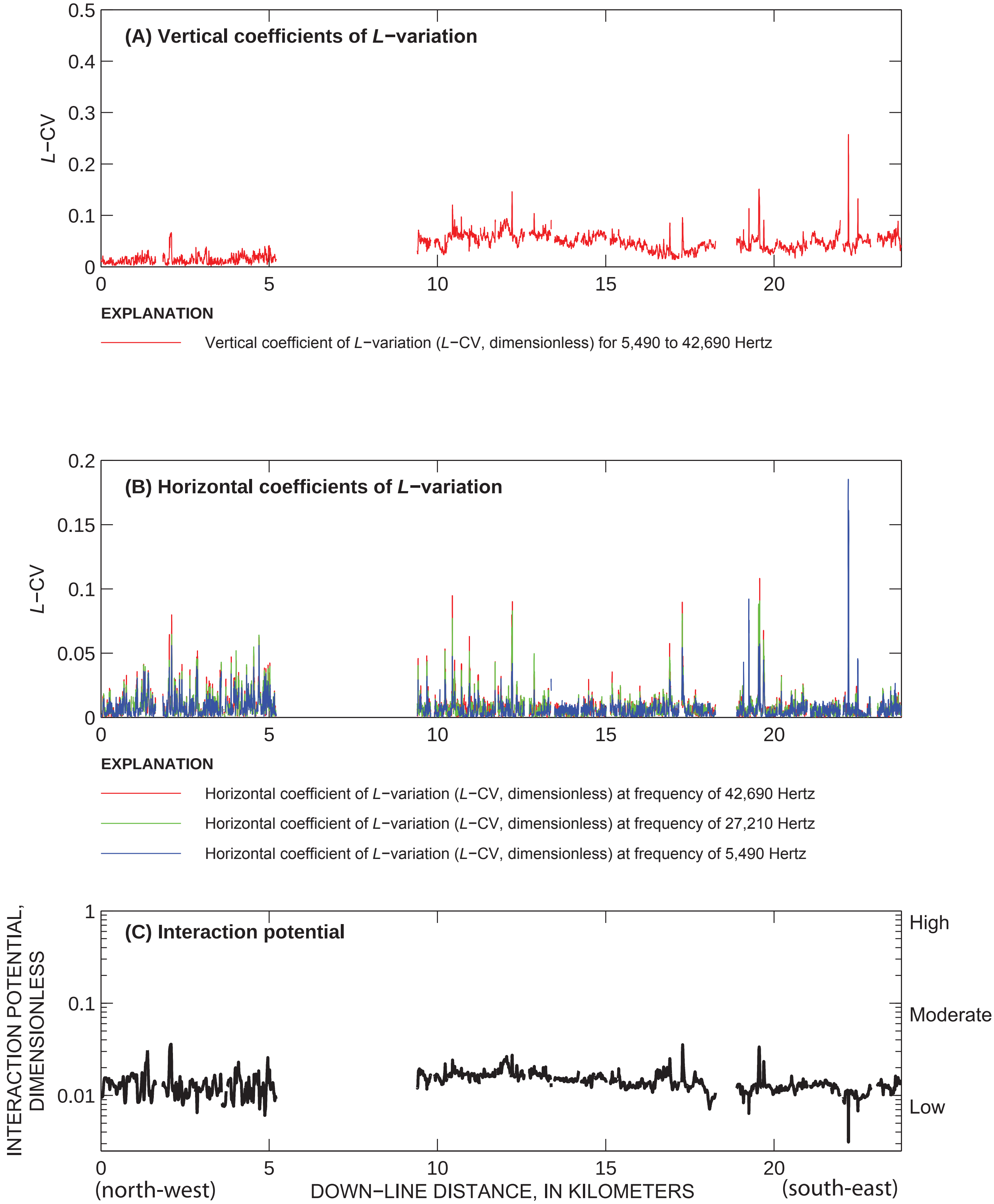

Figure 23. (A) Vertical heterogeneity results, (B) horizontal heterogeneity results, and (C) interaction potential estimated from resistivity data collected along Mirdan and Geranium Canals near Ord, Nebraska, 2006–07.

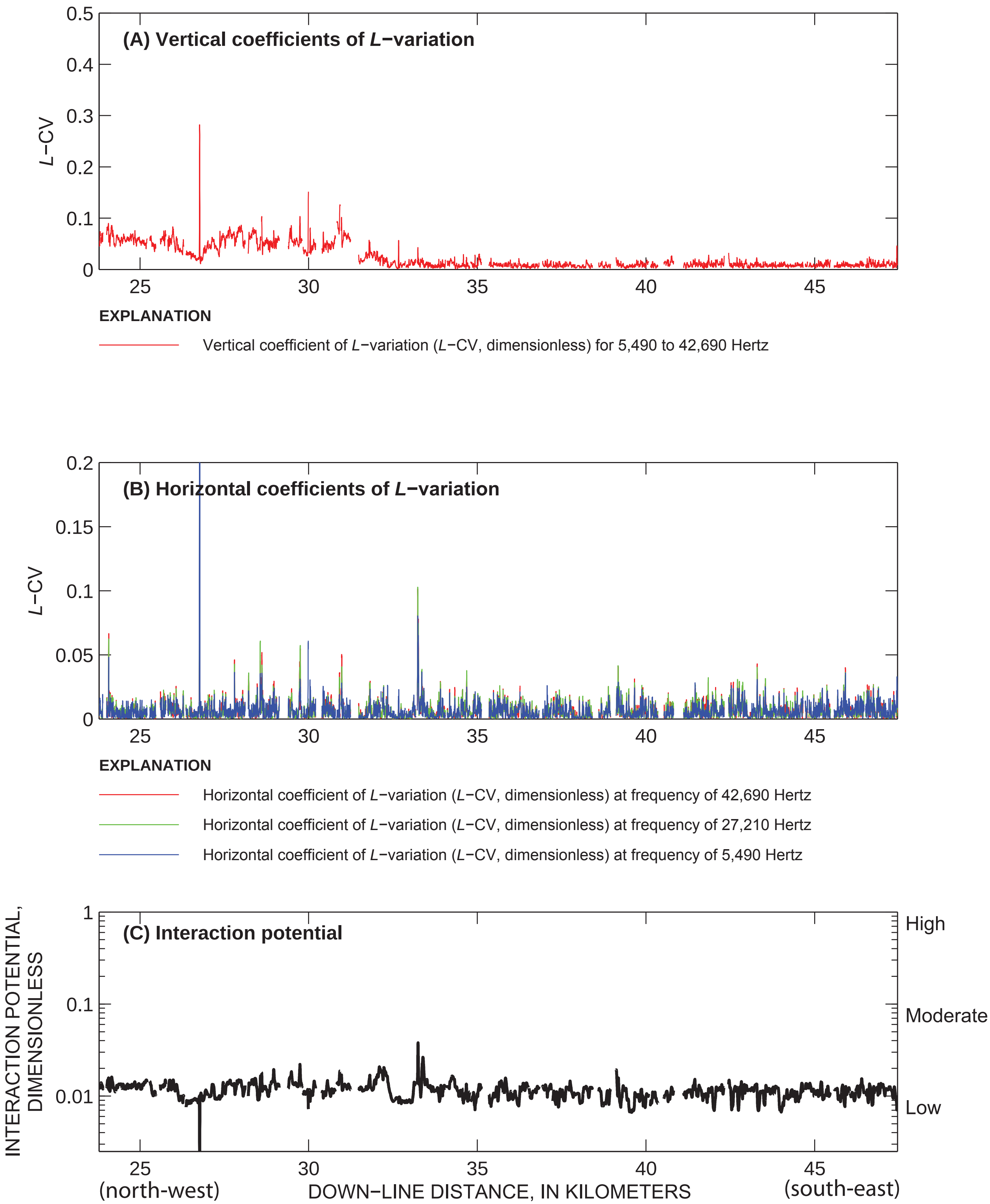

Figure 23.—Continued.

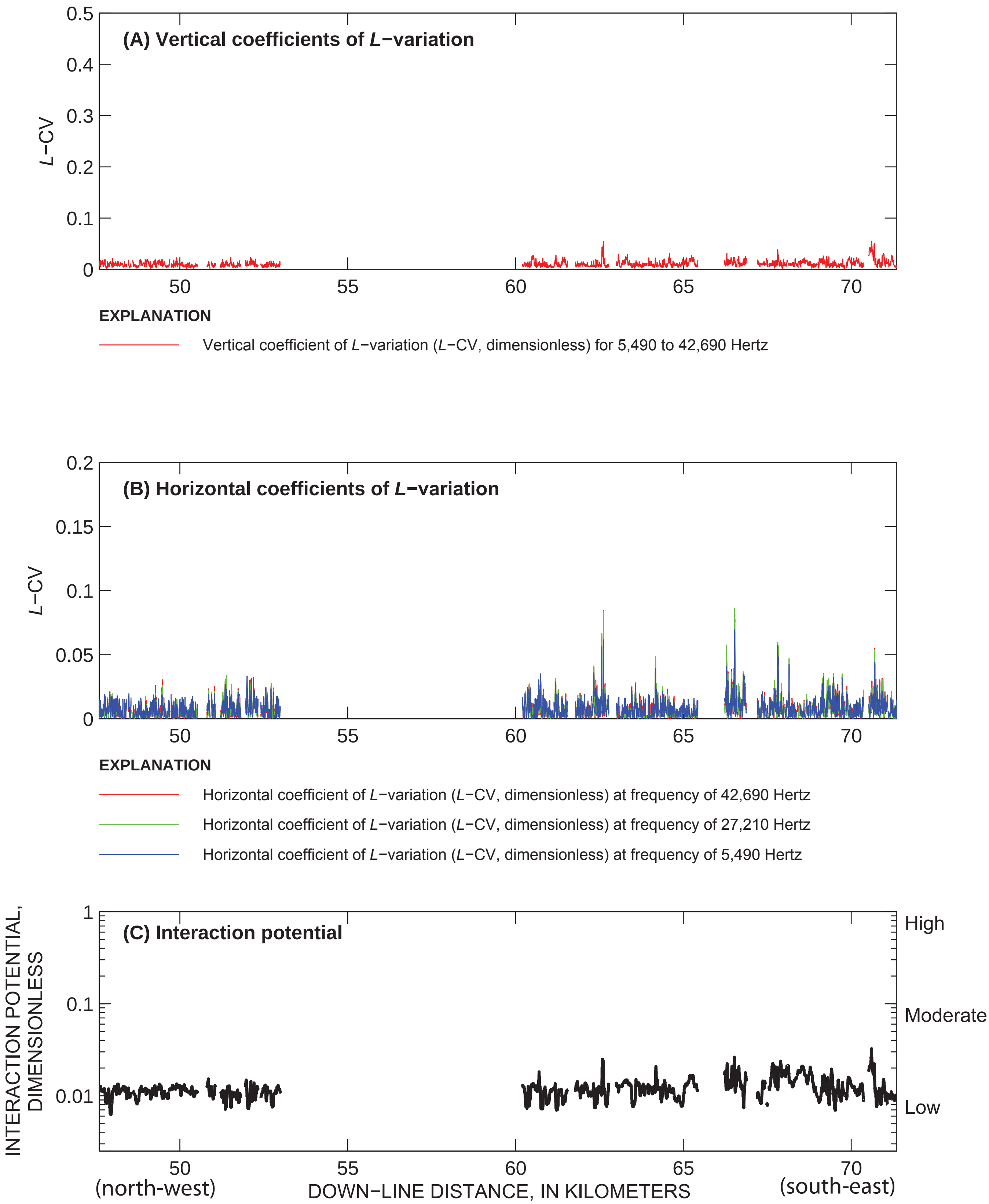

Figure 23.—Continued.

clay and silt textures in sediment samples collected from the test holes (fig. 21B) support a relatively uniform lithologic characterization.

Estimated interaction potential is low to slightly moderate along the profile, ranging from about 0.006 to 0.033 (fig. 23C). Greater fluctuations in interaction potential were observed along this profile than along the profile for the Ainsworth Canal site. This can be attributed to the slightly greater heterogeneity of the near-surface lithology, in both the vertical (fig. 23A) and horizontal (fig. 23B) directions. Overall, the interaction potential at the Mirdan and Geranium Canal site is estimated to be low to slightly moderate, which is consistent with the high percentages of clay and silt textures of the test holes. A color-scaled map of the estimated interaction potential for the Mirdan and Geranium Canal site, as well as the interaction potential estimates for the North Loup River site, is presented in the “North Loup River” section of this report.

North Loup River

The North Loup River site is electrically conductive to moderately resistive, with WDC resistivities of the shallow subsurface ranging from 34 to 633 ohm-m. Both the histogram of the resistivity distribution and the associated summary statistics depict a broader distribution than for either the Ainsworth Canal site or the Mirdan and Geranium Canal site (fig. 24A). Lithologic descriptions of the test holes for this site (Ord-6, Ord-7, Ord-8, Ord-9, Ord-10, and Ord-11) are in table 1. Coarser-grained deposits generally overlie finer-grained materials. Test-hole lithologies as a group (fig. 24B) are approximately 65 percent sand with the remainder silt and clay. The high sand content of sediment samples collected from the test holes is consistent with the higher electrical resistivities relative to the canal sites, and the silt and clay contribute to the relatively broad resistivity distribution (fig. 24A).

Inverse modeling results for the WDC resistivity profile are shown in figure 25 (for ease of visualization, the results for zero depth are not displayed). Resistivity for depths ranging from 0.1 to 3.8 m is depicted as a series of parallel traces along the profile. A wide range of electrical properties is exhibited, with the high resistivities west of test holes Ord-6 and Ord-7 decreasing to substantially lower resistivities to the east. The lowest resistivities of the site (34 ohm-m) were at about 2.0 to 3.8 m below land surface toward the east end of the profile, upstream from the Highway 70 bridge at Ord. The varying resistivity was expected, given the wide range of lithology textures and grain sizes at the test holes (fig. 24B).

Results of the vertical heterogeneity analysis are shown in figure 26A. The 12 depths of the inverted resistivity data were partitioned into three discrete zones for heterogeneity analysis: upper zone (0–0.64 m), middle zone (0.94–2.0 m), and lower zone (2.5–3.8 m). Vertical heterogeneity was moderately high, with the highest *L*-CV (dimensionless) of 0.4 at about 1.6 km down-line distance. The three depth zones showed distinct contrasts. The upper and middle zones tracked closely together along the profile, whereas the lower zone tracked independently. The distinction suggests that the lithologic characterization for the lower zone (2.5–3.8 m) differs from that of the shallower layers. The differences are shown in the resistivity profile (fig. 25), where lower resistivities were more prominent at deeper depths. The lithologic descriptions (table 1) also show that the deeper depths have a tendency for fine sand and clayey silt, consistent with the lower resistivity and vertical heterogeneity.

Results of the horizontal heterogeneity analysis are shown in figure 26B. The horizontal heterogeneity analysis used data for depths of 0.64, 2.0, and 3.8 m as representative of shallow, moderate, and deep depths, respectively. Horizontal heterogeneity ranged from low to moderate with *L*-CV (dimensionless) of 0 to 0.1. Although the fluctuations within this range along the profile show different patterns for each depth, each depth is similarly distributed overall. This indicates similar lateral lithologic variability at each depth as shown in the resistivity profile (fig. 25), where prominent changes in resistivity occur along the profile, but the changes generally coincide at each depth level. The higher resistive variability of this site indicated generally higher lithologic heterogeneity than for either of the canal sites.

Estimated interaction potential (dimensionless) is generally moderate along the data-collection path, ranging from about 0.02 to 0.11 (fig. 26C). The moderate interaction potential is consistent with the relatively variable lithology texture at the site, contributing to both horizontal and vertical heterogeneity. The overall higher resistivities (mean of 156 ohm-m) and broader resistivity distribution (interquartile range of 69 ohm-m) are consistent with moderate but variable interaction. A color-scaled map of the estimated interaction potential for both the North Loup River site and the Mirdan and Geranium Canal site is presented in figure 27.

Middle Loup River

The Middle Loup River site is moderately to highly resistive, with WDC resistivities of the shallow subsurface ranging from 42 to 1,338 ohm-m. A histogram of the inverted resistivity is presented with summary statistics in figure 28A, depicting a relatively broad distribution (interquartile range of 108 ohm-m) with the majority of the values between approximately 80 to 300 ohm-m. Lithologic descriptions of the test holes for this site (Thedford-1, Thedford-2, Thedford-3, and Thedford-4) are in table 1. Test-hole lithologies as a group were approximately 90 percent fine to coarse sand with the remainder silt and clay (fig. 28B). The high sand content of the test holes is consistent with the moderate to high electrical resistivities, with small amounts of silt and clay contributing to the relatively broad resistivity distribution (fig. 28A).

Inverse modeling results for the WDC resistivity profile are shown in figure 29. Resistivity for depths ranging from 0.1 to 3.8 m is depicted as a series of parallel traces along the profile. Depths from 0.4 to 0.9 m below land surface were relatively conductive (resistivities below 100 ohm-m), whereas

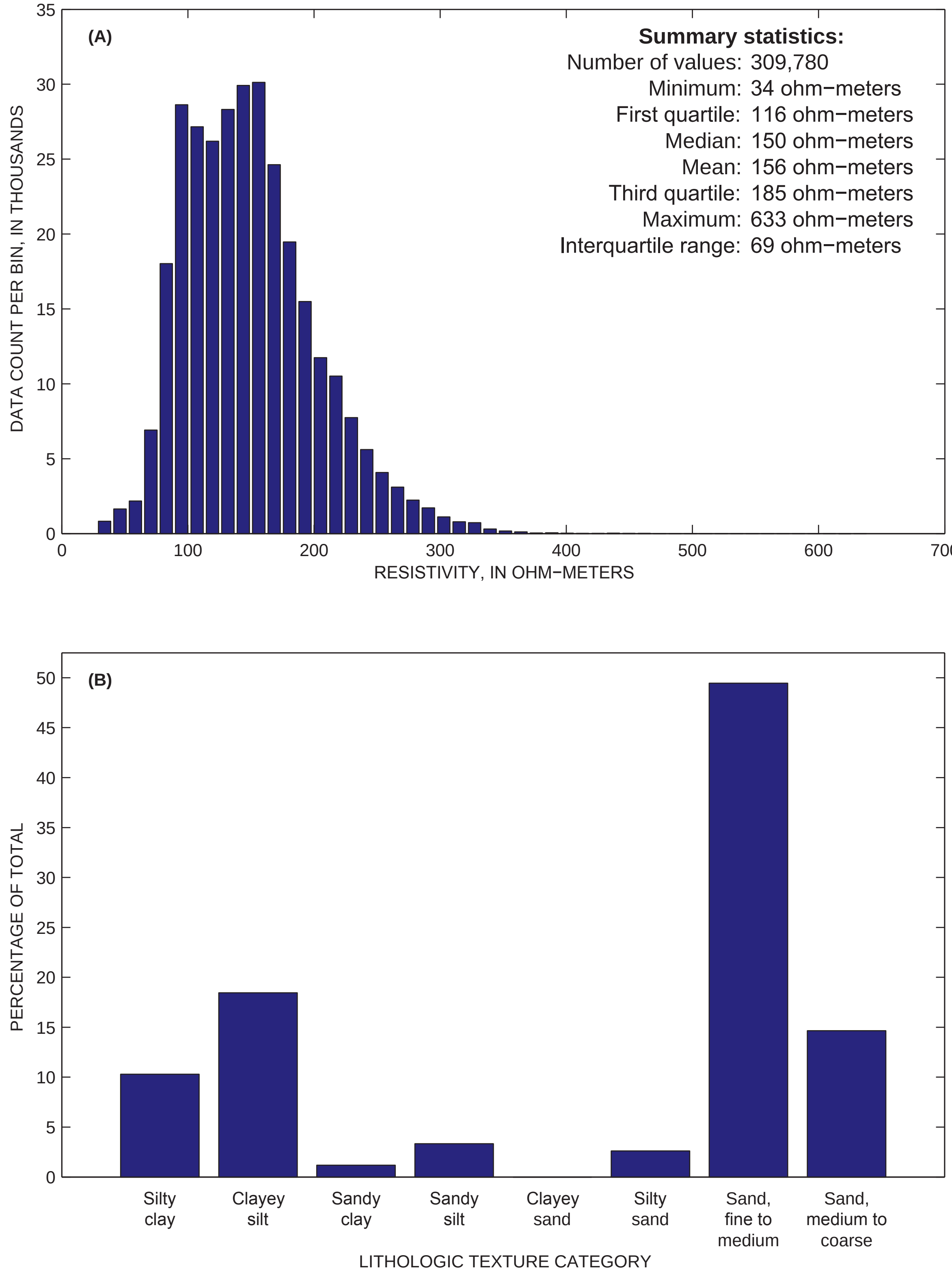

Figure 24. (A) Histogram with summary statistics for inverted direct-current resistivity; and (B) distribution of lithologic texture categories found at test holes Ord-6, Ord-7, Ord-8, Ord-9, Ord-10, and Ord-11 along North Loup River near Ord, Nebraska, 2006–07.

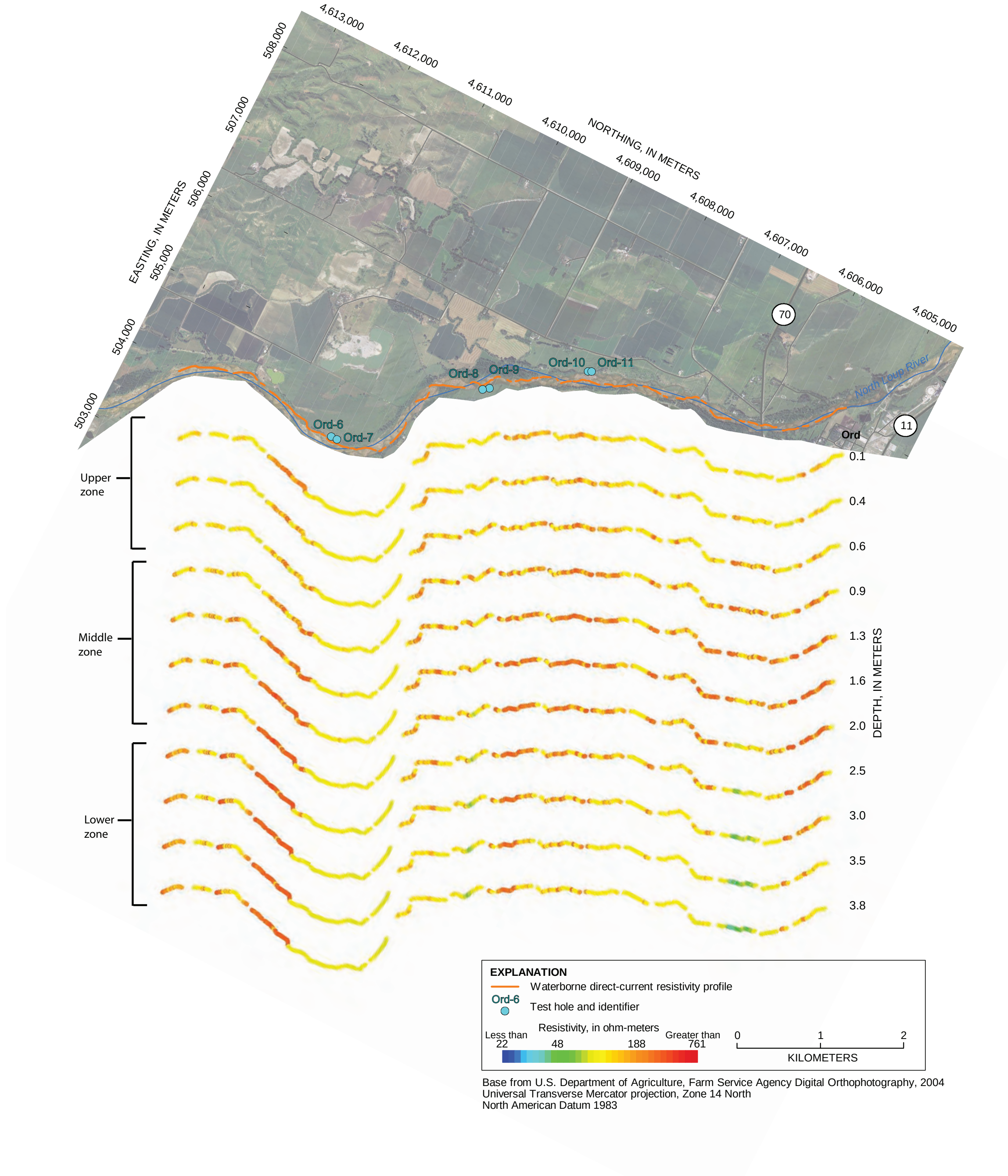

Figure 25. Inverse modeling results for waterborne direct-current resistivity profile along North Loup River near Ord, Nebraska, 2006–07.

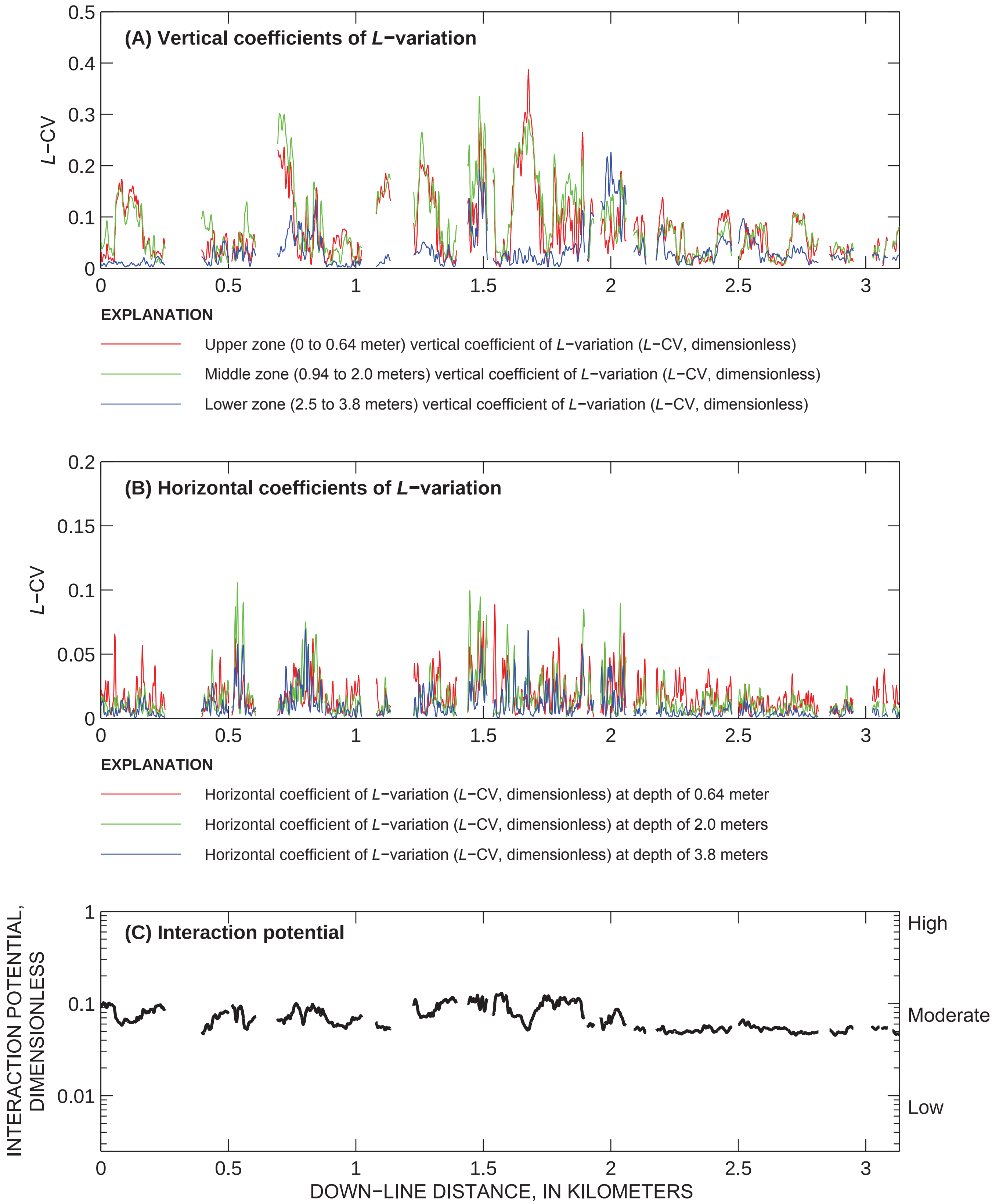

Figure 26. (A) Vertical heterogeneity results, (B) horizontal heterogeneity results, and (C) interaction potential estimated from resistivity data collected along North Loup River near Ord, Nebraska, 2006–07.

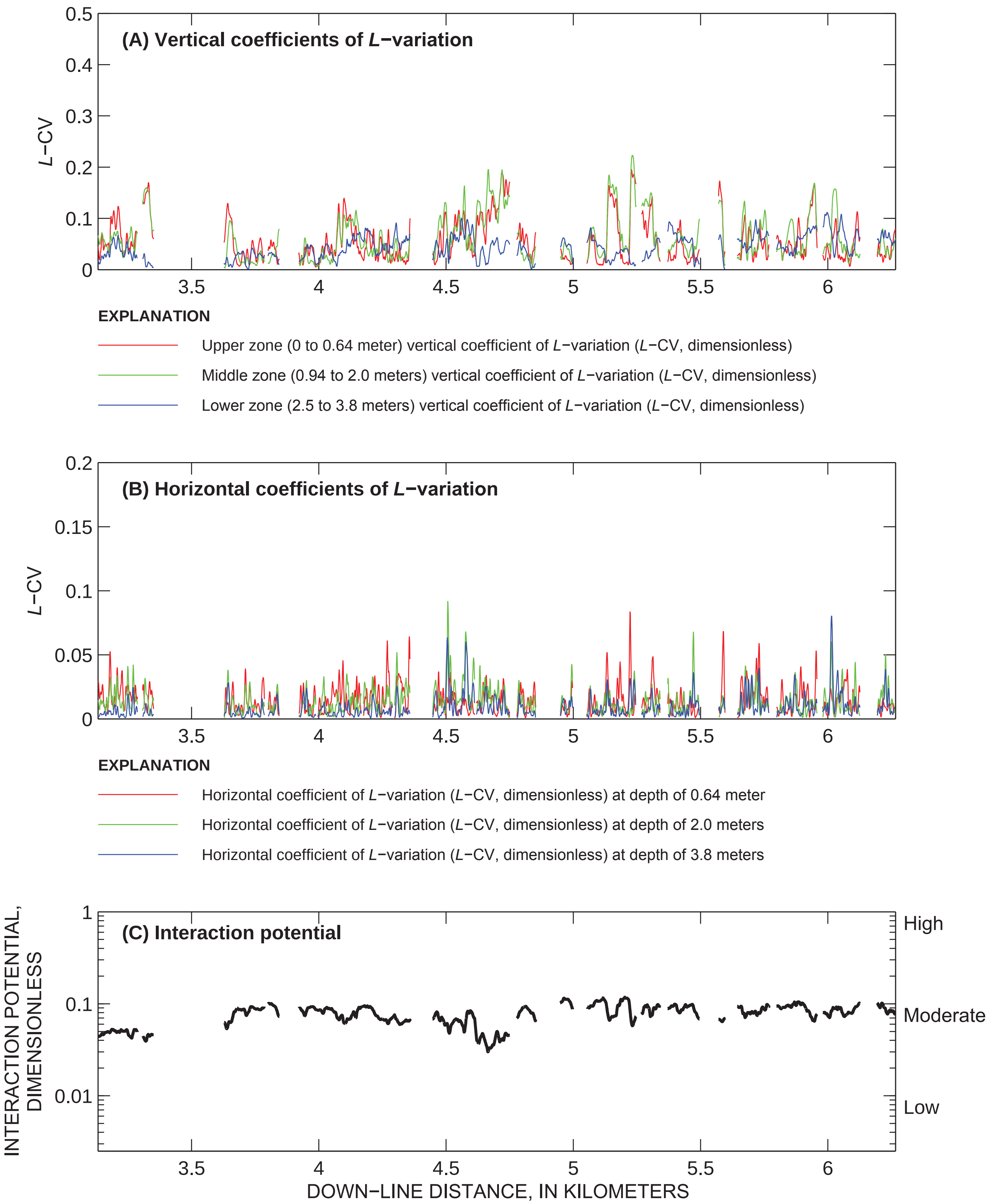

Figure 26.—Continued.

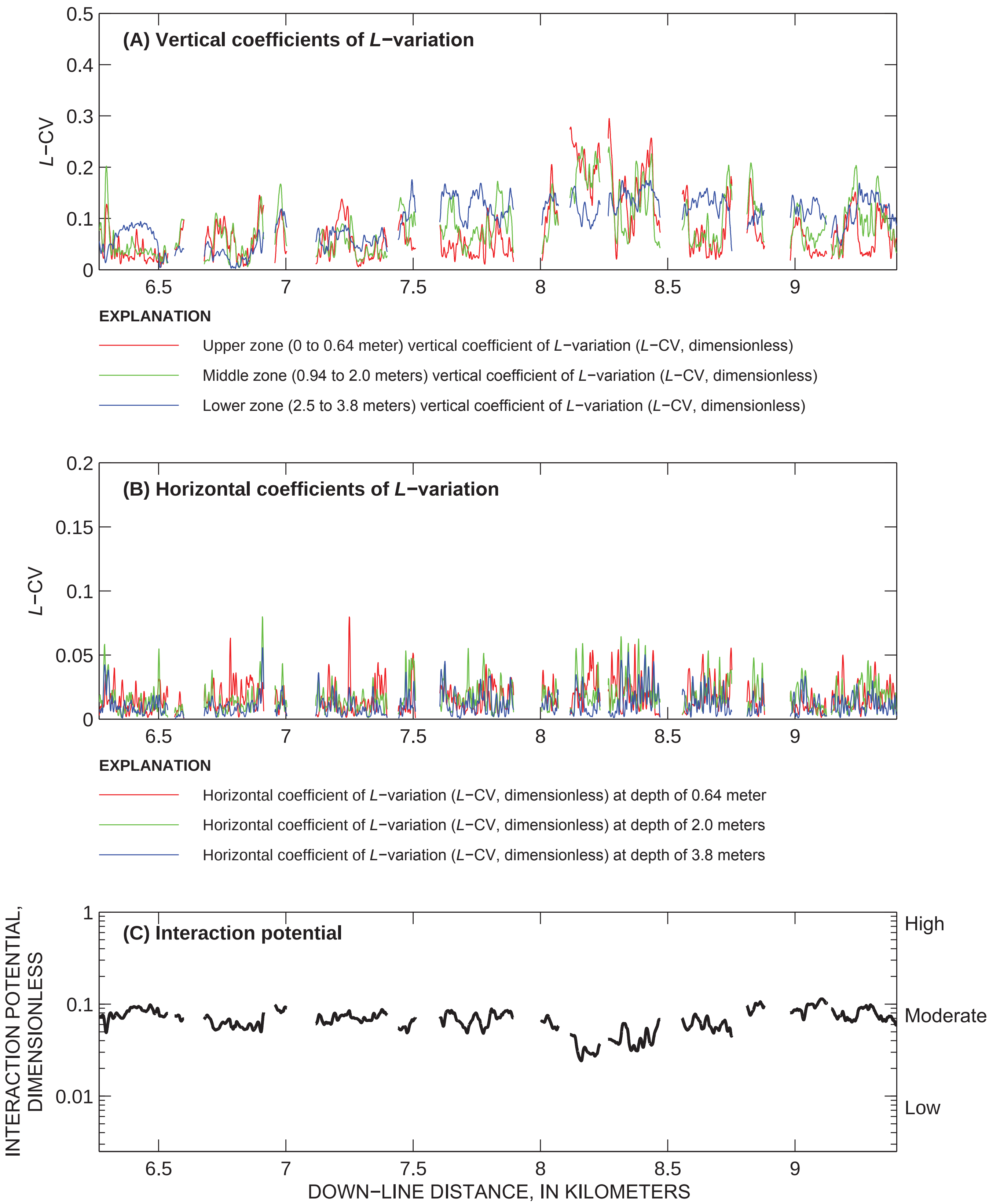

Figure 26.—Continued.

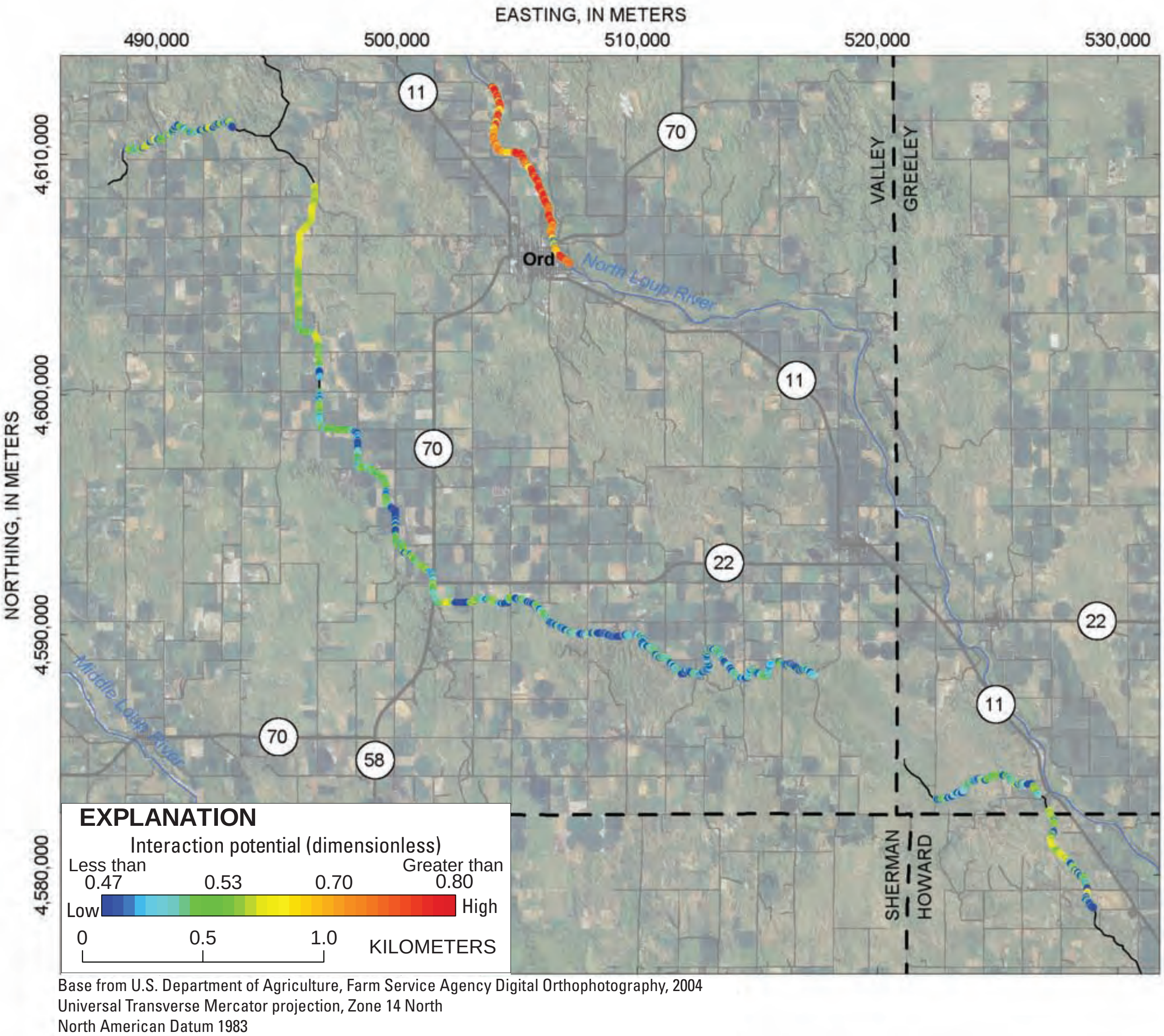

Figure 27. Interaction potential estimates along Mirdan and Geranium Canals and North Loup River near Ord, Nebraska.

deeper depths are consistently more resistive (greater than 100 ohm-m). Resistivities also were higher, about 200 ohm-m, at the 0.1-m depth (immediately below the streambed).

Results of the vertical heterogeneity analysis are shown in figure 30A. As was the case for the North Loup River site, the 12 depths of the inverted resistivity data were partitioned into an upper zone (0–0.64 m), middle zone (0.94–2.0 m), and lower zone (2.5–3.8 m). Vertical heterogeneity was generally high, with the highest *L*-CV (dimensionless) near 0.5. The upper and middle zones tracked closely together along the profile, exhibiting comparatively greater variability than the lower zone, which remained consistently lower in heterogeneity. The relation with depth is shown in the resistivity profile (fig. 29), where the higher resistivities at deeper depths are relatively uniform. The lithologic descriptions (table 1) also show a relation with depth, wherein the upper and middle zones (greater than 2 m below the streambed) are a mixture of fine sand and silty clay, and the lower zone uniformly consists of medium to coarse sand.

Results of the horizontal heterogeneity analysis are shown in figure 30B. The horizontal heterogeneity analysis used data for depths of 0.64, 2.0, and 3.8 m as representative of shallow, moderate, and deep depths, respectively. The horizontal heterogeneity was similar to that of the North Loup River site, with *L*-CV (dimensionless) ranging mostly from 0 to 0.1. Exceptions occurred toward the east end of the survey, where isolated spikes approaching or exceeding 0.15 were observed. Each depth exhibits moderate lateral variability.

Estimated surface-water/groundwater interaction potential is consistently moderate along the surveyed profile, ranging from 0.03 to 0.13 (fig. 30C). A greater interaction potential, as compared to the Ainsworth Canal site and Mirdan

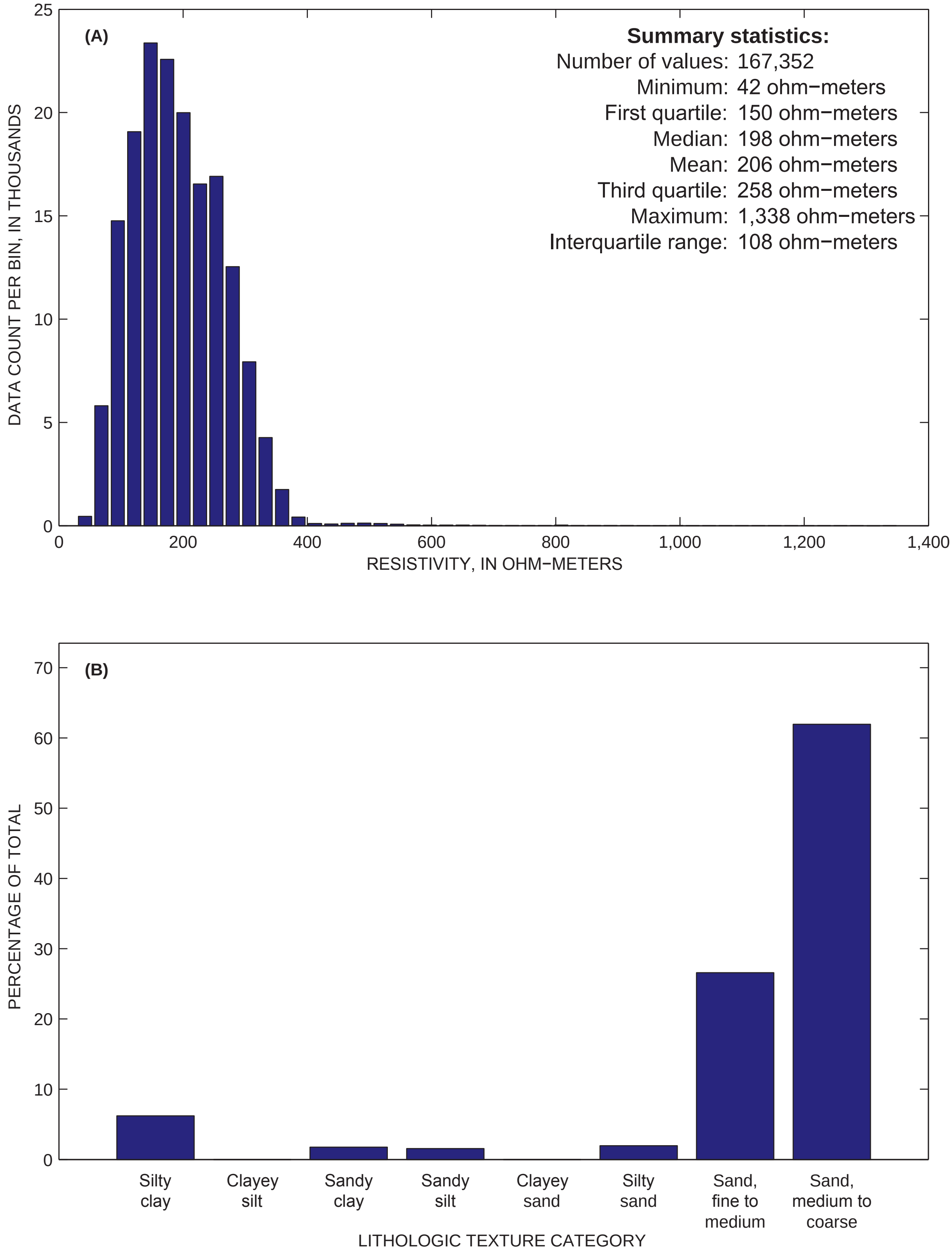

Figure 28. (A) Histogram with summary statistics for inverted direct-current resistivity; and (B) distribution of lithologic texture categories found at test holes Thedford-1, Thedford-2, Thedford-3, and Thedford-4 along Middle Loup River near Thedford, Nebraska, 2006–07.

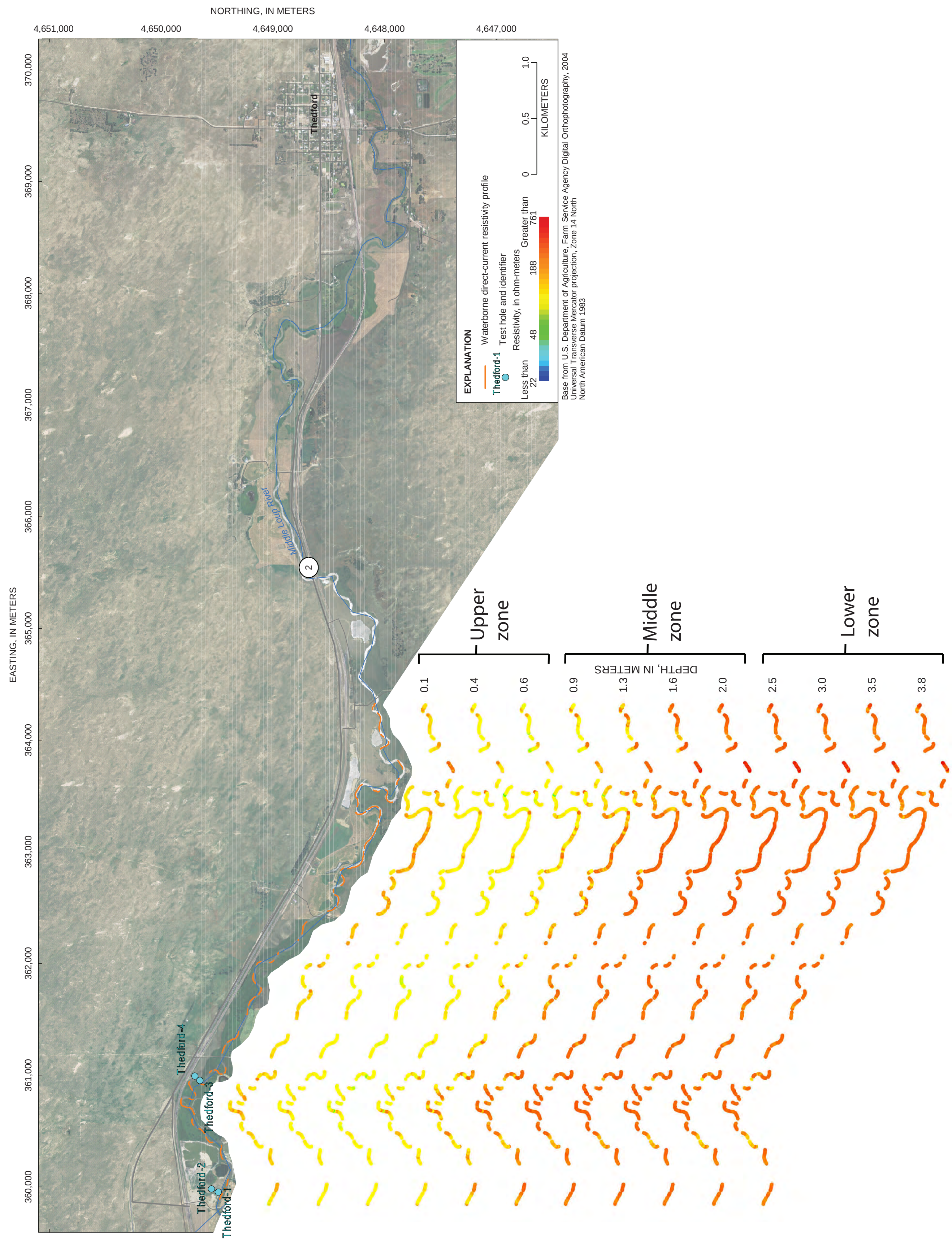

Figure 29. Inverse modeling results for waterborne direct-current resistivity profile along Middle Loup River near Thedford, Nebraska, 2006–07.

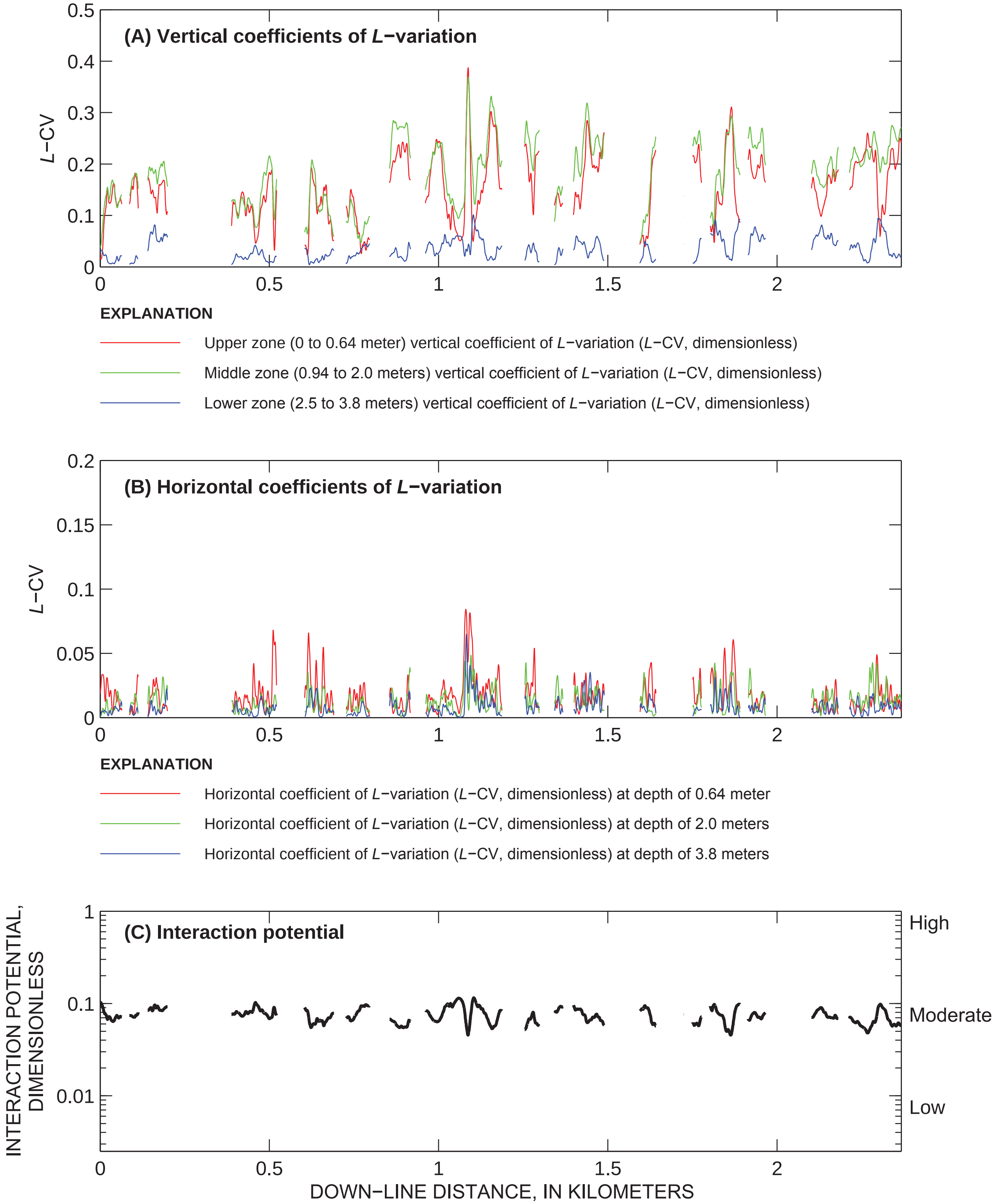

Figure 30. (A) Vertical heterogeneity results, (B) horizontal heterogeneity results, and (C) interaction potential estimated from resistivity data collected along Middle Loup River near Thedford, Nebraska, 2006–07.

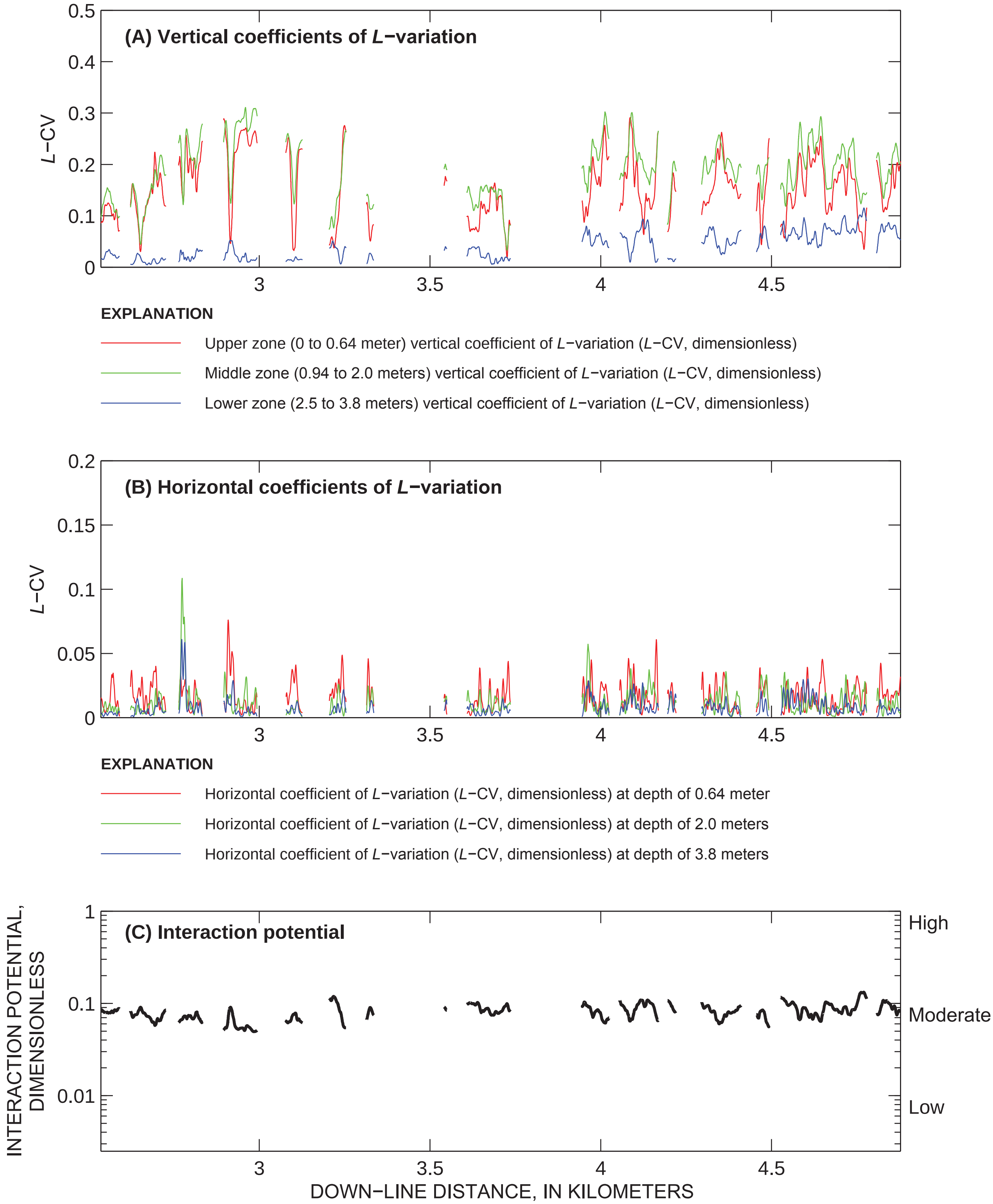

Figure 30.—Continued.

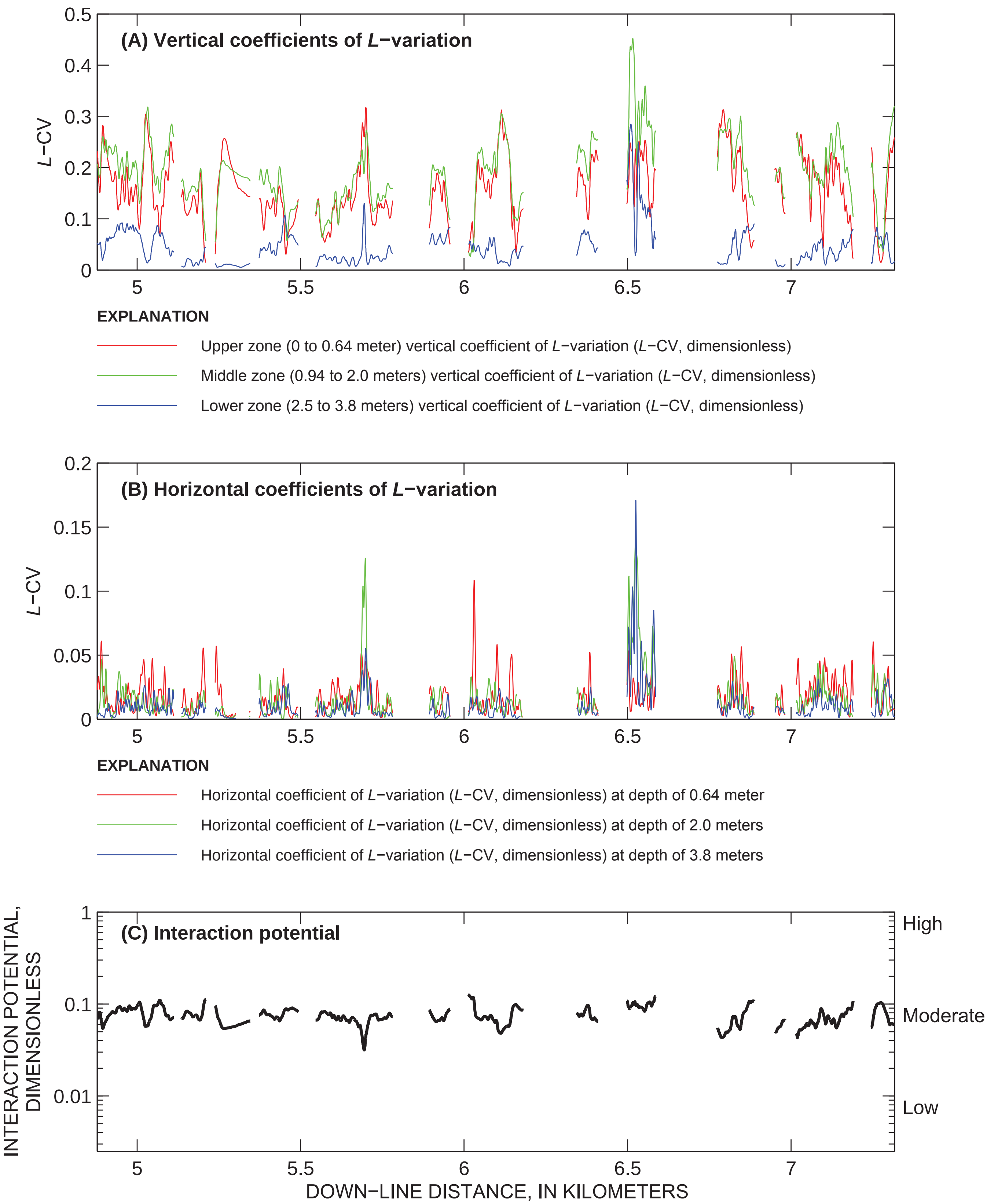

Figure 30.—Continued.

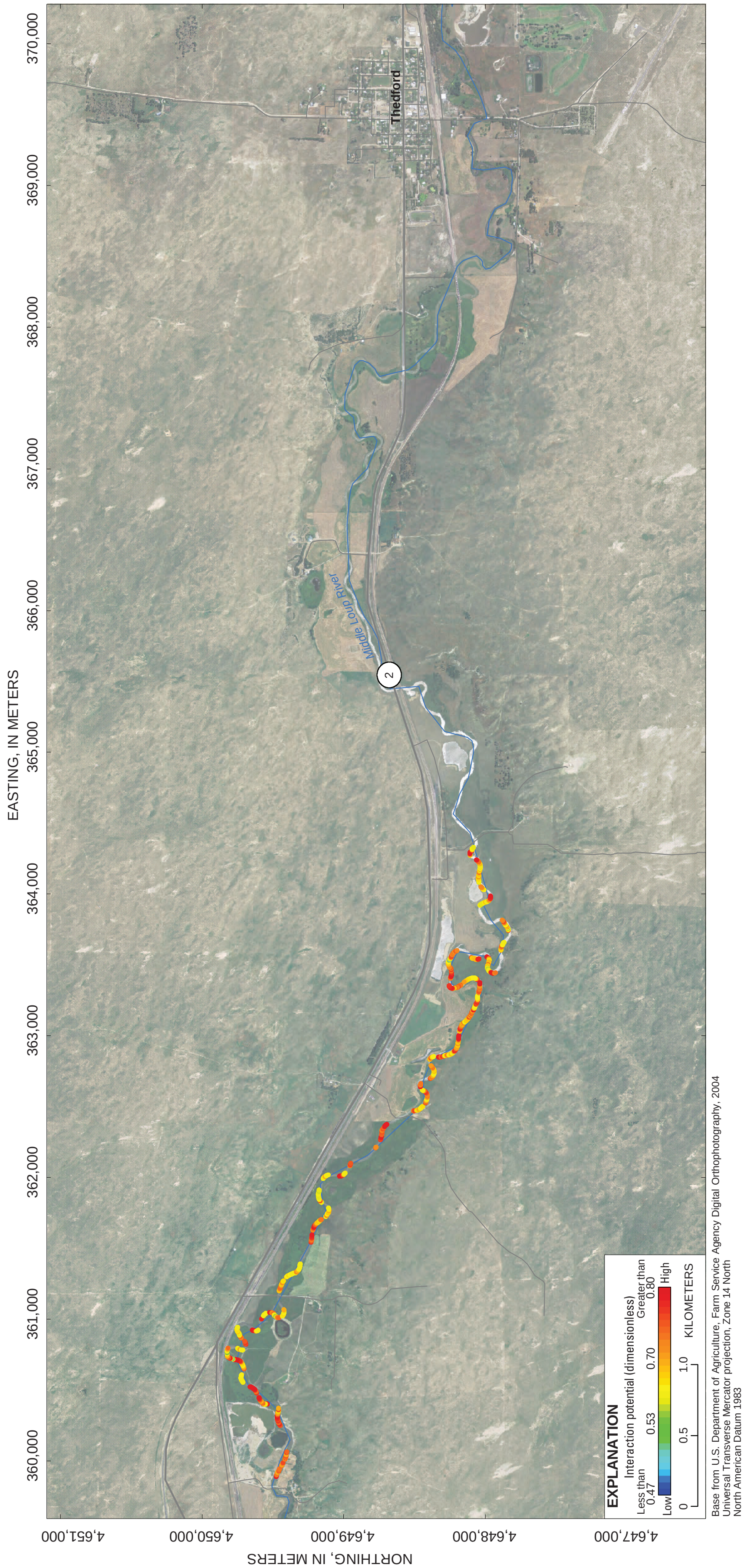

Figure 31. Interaction potential estimates along Middle Loup River near Thedford, Nebraska.

and Geranium Canal site, is estimated because of the higher subsurface resistivity. The finding is also consistent with the high percentage of medium to coarse sand in the test holes. A color-scaled map of the estimated interaction potential for the Middle Loup River site is presented in figure 31.

The North Loup and Middle Loup River sites were surveyed using a different CRP method (WDC) than that used for the Ainsworth Canal site and the Mirdan and Geranium Canal site (FDEM), and the estimated interaction potentials differed substantially. The sites surveyed using the WDC technique exhibited low to moderately low interaction potentials, whereas the sites surveyed using the WDC technique exhibited moderate to moderately high interaction potentials. However, the interaction potential estimated for sites using either the FDEM technique or the WDC technique are consistent with the lithologic descriptions for test holes at each site. The authors therefore conclude that the resistivity results do correlate with the differences in interaction potential estimates.

Summary

In 2005, the State of Nebraska adopted new legislation that in part requires Natural Resources Districts (NRDs) to include the effect of groundwater use on surface-water systems in their groundwater management plan. In response, a study was initiated to investigate surface-water and groundwater interaction within a 79,800-km^2 area in north-central Nebraska. To determine how streambed materials affect surface-water and groundwater interaction, surface geophysical and lithologic data were integrated into a comprehensive framework to characterize the hydrogeologic conditions of streambeds within the study area. During 2006–07 the U.S. Geological Survey, in cooperation with the Upper Elkhorn, Lower Elkhorn, Upper Loup, Lower Loup, Middle Niobrara, Lower Niobrara, Lewis and Clark, and Lower Platte North NRDs (Elkhorn-Loup Model sponsors), used surface geophysical continuous-resistivity profiling (CRP) techniques to map the near-surface lithologies and estimate surface-water/groundwater interaction potentials within the streambeds at Ainsworth, Mirdan, and Geranium Canals and at North Loup and Middle Loup Rivers. Sites were selected because they had contrasting streambed character, stream morphology, stream size, local geology, and local topography. Lithologic data were collected from test holes at each site to aid in the interpretation of the geophysical data. Geostatistical analysis of the CRP data as well as lithologic descriptions were used to interpret the hydrogeology of the surface-water and groundwater system.

Because local lithologic heterogeneity can have direct bearing on groundwater transport, an adjustment method based on inferred heterogeneity was applied to the processed CRP data to estimate the potential for surface-water/groundwater interaction through the subsurface material. The heterogeneity-adjustment method was used to adjust the values of two-dimensional resistivity profiles on the basis of relative variability of the resistivity values, quantified by the coefficient of *L*-variation (*L*-CV) statistic, on a local (5-m by 5-m) scale. Resistivity values were scaled by adjustment factors proportional to the local variability to allow for greater flow potential in lithologically heterogeneous units. To obtain a one-dimensional estimate of interaction potential along the streambed, the minimum of the adjusted resistivity values for each vertical column of points at each down-line distance along the profile was computed. The minimum was selected because water transport through the subsurface is most affected by the least permeable unit, corresponding to the least electrical resistance. The one-dimensional interaction-potential estimates determined by the heterogeneity-adjustment method were normalized to the maximum resistivity value measured during this study, resulting in dimensionless estimates between 0 and 1.

The Ainsworth Canal site is generally electrically conductive, with apparent frequency-domain electromagnetic (FDEM) resistivities ranging from 22 to 71 ohm-m. Sediment samples at nearby test holes were typically fine-to-medium sand and clay and silt. The vertical and horizontal variability of the apparent resistivity data were consistently low. The small variability suggests little lithologic heterogeneity for the site as a whole. Surface-water/groundwater interaction-potential estimates are consistently low along the entire profile, ranging from about 0.01 to 0.025. The interaction-potential estimates are in agreement with the narrow frequency distribution of low apparent resistivities, general homogeneity, and grain-size characteristics of core samples collected from nearby test holes. Overall, the interaction potential at the Ainsworth Canal site is estimated to be low relative to the other three sites.

The Mirdan and Geranium Canal site is generally electrically conductive, with apparent FDEM resistivities ranging from 2 to 120 ohm-m. Core samples at nearby test holes were almost entirely silt and clay (95 percent). For 45 km of the canal, the vertical variability of the apparent resistivity data was similar to that for the Ainsworth Canal site. For 20 km of the canal, high surface resistivities contributed to greater vertical variability. The horizontal variability of the apparent resistivity was moderately higher than that for the Ainsworth Canal site, with *L*-CV generally below 0.05. The relatively small vertical and horizontal variability indicate lithologic homogeneity both laterally and with depth. Interaction-potential estimates are low to slightly moderate along the data-collection path, ranging from about 0.006 to 0.033. Interaction estimates exhibit greater fluctuation along this profile than along the profile for the Ainsworth Canal site, which can be attributed to the slightly greater vertical and horizontal heterogeneity of the near-surface lithology. Overall, the interaction potential at the Mirdan and Geranium Canal site is estimated to be low to slightly moderate.

The North Loup River site is conductive to moderately resistive, with waterborne direct-current (WDC) resistivities ranging from 34 to 633 ohm-m. Lithologic descriptions indicate coarser-grained deposits generally overlie finer-grained

materials. Vertical variability of the inverted resistivity data was moderately high. The heterogeneity of the lower 2.5 to 3.8 m was distinct from the shallower material, consistent with the transition to finer sediment textures in deeper intervals at the test holes. Horizontal variability was low to moderate. The higher resistive variability of this site indicated generally higher lithologic heterogeneity than for either of the canal sites. Interaction-potential estimates are consistently moderate along the profile, ranging from about 0.02 to 0.11. The moderate interaction potential is consistent with the relatively variable lithologic texture at the site, contributing to both horizontal and vertical heterogeneity. Overall, the interaction potential at the North Loup River site is estimated to be moderate.

The Middle Loup River site is moderately to highly resistive, with WDC resistivities ranging from 42 to 1,338 ohm-m. Sediment cores collected from test holes were predominantly fine, medium, and coarse sand (about 90 percent) with the remainder silt and clay. Vertical variability of the inverted resistivity data was generally high. Deeper intervals (2.5 to 3.8 m) consistently exhibited less vertical variability, corresponding to the uniformly medium to coarse sand at the test holes. The horizontal variability was similar to that of the North Loup River site. Interaction potential was consistently moderate along the surveyed profile, with estimates ranging from 0.03 to 0.13. A higher interaction potential, as compared to the Ainsworth Canal site and Mirdan and Geranium Canal site, is estimated because of the higher subsurface resistivity and high percentage of medium to course sand.

References Cited

Abraham, J.D., Deszcz-Pan, Maryla., Fitterman, D.V., and Burton, B.L., 2006, Use of a handheld broadband EM induction system for deriving resistivity depth images, *in* 19th Symposium on the Application of Geophysics to Engineering and Environmental Problems (SAGEEP), Seattle, Wash., April 2–6, 2006, Proceedings: 18 p.

Advanced Geosciences, Inc., 2008, Instruction manual for EarthImager 2D version 2.2.5—Resistivity and IP inversion software: Austin, Tex., Advanced Geosciences, accessed November 1, 2008, at *http://www.agiusa.com/files/pub/softwareproducts.shtml*

Alpha GeoScience, 2007, terraTEM overview: Peakhurst NSW, Australia, Alpha GeoScience, accessed June 1, 2007, at *http://www.alpha-geo.com/instruments/terratem/*

Appel, C.A., and Bredehoeft, J.D., 1976, Status of groundwater modeling in the U.S. Geological Survey: U.S. Geological Survey Circular 737, 9 p.

Asquith, W.H., 2007, *L*- and *TL*-moments of the generalized lambda distribution: Computational Statistics and Data Analysis, v. 51, no. 9, p. 4,484–4,496.

Ball, L.B., Kress, W.H., Steele, G.V., Cannia, J.C., and Anderson, M.J., 2006, Determination of canal leakage potential using continuous resistivity profiling techniques, Interstate and Tri-State Canals, western Nebraska and eastern Wyoming, 2004: U.S. Geological Survey Scientific Investigations Report 2006–5032, 53 p.

Bleed, A.S., 2006, Annual evaluation of availability of hydrologically connected water supplies: Nebraska Department of Natural Resources, accessed December 12, 2008, at *http://www.dnr.state.ne.us/LB962/AnnualReport/2006_AnnualReport.pdf*

Bleed, A.S., 2007, Annual evaluation of availability of hydrologically connected water supplies: Lincoln, Nebraska Department of Natural Resources, accessed December 12, 2008, at *http://www.dnr.state.ne.us/LB962/AnnualReport_2007/AnnualReport2007.pdf*

Constable, S.C., Parker, R.L., and Constable, C.G., 1987, Occam's inversion—A practical algorithm for generating smooth models from EM sounding data: Geophysics, v. 52, p. 289–300.

Darton, N.H., 1903a, Geologic atlas of the United States, Scotts Bluff folio, Nebraska: U.S. Geological Survey Folio 88, 5 p.

Darton, N.H., 1903b, Preliminary report on the geology and water resources of Nebraska west of the one hundred and third meridian: U.S. Geological Survey Professional Paper 17, 69 p., 43 pls.

Friedberg, S.H., Insel, A.J., and Spence, L.E., 1997, Linear algebra (3rd ed.): Upper Saddle River, N.J., Prentice-Hall, 557 p.

Geosoft, Inc., 2008, Oasis montaj, version 7.0.1 (OL): Toronto, Canada, Geosoft, Inc., accessed November 25, 2008, at *http://geosoft.com/support/updates/oasismontaj.asp*

Hosking, J.R.M., 1990, *L*-moments—Analysis and estimation of distributions using linear combinations of order statistics: Journal Royal Statistical Society B, v. 52, no. 1, p. 105–124.

Huang, Haoping, and Won, I.J., 2000, Conductivity and susceptibility mapping using broadband electromagnetic sensors: Journal of Environmental and Engineering Geophysics, v. 5, no. 4, p. 31–41.

Interpex, Ltd., 2007, IX1D version 3 inversion software: Golden, Colo., Interpex, Ltd., accessed June 1, 2007, at *http://www.interpex.com*

IRIS Instruments, 2007a, SYSMAR acquisition for continuous marine survey: Orleans, France, IRIS Instruments, accessed June 1, 2007, at *http://www.iris-instruments.com/Support/Support.html*

IRIS Instruments, 2007b, PROSYS II version 02.08.01 resistivity data management: Orleans, France, IRIS Instruments, accessed June 1, 2007, at *http://www.iris-instruments.com/Support/Support.html*

Keller, G.V., and Frischknecht, F.C., 1966, Electrical methods in geophysical prospecting: Oxford, U.K., Pergamon Press, 519 p.

Loke, M.H., 2000, Electrical imaging surveys for environmental and engineering studies—A practical guide to 2-D and 3-D surveys: M.H. Loke, 62 p., accessed August 2002, at *http://www.terrajp.co.jp/lokenote.pdf*

Loke, M.H., 2004, RES2DINV, version 3.54—Rapid 2D resistivity and IP inversion using the least-squares method—Geoelectrical imaging 2-D and 3-D: Penang, Malaysia, Geotomo Software, 130 p., accessed September 12, 2005, at *http://www.geoelectrical.com/download.html*

Lucius, J.E., Langer, W.H., and Ellefsen, K.J., 2007, An introduction to using surface geophysics to characterize sand and gravel deposits: U.S. Geological Survey Circular 1310, 33 p.

Merry, A.G., Martin, P.J., and Sussman, J.D., 2003, Importance of local geologic structure in a regional groundwater flow and contaminant transport model for Lansing, Michigan, *in* Poeter, Eileen, Zheng, Chunmiao, Hill, Mary, and Doherty, John, MODFLOW and more 2003–Understanding through modeling conference, v. II, September 16, 2003, Denver, Colo., [Proceedings]: p. 655–660.

North Carolina Division of Water Resources, 2004, Time domain electromagnetic geophysics: North Carolina Department of Environment and Natural Resources, accessed July 31, 2006, at *http://www.ncwater.org/Education_and_Technical_ Assistance/Ground_Water/TDEM/*

North Platte Natural Resources District, 2004, NPNRD's Integrated Management Plan: Gering, Nebraska, accessed March 2007, at *http://www.npnrd.org/LB962.htm*

Peterson, S.M., 2007, The Elkhorn-Loup Model study—Proactive Nebraska decision makers initiate science-based integrated water management: Denver, Geological Society of America National Conference, Paper 195–12.

Peterson, S.M., Stanton, J.S., Saunders, A.T., and Bradley, J.R., 2008, Simulation of ground-water flow and effects of pumpage on base flow in the Elkhorn and Loup River Basins, Nebraska: U.S. Geological Survey Scientific Investigations Report 2008–5143, 65 p.

Sharma, P.V., 1997, Environmental and engineering geophysics: Cambridge, United Kingdom, Cambridge University Press.

Smith, Leslie, and Wheatcraft, S.W., 1993, Groundwater flow, Chapter 6, *in* Maidment, D.R., ed., Handbook of hydrology: New York, McGraw-Hill, p. 6.1–6.58.

Souders, V.L., 2000, Geologic maps and cross sections showing configurations of bedrock surfaces, Broken Bow 1° x 2° quadrangle, east-central Nebraska: Nebraska Geological Survey, pamphlet to accompany U.S. Geologic Survey Geologic Investigation Series I–2725, p. 13, accessed November 1, 2008, at *http://pubs.usgs.gov/imap/i-2725/i-2725.pdf*

Stewart, Mark, and Gay, M.C., 1986, Evaluation of transient electromagnetic soundings for deep detection of conductive fluids: Ground Water, v. 24, p. 351–356.

Sumner, J.S., 1976, Principles of induced polarization for geophysical exploration: Amsterdam, Elsevier, 277 p.

Swinehart, J.B., Dreezen, V.H., Richmond, G.M., Tipton, M.J., Bretz, R.F., Steece, F.V., Halberg, G.R., and Goebel, J.E., 1994, Quaternary geologic map of the Platte River 4° x 6° quadrangle: U.S. Geological Survey Quaternary Atlas of the United States, scale 1:1,000,000.

U.S. Army Corps of Engineers, 1995, Geophysical exploration for engineering and environmental investigations, Chapter 4: U.S. Army Engineering Manual 1110–1–1802, p. 25–37.

U.S. Department of Agriculture, 2007, Aerial Photography Field Office: accessed November 3, 2007, at *http://165.221.201.14/NAIP.html*

Won, I.J., Keiswetter, D.A., Fields, G.R.A., and Sutton, L.C., 1996, GEM-2—A new multifrequency electromagnetic sensor: Journal of Environmental and Engineering Geophysics, v. 1, no. 2, p. 129–137.

Zohdy, A.A.R., Eaton, G.P., and Mabey, D.R., 1974, Application of surface geophysics to ground-water investigations: U.S. Geological Survey Techniques of Water-Resources Investigations, book 2, chap. D1, 116 p.

Table 1. Lithologic descriptions of test holes within the Elkhorn-Loup Model study area, north-central Nebraska.

[%, percent; mm, millimeters; some intervals missing due to recovery problems]

Depth (meters)	Lithology	Munsell color
	Ainsworth-1, N42º32'57.3", W99º45'18.2", Brown County, Nebraska, T30N R21W S26	
0.29–0.50	Clayey sand - fine to medium, well sorted, well rounded, medium plasticity, organic, some roots, 90% quartz, 5% feldspar, 5% mafic	2.5Y 3/2
0.50–1.16	Sand-medium well rounded to rounded, moderately sorted, interbedded, coarse sand to fine gravel, rounded, range (2.03–19.05 mm), occasional interbedded coarse gravel, rounded to sub-angular, lenses of clayey sand, medium, rounded, organic (dark brown), hard	2.5Y 6/4
1.16–1.54	Clayey silt - hard, low plasticity, organic, traces of interbedded sand, fine,	2.5Y 2.5/1
1.54–1.8	Clayey silt, hard, low plasticity, interbedded sand, fine, sticky	2.5Y 4/2
1.8–2.4	Sand - fine to medium, well rounded to rounded, moderately sorted, interbedded coarse sand to fine gravel, rounded, range (2.03–12.70 mm), 85% quartz, 10% feldspar, 5% mafic, traces of oxidation	2.5Y 6/4
2.7–3.1	Sand - medium to coarse, well rounded to rounded, poorly sorted, interbedded fine to coarse gravel, rounded to sub-angular, range (4.82–25.4 mm), traces of organics, 80% quartz, 15% feldspar, 5% mafic	2.5Y 5/4
3.1–3.6	Sand - fine to medium, well rounded to rounded, moderately sorted, interbedded coarse sand to fine gravel, rounded, range (2.03–12.7 mm), 90% quartz, 5% feldspar, 5% mafic, occasional interbedded coarse gravel, rounded	2.5Y 7/3
3.6–3.65	Sandy silt - fine, well sorted, well rounded to rounded, soft, interbedded medium sand, rounded to sub-rounded, 90% quartz, 5% feldspar, 5% mafic	2.5Y 6/2
3.65–3.78	Sand, fine - sorted, well rounded to rounded, lenses of sandy silt, (fine, light brown), occasional interbedded medium sand, rounded, 95% quartz, 3% mafic, 2% feldspar	2.5Y 7/3
3.78–4.3	Sand - medium, rounded to sub-rounded, moderately sorted, interbedded coarse sand to fine to coarse gravel, rounded to sub-rounded, range (2.03–25.4 mm), traces of oxidation, 85% quartz, 10% feldspar, 5% mafic	2.5Y 7/4
4.3–4.5	Sand - fine to medium, well sorted, rounded to sub-angular, occasional interbedded, fine gravel, rounded, 90% quartz, 7% feldspar, 3% mafic	2.5Y 7/3
4.5 –4.7	Sand - fine to medium, rounded to sub-rounded, well sorted, occasional interbedded coarse gravel, rounded, traces of organics, 90% quartz, 3% feldspar, 7% mafic	2.5Y 7/3
4.7–4.8	Sand - medium to coarse, rounded to sub-rounded, poorly sorted, interbedded fine gravel, sub-rounded, (4.82–11.43 mm), high appearance of oxidation, 80% quartz, 15% feldspar, 5% mafic	10YR 5/6
5.1–5.2	Sandy silt - fine, well sorted, well rounded to rounded, interbedded medium sand, rounded, organic, traces of oxidation, 90% quartz, 5% feldspar, 5% mafic	2.5Y 4/2
5.2–5.3	Sand - fine, well sorted, well rounded to rounded, interbedded coarse sand, rounded, traces of oxidation, 90% quartz, 3% feldspar, 7% mafic	2.5Y 4/2
5.3–5.5	Sand - fine to medium, rounded to sub-rounded, poorly sorted, interbedded, coarse sand to fine gravel, sub-rounded, with occasional interbedded coarse gravel, rounded to sub-rounded, traces of oxidation, 90% quartz, 5% feldspar, 5% mafic	2.5Y 7/3
5.5–5.6	Sand - fine, well sorted, well rounded, 95% quartz, 2% feldspar, 3% mafic	2.5Y 7/3
5.6–5.9	Sand - medium, moderately sorted, well rounded to rounded, interbedded coarse sand, rounded to sub-rounded, 85% quartz, 10% feldspar, 5% mafic	2.5Y 7/3
5.9–6.0	Sand - medium, moderately sorted, well rounded to rounded, interbedded coarse sand to fine gravel, rounded to sub-angular, oxidation, 85% quartz, 10% feldspar, 5% mafic	10YR 6/6
6.0–6.3	Sand - medium to coarse, poorly sorted, rounded to sub-angular, interbedded fine gravels, rounded to sub-angular, traces of oxidation, 60% quartz, 35% feldspar, 5% mafic	2.5Y 6/6
6.3–8.2	Sand - fine, well sorted, well rounded to rounded, 90% quartz, 5% feldspar, 5% mafic, traces of oxidation	2.5Y 6/2
8.2–8.5	Clayey sand - low to medium plasticity, fine, well rounded to rounded, traces of oxidation, mainly quartz	2.5Y 5/3
	Ainsworth-2, N42º33'07.1", W99º48'47.1", Brown County, Nebraska, T31N R22W S20	
0.36–0.62	Silty clay - organic, low plasticity, interbedded fine sand, well rounded to rounded, some roots, with occasional interbedded fine gravel, rounded to sub-rounded	2.5Y 3/1
0.62–0.78	Sand - fine, well sorted, well rounded to rounded, occasional interbedded coarse sand, rounded, 95% quartz, 3% feldspar, 2% mafic	2.5Y 5/3
0.78–1.16	Clayey silt - organic, low plasticity, some roots and fine sand, well round to rounded	2.5Y 2.5/1

Table 1. Lithologic descriptions of test holes within the Elkhorn-Loup Model study area, north-central Nebraska—Continued.

Depth (meters)	Lithology	Munsell color
	Ainsworth-2, N42º33′07.1″, W99º48′47.1″, Brown County, Nebraska, T31N R22W S20—Continued	
1.4–1.7	Sand, fine - well sorted, well rounded to rounded, 95% quartz, 2% feldspar, 3% mafic	2.5Y 6/3
1.7–2.4	Sandy clay - fine, well rounded to rounded, low to medium plasticity, 95% quartz, 2% feldspar, 3% mafic	2.5Y 6/2
2.6–4.7	Sandy silt - fine, well sorted, well rounded, 95% quartz, 2% feldspar, 3% mafic	2.5Y 7/3
4.7–5.4	Sandy clay - fine, well rounded, low plasticity, 95% quartz, 2% feldspar, 3% mafic	2.5Y 6/4
5.4–6.0	Sandy silt - fine, well sorted, well rounded to rounded, 90% quartz, 5% feldspar, 5% mafic	2.5Y 6/3
6.3–6.8	Sand - fine, well sorted, well rounded to rounded, 90% quartz, 5% feldspar, 5% mafic, traces of oxidation	2.5Y 7/3
6.8–7.3	Sand - fine to medium, well sorted, well rounded to rounded, 90% quartz, 3% feldspar, 7% mafic	2.5Y 7/3
	Ord-1, N41º34′45.9″, W99º02′56.9″, Valley County, Nebraska, T19N R15W S33	
0–0.23	Silty sand - very fine to fine, well rounded, well sorted, soft, 95% quartz, 5% mafic	2.5y 6/4
0.23–0.29	Clayey silt - very fine, sticky, organic	2.5y 2.5/1
0.29–1.16	Silty clay - very fine, loess, hard	2.5y 6/4
1.16–1.59	Silty clay - very fine, traces of fine sand, hard, loess, 95% quartz, 5% mafic	2.5y 6/4
1.59–2.4	Clayey silt - very fine, sticky, occasional interbedded gravel	2.5y 5/3
2.4–7.3	Clayey silt - very fine, sticky, soft	2.5y 5/3
7.3–9.8	Clayey silt - very fine, sticky, soft, traces of oxidation	2.5y 5/3
	Ord-2, N41º34′18″, W99º02′22.5″, Valley County, Nebraska, T19N R15W S33	
0–0.76	Silty clay - very fine, hard, low plasticity, traces of oxidation, lenses of fine silty sand	2.5y 4/2
0.76–2.0	Clayey silt - very fine, soft, sticky, traces of oxidation	2.5y 4/4
2.0–3.4	Sandy clay - very fine to fine, well rounded, 100% quartz, medium plasticity, soft	2.5y 6/5
3.4–3.6	Clayey sand - very fine, sticky, well rounded, 100% quartz	2.5y 6/3
3.9–4.8	Sandy clay - very fine to fine, well rounded, well sorted, 100% quartz	2.5y 6/3
4.8–7.3	Sandy clay - very fine to fine, well rounded, well sorted, 100% quartz	2.5y 6/3
	Ord-3, N41º34′06.9″, W99º02′20.9″, Valley County, Nebraska, T19N R15W S34	
0.25–1.16	Silty clay - very fine, soft, low to medium plasticity	2.5y 5/3
1.16–2.4	Clayey silt - very fine, soft, high plasticity	2.5y 4/3
2.4–3.6	Clayey silt - very fine, soft, high plasticity, traces of oxidation	2.5y 5/4
3.6–4.2	Sandy clay - very fine, rounded, well sorted, high plasticity, 100% quartz	2.5y 5/4
4.2–4.8	Sandy clay - very fine to fine, well sorted, well rounded, soft, 95% quartz, 5% mafic	2.5y 6/3
4.8–6.0	Same as (4.2–4.8)	
6.0–7.3	Same as (4.2–4.8)	

Table 1. Lithologic descriptions of test holes within the Elkhorn-Loup Model study area, north-central Nebraska—Continued.

Depth (meters)	Lithology	Munsell color
	Ord-4, N41º27′01.7″, W98º48′25.6″, Valley County, Nebraska, T17N R13W S15	
0.34–0.58	Clayey silt - hard, low plasticity, organic	2.5Y 3/3
0.58–1.16	Clayey silt - soft, medium to high plasticity, traces of oxidation, sticky	2.5Y 5/4
1.38–1.83	Clayey silt - soft, medium to high plasticity, sticky	2.5Y 5/3
1.83–2.4	Clayey silt - soft, medium to high plasticity, sticky, traces of interbedded fine sand	2.5Y 5/3
2.4–5.8	Clayey silt - soft, medium to high plasticity, sticky, traces of interbedded fine sand, traces of oxidation	2.5Y 5/3
5.8–8.0	Clayey silt - stiffer than above, low to medium plasticity, traces of interbedded fine sand, oxidized	2.5Y 5/3
8.0–8.5	Clayey silt - stiff, low to medium plasticity, interbedded fine sand, well rounded, more sand than the previous samples above, mainly quartz and mafic minerals	2.5Y 5/3
8.8–8.9	Sandy clay - fine, well rounded, well sorted, soft, low to medium plasticity, 95% quartz, 2% feldspar, 3% mafic	2.5Y 6/4
8.9–9.5	Clayey sand - fine, well rounded, well sorted, stiff, low to medium plasticity, traces of oxidation, 95% quartz, 2% feldspar, 3% mafic	2.5Y 5/3
9.5–9.7	Sandy clay - fine, well sorted, well rounded, 95% quartz, 2% feldspar, 3% mafic	2.5Y 6/3
	Ord-5, N41º24′23.3″, W98º41′37.4″, Greeley County, Nebraska, T17N R12W S34	
0–1.16	Clayey silt - hard, low plasticity	2.5Y 5/3
1.16–1.92	Silty clay - soft, very fine	2.5Y 5/3
1.92–2.4	Clayey silt - very fine, hard, low plasticity, traces of oxidation	2.5Y 5/2
2.4–4.8	Clayey silt - soft, medium plasticity, traces of oxidation	2.5Y 5/3
4.8–6.0	Clayey silt - soft, medium plasticity	2.5Y 5/3
6.0–6.4	Clayey silt - soft, medium plasticity, traces of oxidized sand	2.5Y 5/3
6.4–7.3	Clayey silt - soft, medium plasticity	2.5Y 5/3
7.3–7.6	Clayey silt - soft, medium plasticity, traces of oxidized sand	2.5Y 5/3
7.6–8.5	Clay - soft, medium to high plasticity	2.5Y 5/4
8.8–9.4	Clayey silt - soft, medium plasticity, traces of oxidized sand	2.5Y 5/3
9.4–9.6	Clayey sand, - soft, fine, well rounded, medium plasticity, 95% quartz, 2% feldspar, 3% mafic	2.5Y 5/3
	Ord-6, N41º38′57″, W98º57′04″, Valley County, Nebraska, T19N R14W S5	
0.13–0.29	Topsoil - silty clay, very fine, organic, some roots	2.5Y 3/2
0.29–0.70	Silty sand - very fine to fine, well sorted lenses of clay	2.5Y 6/3
0.92–1.16	Sandy silt - very fine to fine, well sorted, well rounded, lenses of sandy clay, with occasional fine gravel, rounded, 96% quartz, 1% feldspar, 3% mafic	2.5Y 7/3
1.71–1.82	Silty clay - very fine, organic, sticky, saturated, more sandy towards bottom, 100% quartz	2.5Y 2.5/1
1.82–2.0	Sand - fine, well sorted, well rounded, 95% quartz, 3% feldspar, 2% mafic	2.5Y 7/2
2.0–3.2	Sand - fine to medium, moderately sorted, well rounded, interbedded coarse sand, occasional coarse gravel, rounded, 95% quartz, 2% feldspar, 3% mafic	2.5Y 5/1
3.2–3.3	Sandy clay - fine to medium, organic, occasional coarse gravel, 100% quartz	2.5Y 7/3
3.3–3.6	Sandy silt - very fine to fine, well rounded, well sorted, 100% quartz	2.5Y 7/2
3.6–4.0	Sand - fine to medium, moderately sorted, interbedded coarse sand, rounded, 95% quartz, 2% feldspar, 3% mafic	2.5Y 7/2

Table 1. Lithologic descriptions of test holes within the Elkhorn-Loup Model study area, north-central Nebraska—Continued.

Depth (meters)	Lithology	Munsell color
	Ord-6, N41º38′57″, W98º57′04″, Valley County, Nebraska, T19N R14W S5—Continued	
4.0–4.3	Arkosic sand - medium to coarse, rounded to sub-angular, poorly sorted, interbedded coarse gravels, 70% quartz, 25% feldspar, 5% mafic	2.5Y 7/3
4.3–4.8	Sand - fine, well sorted, well rounded, 96% quartz, 1% feldspar, 3% mafic	2.5Y 7/2
4.8–6.0	Sand - fine, well sorted, well rounded, occasional interbedded medium to coarse sand, 95% quartz, 1% feldspar, 4% mafic	2.5Y 7/2
	Ord-7, N41º38′54″, W98º57′04″, Valley County, Nebraska, T19N R14W S5	
0.34–0.65	Clayey silt - very fine, organic, some roots, more clayey sand towards the bottom	2.5Y 2.5/1
0.65–0.94	Sand - fine, well sorted, well rounded, 95% quartz, 1% feldspar, 4% mafic	2.5Y 8/1
0.94–1.16	Sand - fine, well sorted, well rounded, some interbedded coarse sand to fine gravel, rounded to sub-angular, traces of organics, 95% quartz, 1% feldspar, 4% mafic	2.5Y 7/1
1.83–2.4	Arkosic sand - fine to medium, well rounded, moderately sorted, interbedded coarse sand and coarse gravels, rounded to sub-angular, 80% quartz, 15% feldspar, 5% mafic	2.5Y 7/2
2.4–2.9	Sand - very fine, well rounded, well sorted, soft, 95% quartz, 2% feldspar, 3% mafic	2.5Y 7/2
2.9–3.6	Arkosic sand - medium to coarse, moderately sorted, rounded, interbedded fine gravels, rounded to sub-angular, 80% quartz, 15% feldspar, 5% mafic	2.5Y 7/3
3.6–3.7	Arkosic sand - medium to coarse, poorly sorted, rounded, interbedded fine to coarse gravels, rounded to sub-angular, 80% quartz, 15% feldspar, 5% mafic	2.5Y 7/3
3.7–4.8	Sand - fine, well sorted, well rounded, 95% quartz, 2% feldspar, 3% mafic	2.5Y 7/2
	Ord-8, N41º38′12″, W98º56′07″, Valley County, Nebraska, T19N R14W S9	
0–0.46	Clayey silt - organic, sticky, some roots, very fine to fine sand toward bottom	10YR 2/1
0.81–1.0	Sandy silt - very fine to fine, well sorted, well rounded, organic traces of plant roots, 95% quartz, 5% mafic	2.5Y 6/1
1.0–1.16	Silty clay - fine, with interbedded sand, very fine, organic traces of plant roots, sticky	2.5Y 5/1
1.16–1.67	Sand - fine, moderately sorted, well rounded, fine to medium sand toward the bottom, interbedded fine to coarse gravels, moderately sorted, rounded, range (10–33 mm), 90% quartz 5% feldspar, 5% mafic	2.5Y 7/1
1.67–2.47	Sand - fine to medium, well rounded, moderately sorted, 90% quartz, 5% feldspar, 5% mafic	2.5Y 7/1
2.47–3.6	Arkosic - sand, medium to coarse, rounded, poorly sorted, interbedded fine to coarse gravel, rounded, range (10–30 mm), more organic sand toward the bottom, 70% quartz, 25% feldspar, 5% mafic	2.5Y 6/2
4.0–4.32	Arkosic - sand, fine to medium, well rounded, well sorted, 90% quartz, 3% feldspar, 7% mafic	2.5Y 7/1
4.32–4.8	Arkosic - sand, medium to coarse, rounded, poorly sorted, interbedded fine gravels, rounded, sand fines upward, more feldspar than (4.0–4.32), 85% quartz, 10% feldspar, 5% mafic	2.5Y 7/1
	Ord-9, N41º38′10″, W98º56′05″, Valley County, Nebraska, T19N R14W S9	
0.31–0.57	Topsoil - silty clay, very fine, organic, some roots	10YR 2/1
0.57–0.83	Silty clay - interbedded sand, very fine to fine, 100% quartz	2.5Y 4/1
0.83–1.16	Sand - fine, well sorted, well rounded, interbedded medium sand, well rounded, 95% quartz, 1% feldspar, 4% mafic	2.5Y 7/2
1.16–3.4	Sand, - fine to medium, poorly sorted, well rounded, interbedded coarse sand and fine gravels, rounded, occasional coarse gravel, 80% quartz, 15% feldspar, 5% mafic	2.5Y 7/2
3.4–3.6	Silty clay - interbedded fine sand, well rounded, 100% quartz, more sandy toward the bottom, organic	2.5Y 4/1
4.0–4.8	Sand - fine, well sorted, well rounded, occasional coarse sand and fine gravel, rounded, 97% quartz, 1% feldspar, 2% mafic	2.5Y 7/1

Table 1. Lithologic descriptions of test holes within the Elkhorn-Loup Model study area, north-central Nebraska—Continued.

Depth (meters)	Lithology	Munsell color
	Ord-10, N41º37′39″, W98º55′34″, Valley County, Nebraska, T19N R14W S9	
0.25–0.41	Topsoil - silty sand, very fine to fine, well rounded, interbedded roots, organic, sandy silt toward the bottom	10YR 3/2
0.41–1.05	Clayey silt - very fine, organic, sticky, silty sand at the bottom, very fine to fine, traces of roots	10YR 3/1
1.05–1.16	Arkosic sand, fine - well sorted, well rounded, 95% quartz, 5% mafic	2.5Y 7/1
1.76–2.06	Arkosic sand - fine, medium, well rounded, well sorted, interbedded coarse sand and fine gravel, rounded, 95% quartz, 2% mafic 3% feldspar	2.5Y 7/1
2.06–2.4	Arkosic sand - medium to coarse, some fine, rounded, poorly sorted, interbedded fine gravels toward the bottom, rounded, 90% quartz, 5% feldspar, 5% mafic	2.5Y 7/1
3.0–3.1	Arkosic sand - medium to coarse, rounded, poorly sorted, more coarse sand than (2.06–2.4), range (2.06–2.4 mm) 85% quartz, 15% feldspar	2.5Y 7/2
3.1–3.6	Clayey silt - organic, very fine, sticky, saturated	2.5Y 3/1
4.0–4.9	Clayey silt - organic, very fine, sticky, silty toward the top, saturated, clayey toward the bottom	2.5Y 5/1
4.9–6.0	Clayey silt - organic, very fine, sticky, very fine sand toward the bottom, saturated	2.5Y 5/1
	Ord-11, N41º37′39″, W98º55′33″, Valley County, Nebraska, T19N R14W S9	
0–0.10	Topsoil - silty clay, very fine, organic, interbedded roots, interbedded fine sand, rounded, 100% quartz	10YR 2/2
0.10–0.26	Sandy clay - very fine to fine, interbedded sand, well rounded, 100% quartz, interbedded roots	10YR 5/2
0.60–0.70	Clayey silt - very fine to fine, organic, well rounded, sticky, 100% quartz	10YR 2/1
0.94–1.16	Clayey silt - very fine to fine, more organic than (0.60–0.70), well rounded, some roots, 100% quartz	10YR 2/1
1.16–1.35	Arkosic sand - fine to medium, well sorted, well rounded, 95% quartz, 1% feldspar, 4% mafic	2.5Y 8/1
1.71–2.4	Arkosic sand - fine to medium, well sorted, well rounded, interbedded fine gravel, rounded, traces of organics, 95% quartz, 2% feldspar, 3% mafic	2.5Y 8/1
3.9–4.8	Clayey silt - organic, sticky, soft, very fine	2.5Y 5/1
	Thedford-1, N41º59′06″, W100º41′26″, Thomas County, Nebraska, T23N R29W S9+	
0.49–0.59	Topsoil, silty - organic, some roots	10YR 2.5/1
0.59–1.01	Silty clay - fine, well sorted, organic, sticky, sandy toward the bottom	2.5Y 4/1
1.01–1.16	Sandy silt - fine to medium, well sorted, well rounded, 90% quartz, 5% feldspar, 5% mafic	2.5Y 6/1
1.72–1.82	Arkosic sand - medium, rounded, poorly sorted, interbedded coarse gravel, rounded, range (19–21 mm), 90% quartz, 5% feldspar, 5% mafic	2.5Y 7/1
1.82–2.1	Arkosic sand - medium, well sorted, well rounded, 90% quartz, 5% feldspar, 5% mafic	2.5Y 7/1
2.1–2.4	Arkosic sand - medium, rounded to sub-angular, poorly sorted, interbedded coarse sand to coarse gravel, range (20–40 mm), 80% quartz, 15% feldspar, 5% mafic	2.5Y 7/2
3.1–3.3	Arkosic - sand, medium to coarse, rounded, sub-angular, poorly sorted, interbedded coarse gravel, rounded, range (20–23 mm), 60% quartz, 35% feldspar, 5% mafic	2.5Y 7/4
3.3–3.6	Arkosic sand, - fine to medium, rounded, moderately sorted, interbedded coarse sand and fine gravel, rounded, 80% quartz, 15% feldspar, 5% mafic	2.5Y 7/2
4.2–4.8	Arkosic sand - medium to coarse, rounded to sub-angular, poorly sorted, interbedded coarse gravel, rounded, range (20–22 mm), sand fines toward the bottom, 60% quartz, 35% feldspar, 5% mafic	2.5Y 7/2
	Thedford-2, N41º59′08″, W100º41′25″, Thomas County, Nebraska, T23N R29W S4	
0.43–0.60	Topsoil - silty clay, very fine, organic, sticky, some roots	10YR 2/1
0.60–0.77	Sandy clay - very fine to fine, well rounded, well sorted, sticky, organic, mostly quartz	2.5Y 6/2

Table 1. Lithologic descriptions of test holes within the Elkhorn-Loup Model study area, north-central Nebraska—Continued.

Depth (meters)	Lithology	Munsell color
	Thedford-2, N41º59′08″, W100º41′25″, Thomas County, Nebraska, T23N R29W S4—Continued	
0.77–1.16	Sand - fine, well sorted, well rounded, 95% quartz, 1% feldspar, 4% mafic	2.5Y 8/1
1.16–1.35	Arkosic sand - medium to coarse, rounded to sub-angular, poorly sorted, interbedded fine to coarse gravel, rounded, 85% quartz, 10% feldspar, 5% mafic	2.5Y 7/2
1.77–1.98	Sand - fine to medium, well sorted, well rounded, 95% quartz, 1% feldspar, 4% mafic	2.5Y 7/2
2.4–3.9	Arkosic sand - medium to coarse, rounded to sub-angular, poorly sorted, interbedded fine to coarse gravel, rounded, 75% quartz, 20% feldspar, 5% mafic	2.5Y 7/3
	Thedford-3, N41º59′12″, W100º40′43″, Thomas County, Nebraska, T23N R29W S4	
0.30–0.90	Topsoil - silty, fine, well sorted, silty sand toward bottom, some roots, mostly quartz	2.5Y 3/2
0.90–1.16	Sand - fine, well sorted, well rounded, soft, 97% quartz, 1% feldspar, 2% mafic	2.5Y 8/2
1.53–2.11	Sand - fine, well sorted, well rounded, soft, traces of organics, 97% quartz, 1% feldspar, 2% mafic	2.5Y 6/2
2.11–2.8	Arkosic sand - medium to coarse, poorly sorted, rounded to sub-angular, interbedded fine to coarse gravel, rounded, 80% quartz, 15% feldspar, 5% mafic	2.5Y 7/2
2.8–3.6	Arkosic sand - medium to coarse, poorly sorted, rounded to sub-angular, interbedded fine to coarse gravel, rounded, coarse sand and gravel at the bottom, 70% quartz, 25% feldspar, 5% mafic	2.5Y 7/2
4.2–4.8	Arkosic sand - medium to coarse, poorly sorted, rounded to sub-angular, interbedded fine to coarse gravel, rounded to sub-angular, 60% quartz, 35% feldspar, 5% mafic	2.5Y 7/3
	Thedford-4, N41º59′13″, W100º40′41″, Thomas County, Nebraska, T23N R29W S4	
0.46–0.65	Topsoil - silty sand, fine, soft, some roots	2.5Y 3/2
0.65–0.83	Silty clay - organic, very fine, soft, sticky, some roots	2.5Y 2.5/1
0.83–1.16	Sand - fine, well sorted, well rounded, 90% quartz, 5% feldspar, 5% mafic, some roots	2.5Y 8/1
1.57–1.92	Sand - medium to coarse, rounded to sub-angular, interbedded fine to coarse gravel, rounded poorly sorted, 45% quartz, 50% feldspar, 5% mafic	2.5Y 7/2
1.92–2.4	Arkosic sand - medium to coarse, rounded to sub-angular, interbedded fine to coarse gravel, rounded, poorly sorted, 65% quartz, 30% feldspar, 5% mafic	2.5Y 7/1
2.9–3.3	Arkosic sand - medium to coarse, rounded to sub-angular, interbedded fine to coarse gravel, rounded, poorly sorted, 45% quartz, 50% feldspar, 5% mafic	2.5Y 7/2
3.3–3.6	Arkosic sand - fine to medium, rounded to sub-angular, interbedded coarse sand and fine gravel, sub-angular, moderately sorted, 60% quartz, 35% feldspar, 5% mafic	2.5Y 7/2
4.1–4.3	Arkosic sand - fine to medium, rounded to sub-angular, interbedded coarse sand and fine gravel, sub-angular, moderately sorted, 60% quartz, 35% feldspar, 5% mafic	2.5Y 7/2
4.3–4.6	Arkosic sand - medium to coarse, rounded to angular, poorly sorted, interbedded large coarse gravel, range (19–39 mm), sub-angular to angular, 35% quartz, 60% feldspar, 5% mafic	2.5Y 7/2
4.6–4.9	Arkosic sand - medium to coarse, moderately sorted, rounded to sub-angular, interbedded fine gravel, angular, 55% quartz, 40% feldspar, 5% mafic	2.5Y 7/2

Appendix 1—Sampling Delays and Widths used with the High-Resolution Time-Gate Sampling Rate for the Time-Domain Electromagnetic Soundings

Blank Page

Appendix 1. Sampling delays and widths used with the high-resolution time-gate sampling rate for the time-domain electromagnetic soundings.

[In milliseconds; --, not available]

Delay	Width	Delay (continued)	Width	Delay (continued)	Width	Delay (continued)	Width
0.002	0.002	0.141	0.008	0.817	0.032	4.001	0.128
.004	.002	.149	.008	.849	.032	4.193	.256
.006	.002	.157	.008	.881	.032	4.449	.256
.008	.002	.165	.008	.913	.032	4.705	.256
.010	.002	.173	.008	.945	.032	4.961	.256
.012	.002	.181	.008	.977	.032	5.217	.256
.014	.002	.189	.008	1.025	.064	5.473	.256
.016	.002	.197	.008	1.089	.064	5.729	.256
.018	.002	.205	.008	1.153	.064	5.985	.256
.020	.002	.213	.008	1.217	.064	6.241	.256
.022	.002	.221	.008	1.281	.064	6.497	.256
.024	.002	.233	.016	1.345	.064	6.753	.256
.026	.002	.249	.016	1.409	.064	7.009	.256
.028	.002	.265	.016	1.473	.064	7.265	.256
.030	.002	.281	.016	1.537	.064	7.521	.256
.032	.002	.297	.016	1.601	.064	7.777	.256
.035	.004	.313	.016	1.665	.064	8.033	.256
.039	.004	.329	.016	1.729	.064	8.417	.512
.043	.004	.345	.016	1.793	.064	8.929	.512
.047	.004	.361	.016	1.857	.064	9.441	.512
.051	.004	.377	.016	1.921	.064	9.953	.512
.055	.004	.393	.016	1.985	.064	1.465	.512
.059	.004	.409	.016	2.081	.128	1.977	.512
.063	.004	.425	.016	2.209	.128	11.489	.512
.067	.004	.441	.016	2.337	.128	12.001	.512
.071	.004	.457	.016	2.465	.128	12.513	.512
.075	.004	.473	.016	2.593	.128	13.025	.512
.079	.004	.497	.032	2.721	.128	13.537	.512
.083	.004	.529	.032	2.849	.128	14.049	.512
.087	.004	.561	.032	2.977	.128	14.561	.512
.091	.004	.593	.032	3.105	.128	15.073	.512
.095	.004	.625	.032	3.233	.128	15.585	.512
.101	.008	.657	.032	3.361	.128	16.097	.512
.109	.008	.689	.032	3.489	.128	16.865	1.024
.117	.008	.721	.032	3.617	.128	17.889	1.024
.125	.008	.753	.032	3.745	.128	18.913	1.024
.133	.008	.785	.032	3.873	.128	--	--

Blank Page

Appendix 2—Inverse Modeling Results for Time-Domain Electromagnetic Soundings, North-Central Nebraska, 2006–07

Blank Page

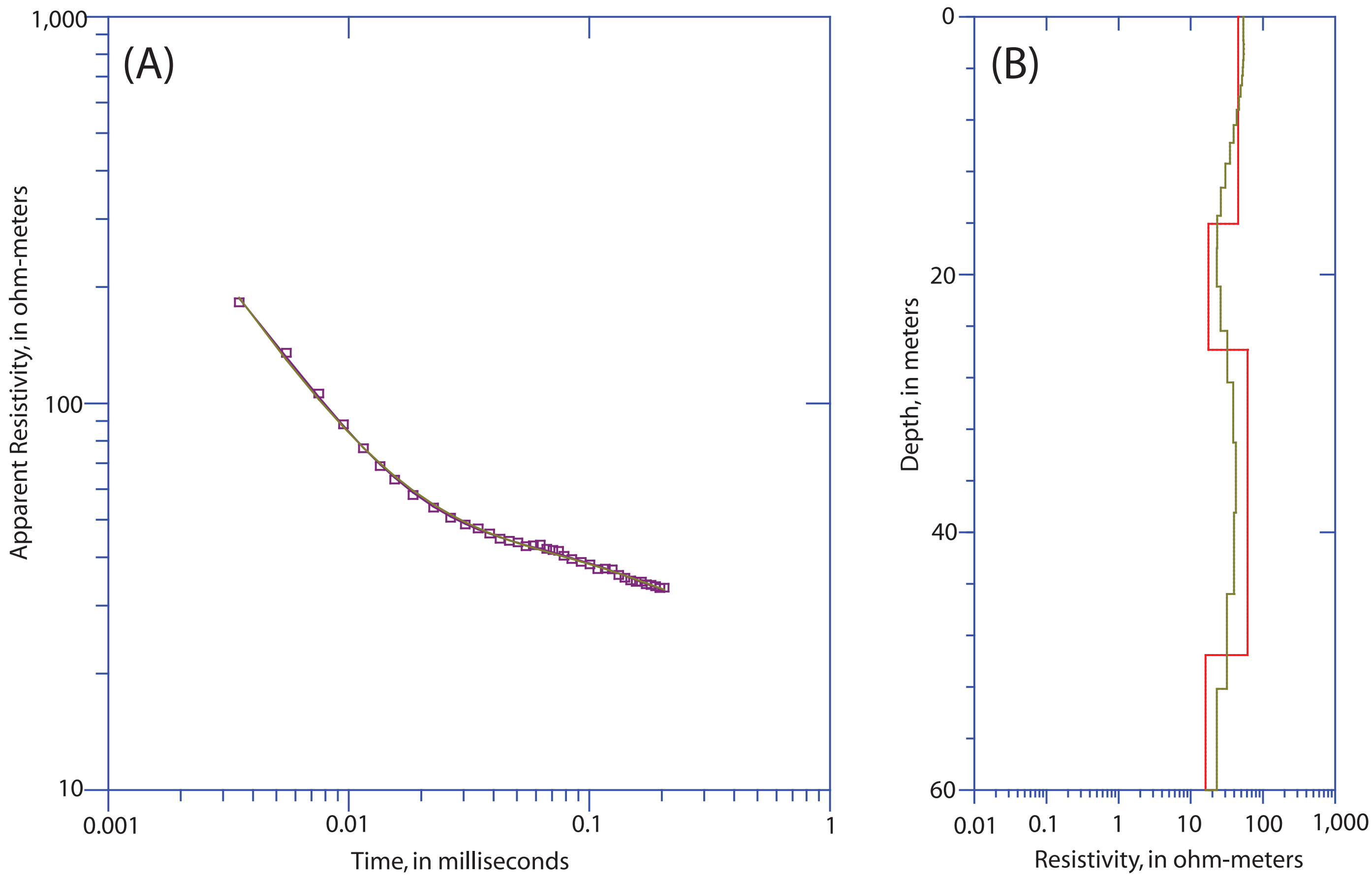

EXPLANATION

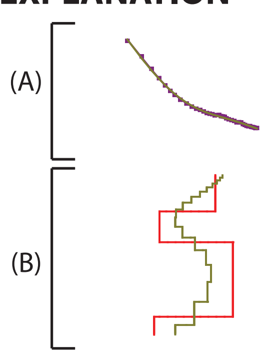

(A) Raw data converted to apparent resistivity shown as squares (purple, low current)
Model fit to the data shown as a line through the data points (colored line is the layered model fit, and brown line is the smooth model fit)

(B) Smooth model inversion results shown as a brown line
Layered model inversion results shown as a red line

Figure 2.1. Sounding site Ainsworth-1: (A) time-domain electromagnetic (TDEM) sounding raw data (apparent resistivity from field measurements) as a function of time; and (B) inverse modeling results (smooth and layered model of estimated true resistivity) as a function of depth.

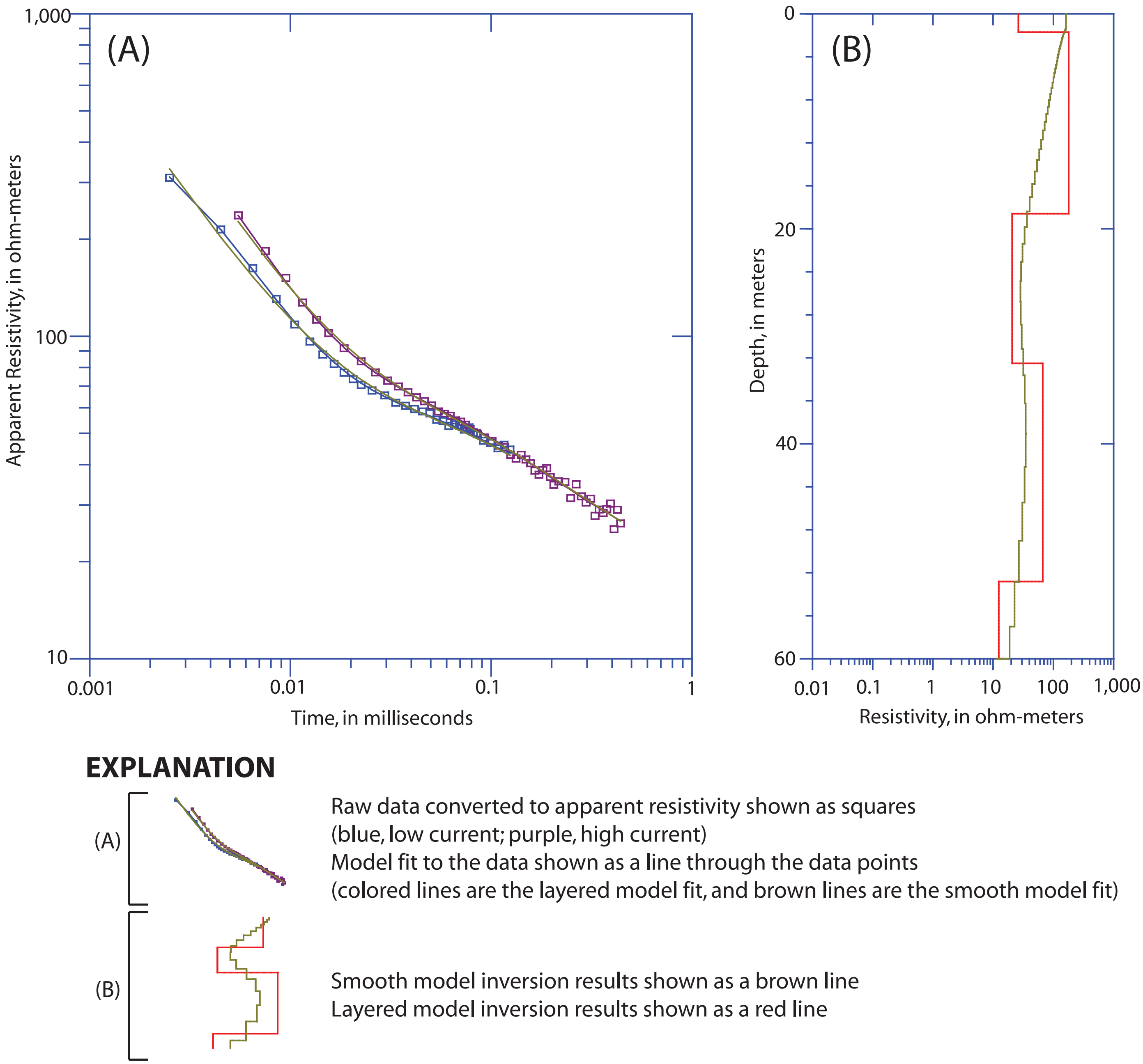

Figure 2.2. Sounding site Ainsworth-2: (A) time-domain electromagnetic (TDEM) sounding raw data (apparent resistivity from field measurements) as a function of time; and (B) inverse modeling results (smooth and layered model of estimated true resistivity) as a function of depth.

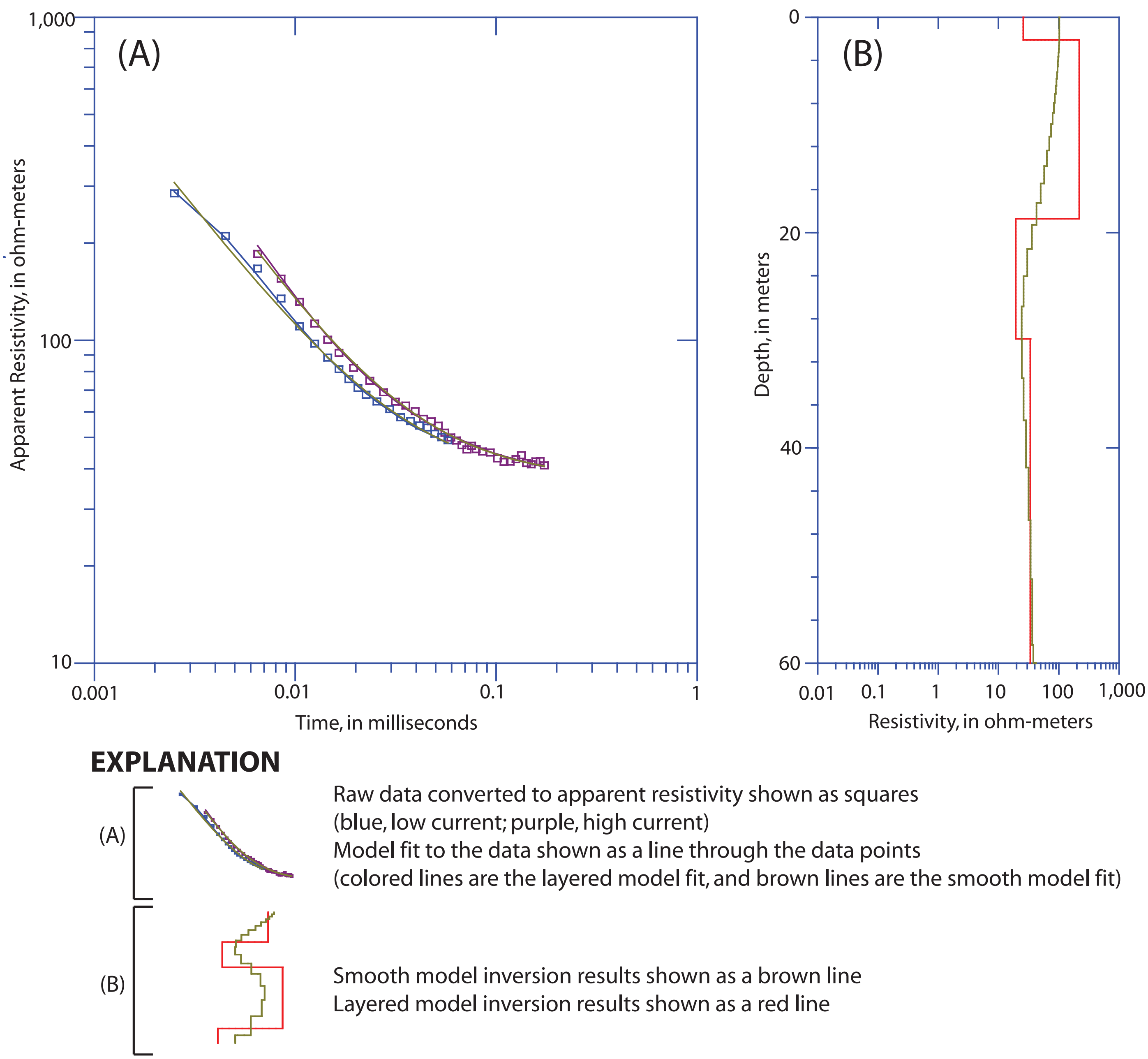

Figure 2.3. Sounding site Ainsworth-3: (A) time-domain electromagnetic (TDEM) sounding raw data (apparent resistivity from field measurements) as a function of time; and (B) inverse modeling results (smooth and layered model of estimated true resistivity) as a function of depth.

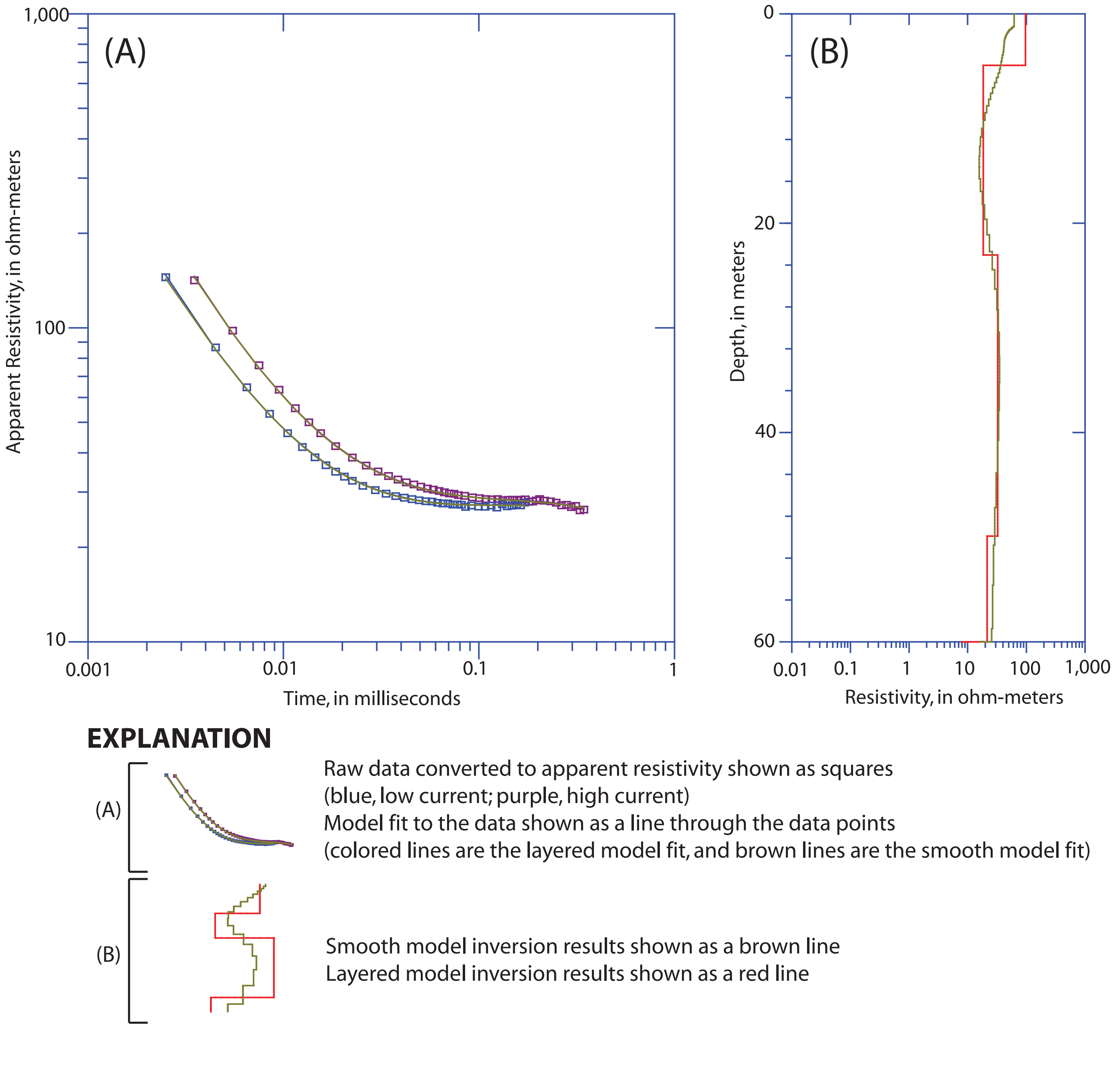

Figure 2.4. Sounding site Ord-1: (A) time-domain electromagnetic (TDEM) sounding raw data (apparent resistivity from field measurements) as a function of time; and (B) inverse modeling results (smooth and layered model of estimated true resistivity) as a function of depth.

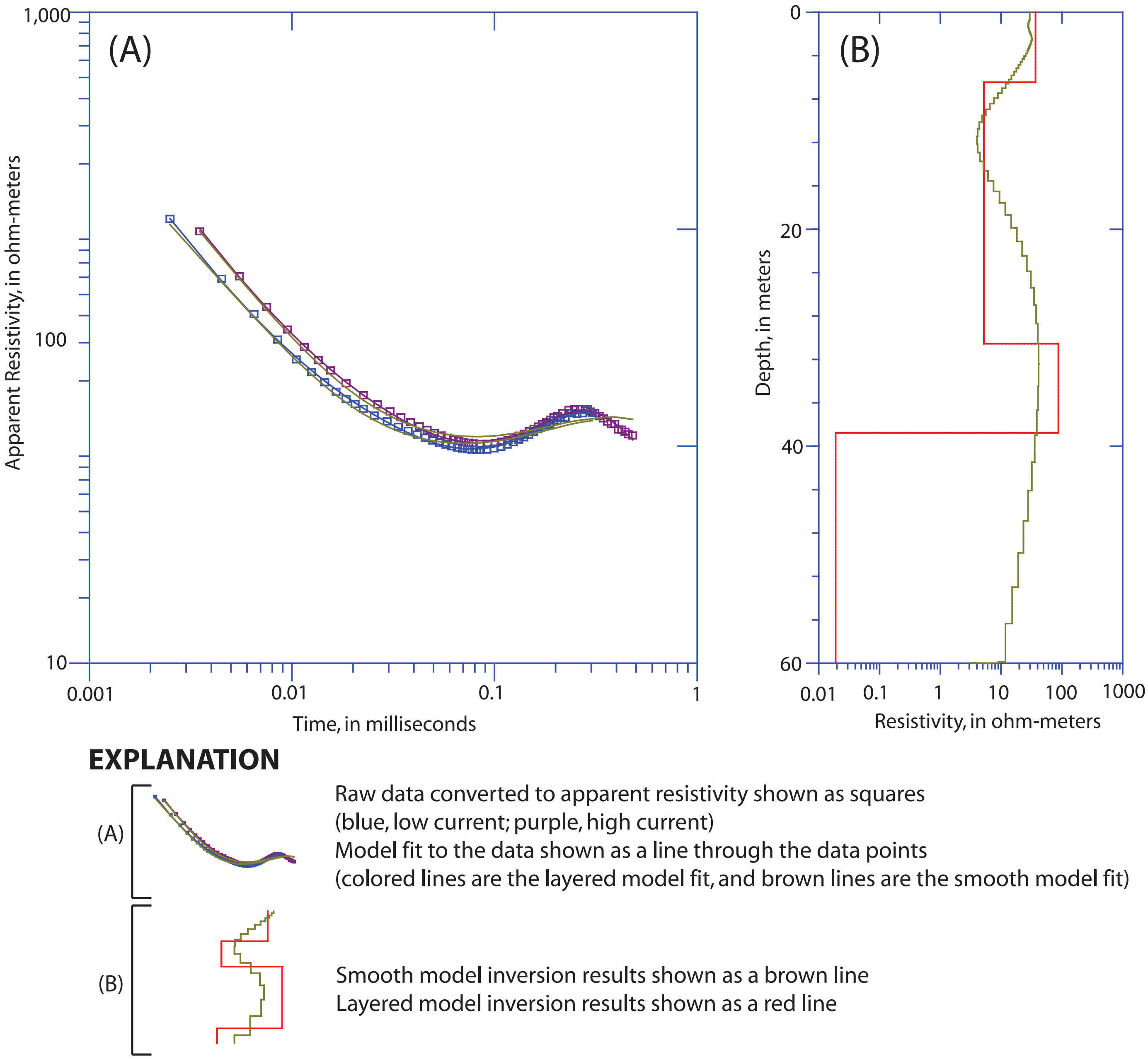

Figure 2.5. Sounding site Ord-2: (A) time-domain electromagnetic (TDEM) sounding raw data (apparent resistivity from field measurements) as a function of time; and (B) inverse modeling results (smooth and layered model of estimated true resistivity) as a function of depth.

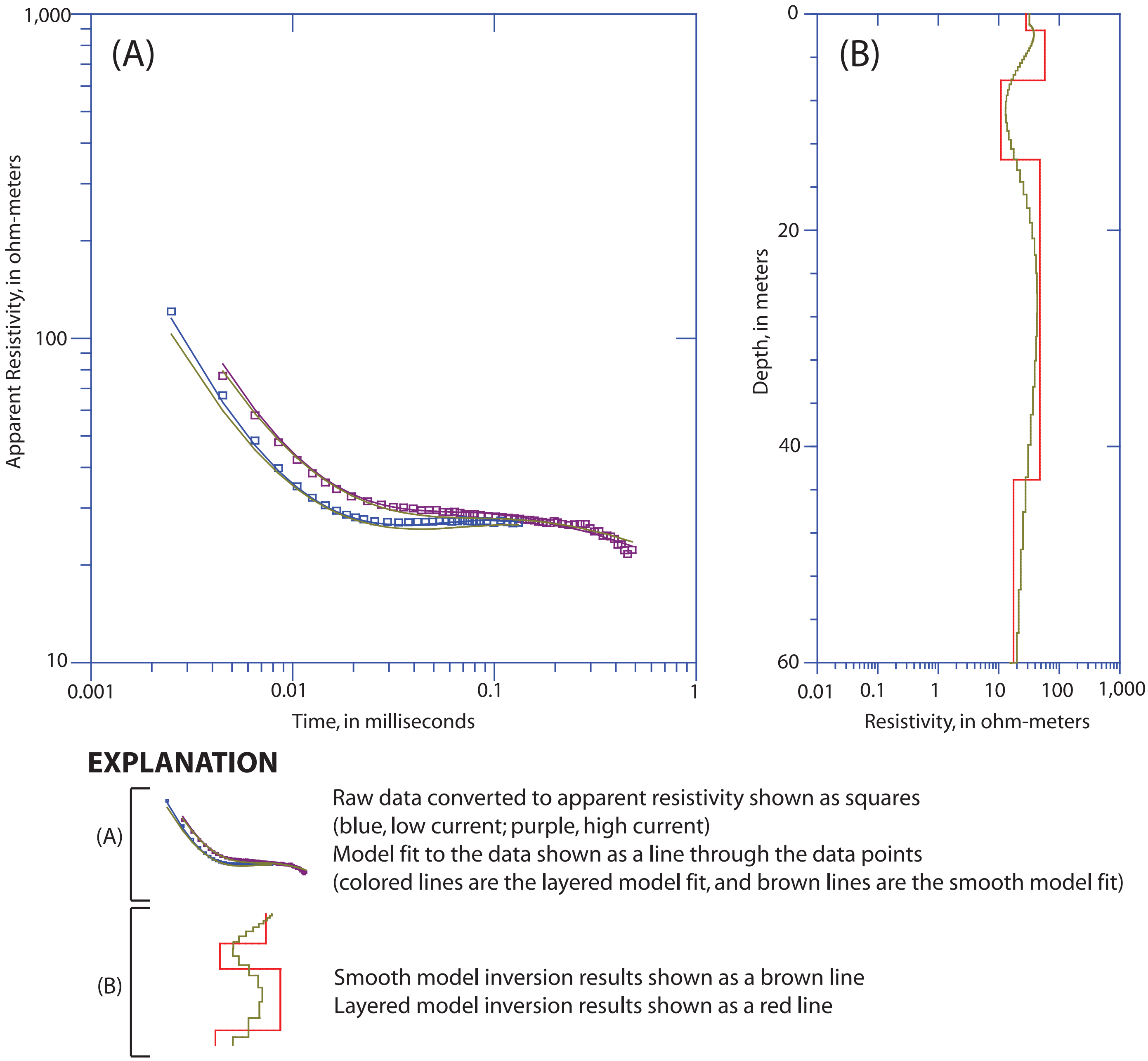

Figure 2.6. Sounding site Ord-3: (A) time-domain electromagnetic (TDEM) sounding raw data (apparent resistivity from field measurements) as a function of time; and (B) inverse modeling results (smooth and layered model of estimated true resistivity) as a function of depth.

Publishing support provided by
Lafayette Publishing Service Center

≈USGS

Teeple, Vrabel, Kress, and Cannia—Apparent Resistivity and Estimated Interaction Potential of Surface Water and Groundwater, North-Central Nebraska—SIR 2009–5171